Implementing GaN Technology in the Design of a High Efficiency RF Power Amplifier

by

Evan Court

Thesis submitted in fulfilment of the requirements for the degree

Master of Engineering: Electrical Engineering

in the Faculty of the Department of Electrical, Electronic and Computer Engineering

at the Cape Peninsula University of Technology

Supervisor: Dr. Vipin Balyan

Bellville
Date submitted (January 2024)

CPUT copyright information

The thesis/dissertation may not be published either in part (in scholarly, scientific or technical journals), or as a whole (as a monograph), unless permission has been obtained from the University

Declaration

I, Evan Court, declare that the contents of this thesis represent my own unaided work, and that the thesis/dissertation has not previously been submitted for academic examination towards any qualification. Furthermore, it represents my own opinions and not necessarily those of the Cape Peninsula University of Technology.

Signed: Date: 07 November 2024

Abstract

The output signal of a radio frequency (RF) power amplifier (PA) is referred to as the transmitted signal. The purpose of a RF PA is to amplify/increase the power level of the transmitted signal such that the level of the received signal is at a suitable level above the noise floor to enable detection.

RF PA's implement amplification by converting the DC power applied to the PA into RF output power. Thus, the output signal of the PA is an amplified representation of the input signal. It is practically impossible to convert all the applied DC power into RF output power. Any DC power that is not converted into RF output power is dissipated as heat. This measure of power conversion is defined by two parameters termed the power added efficiency (*PAE*) and the power conversion efficiency (*PE*). Although the actual process of amplification is highly non-linear, the output signal of the PA is a linear amplified representation of the input signal.

A CubeSat is a miniature satellite in the shape of the cube, with the dimensions of 10 cm x 10 cm x 10 cm. On-board the satellite is a RF communication system which enables communication and data transfer with the satellite. As for any RF communication system and especially satellite communications, a high efficiency PA is required at the final stage of the transmitter due to the limited/restricted available on-board resources. Based on the condition of high efficiency, several PA design methods, techniques and classes of operation were studied. The class E switch-mode PA (zero-voltage switching) satisfies the condition of a high efficiency PA. This thesis presents the design of a class E switch-mode PA using Wolfspeed Cree CGH40010F power active device. Design methods were tested by means of simulation using Agilent Advanced Design Systems (ADS) and results are analysed for correct class-E operation.

Contents

Declaration ii

Abstract iii

Table of Contents iv

List of Figures vi

List of Tables vii

Introduction 1
- 1.1 Motivation 1
- 1.2 Objectives 2
- 1.3 Research Methodology 2
- 1.4 Conclusion 3

Overview of RF Power Amplifiers 4
- 2.1 History of the RF Power Amplifier 4
- 2.2 History of the Active Device 4
- 2.3 Operating Regions of a Field Effect Transistor 7
  - 2.3.1 The Cut-Off Region 7
  - 2.3.2 The Active Region 8
  - 2.3.3 The Ohmic Region 8
- 2.4 Operation Theory of RF Power Amplifiers 9
  - 2.4.1 Operating the Active Device as a Switch 10
  - 2.4.2 Operating the Active Device as a Current Dependant Source 11
- 2.5 Classes of Operation of RF Power Amplifiers 12
  - 2.5.1 Linear Power Amplifier Classes 14
  - 2.5.2 Synopsis of Linear Power Amplifiers 18
  - 2.5.3 Switching Class Power Amplifiers 19
  - 2.5.4 Active Device Technology for RF Power Amplifiers 24

2.6 Performance Parameters of a Power Amplifier 26
2.6.1 Output Power 26
2.6.2 Power Gain 26
2.6.3 Power Conversion Efficiency 27
2.6.4 Power Added Efficiency 27
2.6.5 Linearity 28
2.7 Design Techniques and Principles 33
2.7.1 Load-Line Theory 33
2.7.2 Load-Pull Technique 34
2.8 Conclusion 33
Class-E Power Amplifiers with Shunt Capacitance 37
3.1 Introduction 37
3.2 Switching Transitions of the Active Device 38
3.3 Assumptions for Theoretical Analysis 39
3.4 Limitations on Maximum Achievable *PE* 40
3.5 Maximum Operating Frequency Before Experiencing Degradation 41
3.6 Conclusion 33
The Design of a Class-E PA with Shunt Capacitance 44
4.1 Specifications 44
4.2 Choice of Active Device 44
4.3 DC Biasing 45
4.4 Design Procedure 45
4.4.1 Determining the Optimum Load Network Conditions 46
4.4.2 Load Network Design 49
4.5 Load Network Simulation Results 52
4.6 Lumped Component Class-E PA 52
4.6.1 Simulation Results of Lumped Component Class-E 53
4.7 Ideal Transmission Line Class-E 55
4.8 Microstrip Class-E PA Simulation Results 58
4.9 Optimised Class-E PA Simulation Results 60
Conclusion, Recommendations and Future Work 64
Bibliography 81

List of Figures

Figure 2.3: V-I Characteristics of a JFET ....**Error! Bookmark not defined.**
Figure 2.4.1: Energy Schematic of a PA (modified from Eroglu, 2018: 126)................ **Error! Bookmark not defined.**
Figure 2.4.2: Simplified schematic of a power amplifier (modified from Colantonio *et al*., 2009:178) ....**Error! Bookmark not defined.**
Figure 2.5: Quiescent Bias Conditions for Operating Classes (modified from Kazimierczuk, 2008: 4) ....**Error! Bookmark not defined.**
Figure 2.6: Summary of PA classification (modified from) ...**Error! Bookmark not defined.**
Figure 2.5.1: Simplified schematic of a linear power amplifier (modified from Colantonio *et al*., 2009: 178) ....**Error! Bookmark not defined.**
Figure 2.5.1.1: Drain voltage and current waveforms of an ideal class A PA (modified from Raab) ....**Error! Bookmark not defined.**
Figure 2.5.1.2: Drain voltage and current waveforms of an ideal class B PA (modified from Raab) ....**Error! Bookmark not defined.**
Figure 2.5.1.3: Drain voltage and current waveforms of an ideal class AB PA (modified from) ....**Error! Bookmark not defined.**
Figure 2.5.1.4: Drain voltage and current waveforms of an ideal class C PA (modified from) ....**Error! Bookmark not defined.**
Figure 2.5.2: Comparison of linear class PAs..........................**Error! Bookmark not defined.**
Figure 2.5.3.1: Simplified schematic of a class D PA with series resonant circuit .... **Error! Bookmark not defined.**
Figure 2.5.3.2: Simplified schematic of a current-mode class D (CMCD) PA .... **Error! Bookmark not defined.**
Figure 2.5.3.3: Drain voltage and current waveforms of an ideal class D PA (modified from) ....**Error! Bookmark not defined.**
Figure 2.5.3.4: Simplified schematic of a class E PA.............**Error! Bookmark not defined.**
Figure 2.5.3.5: Drain voltage and current waveforms of an ideal class E PA (modified from) ....**Error! Bookmark not defined.**
Figure 2.5.3.6: Simplified schematic of a class F PA.............**Error! Bookmark not defined.**

Figure 2.5.3.7: Drain voltage and current waveforms of an ideal class F PA (modified from) ....**Error! Bookmark not defined.**
Figure 2.5.4: Output power of a single device as a function of frequency (modified from Colantonio *et al*., 2008: 26)..**Error! Bookmark not defined.**
Figure 2.6.4: Performance of a PA as a function of RF input power (modified from Colantonio, 2009: 5) ....**Error! Bookmark not defined.**
Figure 2.6.5.1: Illustration of the 1 dB compression point (modified from Colantonio *et al.,* 2009:3) ....**Error! Bookmark not defined.**
Figure 2.6.5.2: Illustration of the third-order intercept point (adapted from M. Golio et al., 2018: 9-25) ....**Error! Bookmark not defined.**
Figure 2.6.5.3: Error vector magnitude and dependant quantities (modified from Colantonio *et al*., 2009:3) ....**Error! Bookmark not defined.**
Figure 2.7.1: Illustration of the load-line technique (modified from MacPherson & Whaits, 2007: 14) ....**Error! Bookmark not defined.**
Figure 2.7.2: Load-pull measurement and equipment setup (modified from ...) .... **Error! Bookmark not defined.**
Figure 3.1: Schematic of a low-order class E PA (modified from Sokal, 2003: 31) 35
Figure 3.2: Drain waveforms of FET in low-order class E PA (modified from Sokal, 2003: 31)……………………………………………………………………………………**E rror! Bookmark not defined.**
Figure 3.3: Waveforms of ideal switch model……………………………………………..38
Figure 4.2: The Wolfspeed Cree CGH40010F GaN HEMT…………………………………41
Figure 4.3: Choice of quiescent operating point……………………………………………42
Figure 4.4.2.1: Class-E equivalent circuit…………………………………………………46
Figure 4.4.2.2: Splitting the pi-network……………………………………………………46
Figure 4.4.2.3: Pi-network with relevant reactance values…………………………………48
Figure 4.4.2.4: Realizable class-E amplifier………………………………………………48
Figure 4.5: Input and output return loss of the load network………………………………....49
Figure 4.6: Lumped circuit schematic of designed class-E PA……………………………50
Figure 4.6.1: Simulated drain voltage and current waveforms……………………………50

List of Tables

Table 3.5: Suboptimum operation of a class-E PA above $f_{\max}$ (adapted from Grebbenikov & Sokal, 2007:191) 42

Table 4.9: Comparison of Class-E Power Amplifiers……………………………………..51

Chapter 1

Introduction

Presented in the introductory chapter are the reasons and motivation for which the author undertook the research, in conformance with the French South African Institute of Technology (F'SATI). The objectives of this research and the methodology to achieve such are presented in this chapter. Due to the broad research field of RF power amplification, the specific topic and the focus area of the thereof are presented.

1.1 Motivation

The Cape Peninsula University of technology develops miniature satellites (CubeSat) under the French South African Institute of Technology (F'SATI). The communication system of the most recently developed CubeSat (ZACUBE-2) uses a 2W S-band transmitter (STX) developed by the F'SATI which forms part of the satellite communication system. The STX transmitter however only boasts a power conversion efficiency (PE) of 25%. This means that 75% of the applied DC power is generated as heat and only 25% is converted in useful RF output power. With a priori knowledge of CubeSats having limited resources and space, losing 75% of the DC power not only poses a major problem, the heat dissipation could cause damage to other systems on-board the satellite.

As per research by Moise Safari Mugisho, a high efficiency inverse class-F power amplifier was designed. This research proposes the class-E power amplifier as a method of maximizing the amplification of the transmitted signal and minimizing the dissipation of DC power(heat). A high efficiency power amplifier suitable for the use in an RF/wireless communication system including (and suitable) for CubeSat applications.

1.2 Objectives

The primary objective of the research is to design a high efficiency RF power amplifier (operating in the S-Band) suitable for CubeSat applications. The amplifier design will be simulated and evaluated with respect to the performance in comparison to existing class-E designs.

Supplementary objectives include but are not limited to the following:

- Study and understand RF power amplifiers in a general sense.
- Provide a distinction between the operation of various PA classes.
- Know the advantages and disadvantages of each class of PA.
- Evaluate and compare results of the designed and simulated PA with respect to existing PA's relative to the area of application.

1.3 Research Methodology

- With a priori knowledge of the PA on-board ZA-Cube2, conduct a literature study on various existing PAs with respect to output power as well as maximum obtainable efficiency, but not limited to these parameters.
- The PA's investigated will be specific to the type required/the use in a CubeSat.
- Study existing design techniques for PA's and the select class of operation as well as the configuration or topology most suitable to achieve the desired specification/output/performance.
- Study various active devices, that is, RF power transistors with a bias to ones most suitable for space applications.
- Define specifications/performance parameters of the PA to be designed and built.
- Select an active device suitable to achieve the desired specifications.
- Design and simulate the PA using "Keysight Advanced Design System (ADS)".
- Analyse the simulated results with respect to the desired/defined specification.
- Compare the performance of the simulated PA to the performance of existing PA's and determine the degree of improvement/comparison/degradation/etc.

1.4 Conclusion

A CubeSat, as per any wireless communication system, requires a PA to facilitate communication. There is a continuous drive to improve reliability, reduce manufacturing cost, and in most cases, reduce physical size. Managing the thermal aspects of a CubeSat is important in an operational sense and designing a PA capable of meeting all the above-mentioned characteristics is possible, by careful selection and implementation of design techniques, components and suitable active devices.

Chapter 2

Overview of RF Power Amplifiers

2.1 History of the RF Power Amplifier

The early generations of RF power amplifiers were designed exclusively using vacuum tube devices. One of the most common tube amplifier applications still in use is the microwave oven (900 W) which uses a 2,45 GHz magnetron. The achievable power levels using solid-state devices have made considerable advances and the output capabilities are continuously improving, although there still power levels achievable with tube amplifiers that are beyond that of any solid-state device [1, p. 14]

2.2 History of the Active Device

Thomas Edison discovered in 1880's that electric current could flow across an empty space between a hot electric filament and another metal conductor (collector electrode or anode), contained in the same evacuated glass bulb (thermionic emission). He observed a very important phenomenon in that current travelled in one direction only. It was the discovery of the electron, made by J.J. Thompson in 1899 that really gave clarity to this phenomenon of current flow (flow of electrons) [2, pp. Section B, 1-3].

In 1904, John A. Fleming used thermionic emission to create the first electric "valve" and called it "The Fleming Valve". It was a device capable of allowing current flow in one direction and prohibiting/isolating current flow in the opposite direction. In doing so, the Fleming valve creates a dc output current for an ac rf input current. This was one of the earliest methods of detection of rf signals. Since 1904, advances in wireless techniques and systems have been dependant on the understanding and evolution of the electric valve (also known as the vacuum tube, due to its evacuated glass enclosure). Today, even though the electric valve (vacuum tube) devices have been replaced by much smaller solid-state (BJT and FET) devices (certain applications still use vacuum tubes), the forefront and advances of wireless communication is still in understanding and improving the construction, operation and application of the active device [2, pp. Section B, 1-3].

The improvement that was made to the Fleming valve revolutionized electronics and the method that was introduced by Dr Lee de Forest in 1907 is still the very method employed to control modern active devices. What de Forest did was take an electric valve like Fleming's and interposed a grid of wire between the cathode and the anode (in an evacuated glass bulb/tube), which formed a third electrode in the valve, called the grid. This three-electrode valve is known as the "triode". de Forest discovered that the potential of the grid (voltage potential) had overwhelming control over the current conducted by the anode [2, pp. Section B, 1-3].

In years that followed they designed valves (vacuum tubes) with additional electrodes, which allowed various properties of the vacuum tube to be utilized for different applications. The descriptions diode, triode, tetrode, pentode, hexode, octode, etc., are used to indicate the number of electrodes within the make-up of the valve. All of these above-mentioned (later) versions of the electric valve (vacuum tube) were based upon de Forest's discovery that, "the magnitude of the anode current may be controlled by the voltage potential of an interposed grid [2, pp. Section B, 1-3].

The electrodes might have adopted different names, but the fundamental basis of operation and control has remained the same. In transistors (BJT) the collector current is controlled by the base current (which is dependent on the voltage potential across the base-emitter junction, V_{BE}), exactly the basis of operation of the triode. Similarly, for field-effect transistors (FET) the drain current I_{D} is dependent on the voltage potential across the gate-to-source junction V_{GS} of the device.

Following the diode, triode, etc. family of vacuum tubes, electron emission led to the discovery of the electron tube. The electrons emitted by the cathode are accelerated and then by using electric or magnetic fields, the accelerated electrons are constricted into a narrow beam. It was discovered that these narrow electron beams could be deflected by means of an electric or magnetic field. This principle has led to the invention of the cathode-ray tube, which was used in television and laboratory equipment like oscilloscopes and radar displays. In television, the cathode-ray tube is also known as the kinescope [3, pp. 131-158].

More sophisticated versions of the cathode-ray tube (electron beam) were later developed such as iconoscopes, the magnetron (also known as a cavity-magnetron), the Orthicon and the Klystron, which made a strong contribution to the development of television and motion cameras (television camera). It was in the late 1930's to 1940 when the capability of the magnetron and the klystron as high-power sources were discovered. These are devices capable of generating high power levels (at a relatively high frequency) in comparison to the power required to drive the device. Stanford University was largely accredited for discovery of the average power amplification characteristics of the klystron [4, pp. 25-26].

Certain applications still use the cavity-magnetron, the cavity-klystron and the travelling-wave guide, all of which are by large to the credit of Stanford University for the evolution of the magnetron and the klystron. In comparison to these early (traditional) devices, solid-state devices and amplifiers designed using solid-state devices are relatively recent.

All the above-mentioned devices were designed with the intention of providing some degree of controlled amplification of an electronic signal. Advanced semiconductor materials have been developed since the magnetron which allows for manufacture of high performing active devices and electronics.

The review of past developments demonstrates the essential role active devices play in technology. Currently technology is evolving at such a rapid pace which is driving standards and goals for future designs in RF amplification. Currently technology requires high data rate with efficient power transfer. This has resulted in a paradigm of physical makeup of devices and configurations implemented to accommodate higher frequencies and power efficiency objectives.

The most recent active device technology and the semiconductor composition suitable for RF power amplifiers is further discussed in Chapter 2.5.4.

2.3 Operating Regions of a Field Effect Transistor

The operating region of an active device is best understood by means of the voltage-current (V-I) characteristic curves of the device. Based on the bias conditions selected by the designer, it allows a visual representation of the boundary conditions of operation. We analyse the V-I characteristic curves of an N-channel power MOSFET, as per Figure 2., and we observe that there are three regions of operation. Namely, the active region, the ohmic region and cut-off region. Designers are guided by the specification and application of the required PA; these two factors determine the class best suited for the desired implementation.

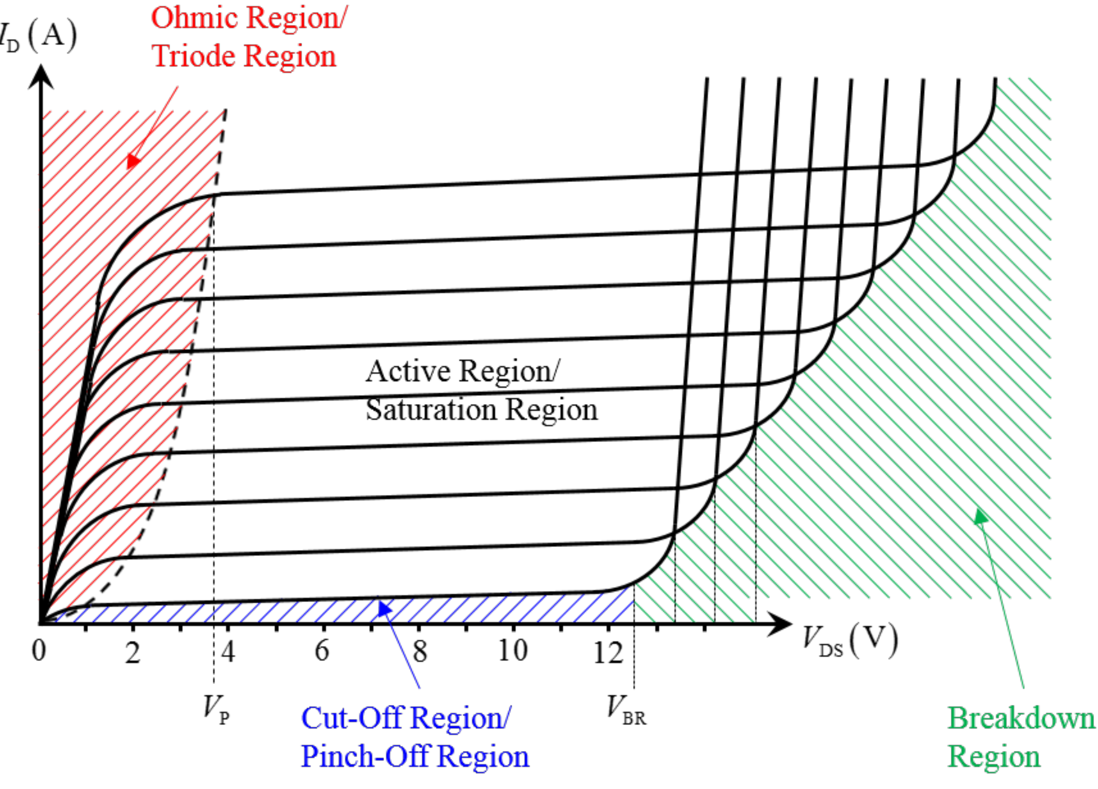

Figure 2.3: V-I Characteristics of a JFET

2.3.1 The Cut-Off Region

The MOSFET enters the cut-off region when the gate-to-source voltage, v_{GS}, is less than the threshold voltage, V_t of the device under scrutiny. When operating in the cut-off region, the

magnitude of the drain current i_D is negligible, thus the MOSFET is said to be “OFF” [5, p. 55].

2.3.2 The Active Region

In terms of FETs, the active region is also referred to as the saturation region. Very importantly though, this is not to be mistaken with the saturation region of a BJT. When a MOSFET is operated in the active region, the variation in drain current magnitude is minimal and of a linear nature, controlled by the gate-to-source voltage v_{GS}. We maintain a MOSFET in the active region by satisfying the following conditions and criteria [6, p. 33]:

$$v_{DS} > v_{GS} - V_t \quad \text{and} \quad v_{GS} > V_t \tag{2.3.2}$$

2.3.3 The Ohmic Region

The ohmic region is also at times referred to as the “triode region” or “the constant resistance region”. A FET behaves exactly like a constant resistance when it is operated in the ohmic region and this constant resistance represents the drain-to-source resistance of the device, denoted as $R_{DS(on)}$. $R_{DS(on)}$ is usually indicated on the manufacturer datasheet and can vary between a few milliohm $(m\Omega)$ to a few ohm (Ω), depending the device used [6, p. 33].

$R_{DS(on)}$ is linearly proportional to both, the drain-to-source voltage v_{DS} as well as the drain current i_D. The conduction power loss of a FET is determined by the drain current i_D and the value of $R_{DS(on)}$. We maintain a FET in the ohmic region by satisfying the following conditions and criteria [6, p. 33]:

$$v_{DS} < v_{GS} - V_t \quad \text{and} \quad v_{GS} > V_t \tag{2.3.3}$$

The FET is a voltage-controlled device in the sense that the amount of drain current flowing through the active device is controlled by the voltage drop across the gate-source junction, v_{GS}.

2.4 Operation Theory of RF Power Amplifiers

The output signal of a radio frequency (RF) power amplifier (PA) is referred to as the transmitted signal. The purpose of a RF PA is to amplify (increase) the power level of the transmitted signal such that the level of the received signal is at a suitable level above the noise floor to enable detection.

RF PA's implement amplification by converting the DC power applied to the PA into RF output power. Thus, the output signal of the PA is an amplified representation of the input signal. It is practically impossible to convert all the applied DC power into RF output power. Any DC power that is not converted into RF output power is dissipated as heat. This process is graphically illustrated in Figure 2.4.1.

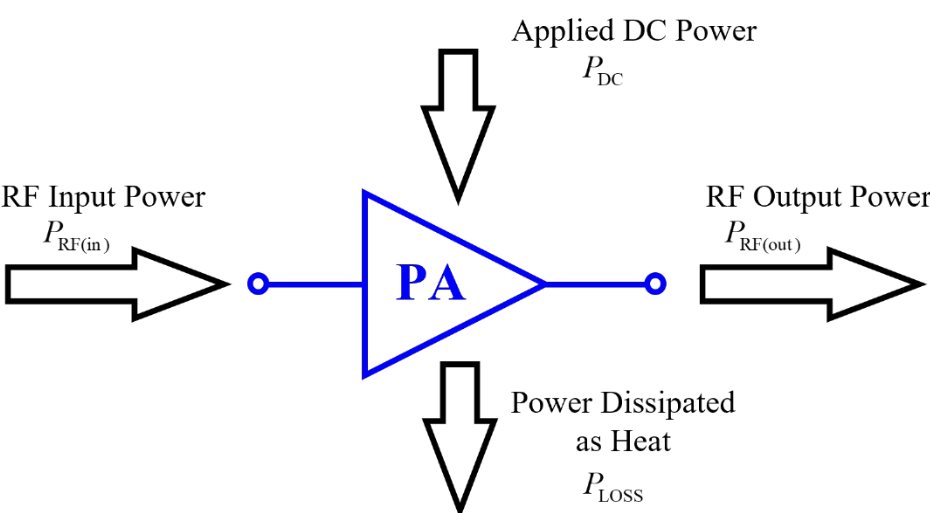

Figure 2.4.1: Energy Schematic of a PA (modified from Eroglu, 2018: 126)

To understand the function and operation of RF power amplifiers, it is important to introduce some fundamentals about the behaviour of a PA and the parameters that affect the behaviour and response of the amplifier.

In RF power amplifiers, the active device can be operated in three ways:

- as a switch
- as a dependant current or voltage source
- in overdriven mode (partially as a dependant current source and partially as a switch)

If the active device is driven by sinusoidal gate-to-source voltage v_{DS} of high amplitude, the active device is said to be overdriven. In such a case, the active device operates in the active region (as a dependant current source) when the instantaneous values of v_{GS} are low, and in the ohmic region (as a switch) when the instantaneous values of v_{GS} are high [7, p. 3].

The main function of the output network of the active device is:

- wave shaping for the voltage and current waveforms.
- impedance transformation.
- harmonic suppression.
- filtering of the spectrum of a signal with some bandwidth *BW*, to avoid interference with communication signals in adjacent channels [7, p. 3].

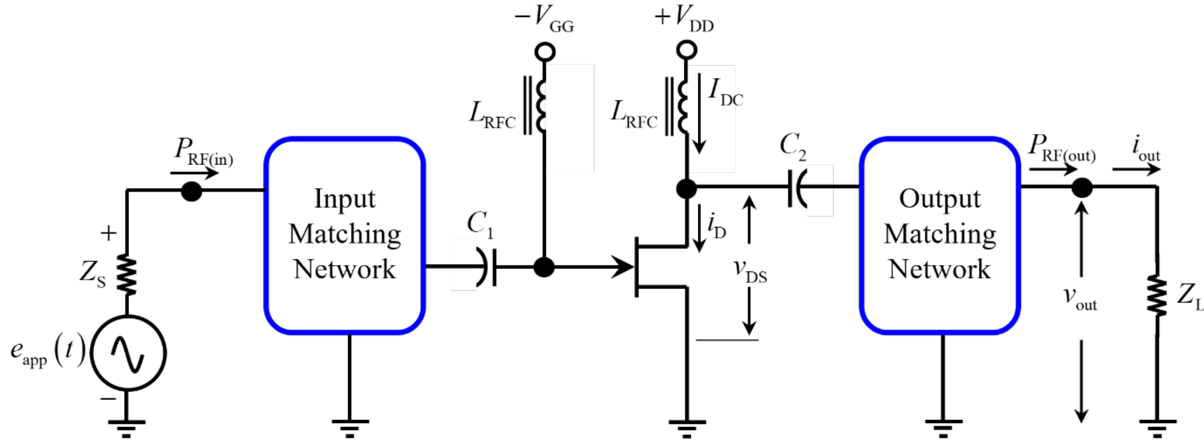

Figure 2.4.2: Simplified schematic of a power amplifier (modified from Colantonio *et al.*, 2009:178)

2.4.1 Operating the Active Device as a Switch

To operate a FET as a switch, the active device (FET) cannot enter the active region (also known as the pinch-off region). It is required that we maintain the device in the ohmic region when it is ON, i.e. the switch is closed, and in the cut-off region when the device is OFF, i.e. the switch is open [7, p. 2].

Maintaining a device in the ohmic region (in our case a GaN device), requires the following condition to hold true, $v_{DS} < v_{GS} - V_t$. By increasing the amplitude of gate-to-source voltage

v_{GS} for some given load impedance, the amplitude of the drain-to-source voltage v_{DS} will also increase. This will cause the active device to initially operate in the active region, and then in the ohmic region [7, p. 3]. For switch-mode operation, the magnitudes of the drain current i_{D} and the drain-to-source voltage v_{DS} are independent of the magnitude of gate-to-source voltage v_{GS}.

Operating at low RF frequencies, the gate-to-source voltage v_{DS} (which is used to drive the active device) is a rectangular waveform. At very high frequencies, a sinusoidal waveform is used for the gate-to-source voltage v_{GS}. This is because it is difficult to generate rectangular voltage waveforms at high frequencies [7, p. 3].

The sole purpose for using the active device (FET) as a switch is to achieve high efficiency of an amplifier. When the drain-to-source voltage v_{DS} is low, the active device conducts a high drain current i_{D} , and this results in low power loss [7, p. 3].

2.4.2 Operating the Active Device as a Current Dependant Source

When the active device is operated as a dependant current source, the waveform of the drain current i_{D} is determined by the operating point of the active device and the waveform of the gate-to-source voltage v_{GS}. The waveform of the drain-to-source voltage v_{DS}, is determined by the impedance of the load network (i.e. the impedance presented to the output port of the active device) and the dependant current source [7, p. 1].

Achieved by operating the device in the active region, also known as the saturation region in FETs and ensuring that it does not enter the ohmic region. We prevent the device from entering the ohmic region by keeping the drain-to-source voltage v_{DS} higher than its minimum value $V_{\mathrm{DS(min)}}$. In other words, $v_{\mathrm{DS}} > V_{\mathrm{DS(min)}} = V_{\mathrm{GS}} - V_{\mathrm{t}}$, where V_{t} is the threshold voltage of the active device [7, p. 1].

When the active device is operated as a dependant current source, the magnitude of the drain-to-source voltage v_{DS} and the drain current i_D are very nearly proportional to the magnitude of the gate-to-source voltage v_{GS}. Therefore, this type of operation (as a dependant current source) is very suitable for linear power amplifiers, where amplitude linearity is an important requirement [7, p. 2].

2.5 Classes of Operation of RF Power Amplifiers

RF/Microwave power amplifiers have designated classes of operation, namely class A, B, AB, C, D, E, F, inverse class E and inverse class F, class S, among others. There seems to be ambiguous definitions about the classes of operation of power amplifiers and how each class is actually defined. With reference to the traditional amplifier classes (class A, B, AB, C), they are implemented by selecting very specific biasing conditions for the active device. It is where the quiescent point (Q-point) lies on the DC load line of the active device that determines the class of operation. The Q-point is determined by the quiescent DC bias conditions of the active device [4, p. 24].

These traditional classes are sometimes defined in terms of the conduction angle of the active device. This definition can be misleading at times, since the conduction angle is ultimately a function of the RF input signal and not only dependent on bias conditions. Considering class A and B PAs, increasing the RF input power such that the active device is driven into compression (saturated or overdriven) will cause a decrease in the conduction angle. As for a class C, an increase in RF input power level will result in an increase in conduction angle [4, p. 23]. Figure 2.5 illustrates the Q-point for each of the traditional power amplifier operating classes.

More advanced power amplifier (PA) classes (class D, E, F, S, etc) were later developed to improve on amplifier characteristics like efficiency, linearity and output power (gain). These PA classes are defined by the operating conditions of the active device. i.e. whether the active device is operating as a dependant current source or as a switch. When using the active device as a current source, the PA is classed based on the harmonic suppression and wave-shaping of the output matching network (class F) [4, pp. 24-25].

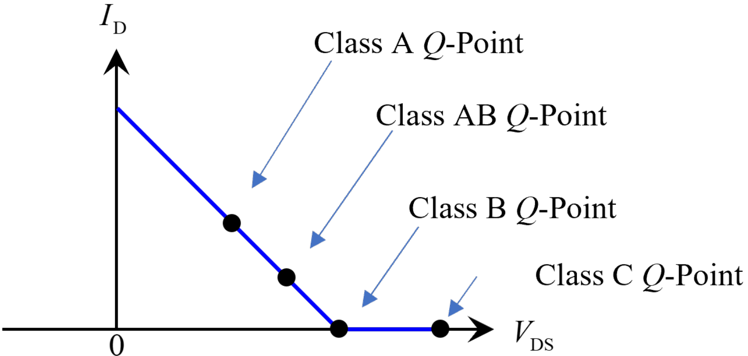

Figure 2.5: Quiescent Bias Conditions for Operating Classes (modified from Kazimierczuk, 2008: 4)

When the active device is operated as a switch, the PA is classed as either a class D, E, G, H or S. The distinction between each of these classes is defined by the switching duty-cycle and/or the switching combination of the active device [4, p. 25]. It is required that we build a suitable input matching and output matching network to meet the design requirements in terms of gain (output power), noise figure, efficiency, cost, etc [8, p. 185].

Classes of PAs are investigated where the fundamental standards and techniques implemented which categorize them are discussed. These categories guide the desired outcome of PA design, including the methodology and essential parameters that will be considered to achieve such.

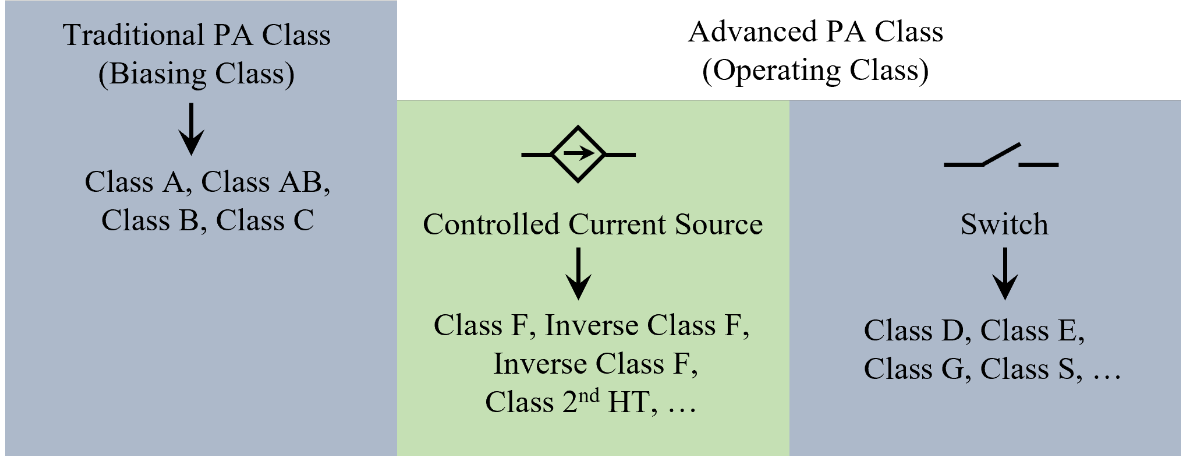

Figure 2.6: Summary of PA classification

2.5.1 Linear Power Amplifier Classes

Linear amplifiers are labelled such due to the fact they always operate within the linear constraints of the device under scrutiny. They are linear in the sense that the RF output signal is an amplified replica of the RF drive signal, and the magnitude of the drive signal is maintained to a level where the active device is never driven into compression or saturated [9] [7, p. 5]. Practically, linear amplifiers are analysed for small-signal applications where the RF output power consists mainly of power at the fundamental frequency as opposed to the large-signal analysis where RF output power consists of power at the harmonic components(integer values) of the fundamental frequency [10, pp. 5-12]. The traditional amplifier classes constitute the family of linear amplifiers. Namely, class A, B and AB. Class C amplifiers are vastly nonlinear and of a switching nature, however, certain texts still classify them as linear amplifiers.

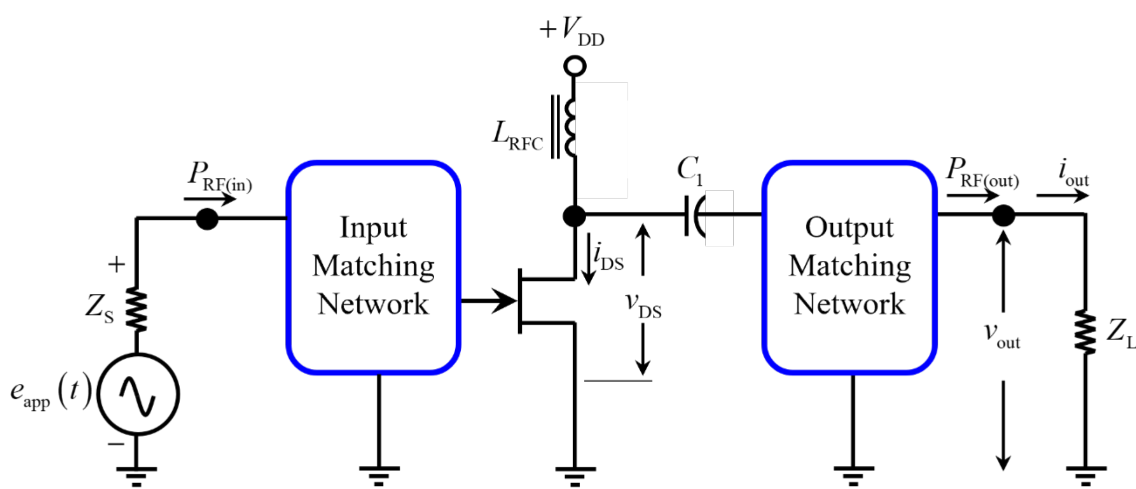

Figure 2.5.1: Simplified schematic of a linear power amplifier (modified from Colantonio *et al.*, 2009: 178)

2.5.1.1 Class A

Biased with the intention of allowing the active device to conduct for the full period ($360°$) of the RF input signal and ensuring that the power level of the drive signal does not exceed the boundary conditions of the active device, class A PAs are linear in the sense that the RF output signal is an amplified replica of the RF input signal provided [11, p. 18]. Limited to a maximum theoretical power efficiency (*PE*) of 50%, the applications for class A PAs are such where efficiency and power dissipation are not critical parameters. Commonly used for low output power applications.

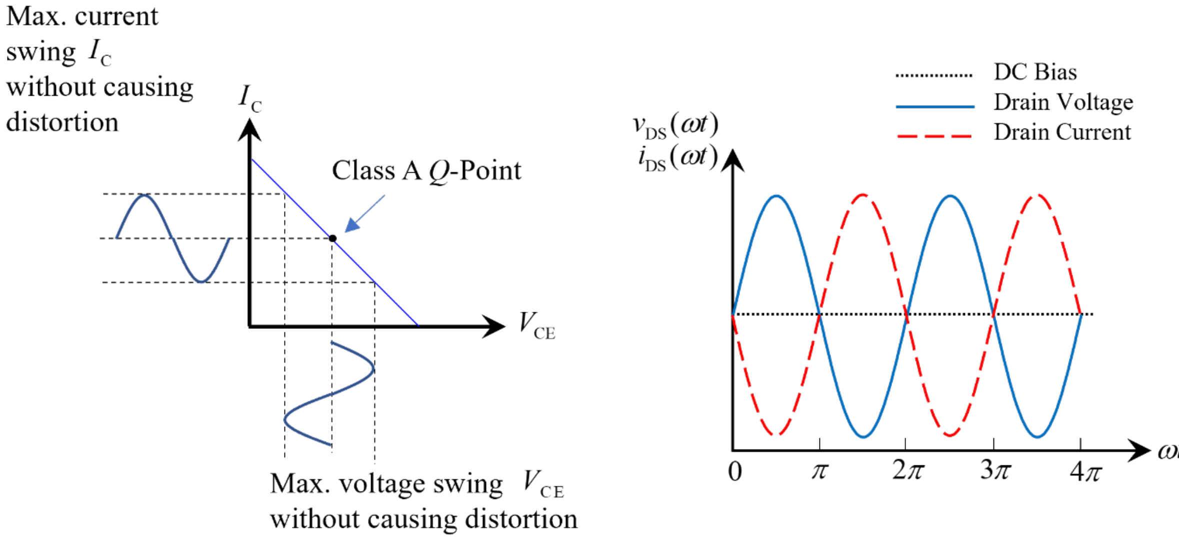

Figure 2.5.1.1: Drain voltage and current waveforms of an ideal class A PA (modified from Kazimierczuk, 2008)

The overlap between the drain voltage and the drain current waveforms, as illustrated in Figure 2.5.1.1, provides a graphical representation of why the maximum achievable *PE* is 50% for class A PAs. This means that 50% of the supplied DC power is radiated and dissipated through the active device, the heat sink and into the peripheral circuitry.

2.5.1.2 Class B

The active device of a class B PA is biased such that its operating point is at the boundary between the active region and the cut-off region. This reduces the conduction angle of the device to 180° of the RF input signal, resulting in a half-sine wave drain current waveform as opposed to a full sine wave drain current for the class A counterpart [7, pp. 75-77]. As illustrated in Figure 2.5.1.2, the overlap between the drain voltage and drain current waveforms is considerably reduced in comparison to the drain waveforms of a class A PA. This emphasises the improved power efficiency of a class B PA in comparison to a class A.

Theoretically, a *PE* of 78.5% can be achieved for a class B PA. Class B PAs are generally implemented in systems and designs where *PE* and output power level are more critical parameters than for class A PAs [12, p. 443].

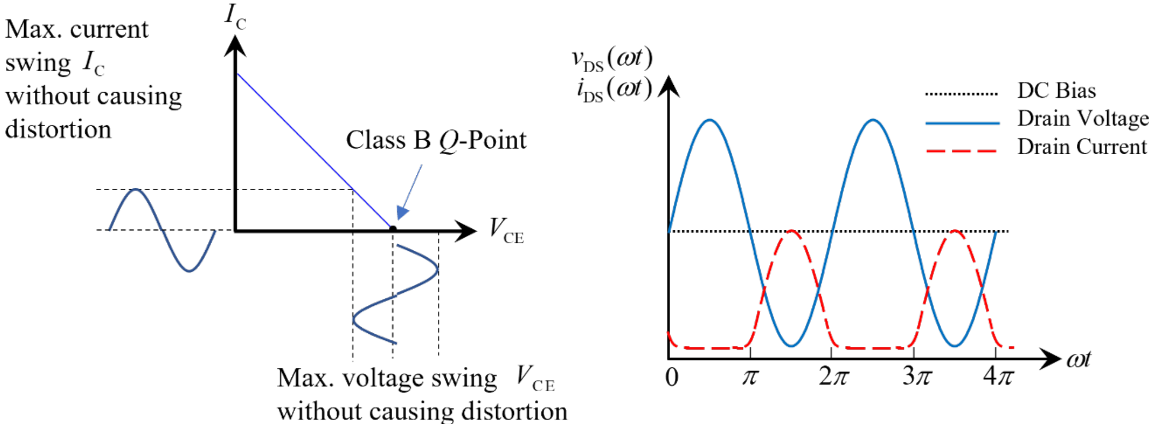

Figure 2.5.1.2: Drain voltage and current waveforms of an ideal class B PA (modified from Kazimierczuk, 2008)

2.5.1.3 Class AB

Class A PAs have an inferior *PE* in comparison to a class B PAs due to the increased overlap of the drain voltage and current waveforms, which is evident when comparing the two. Class B PAs have inferior linearity in comparison to class A PAs due to the reduced conduction angle of the active device.

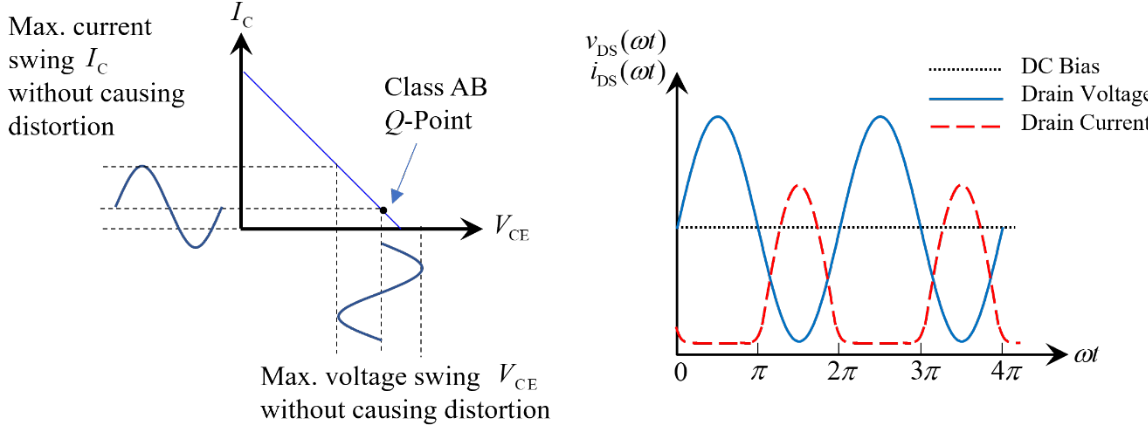

Figure 2.5.1.3: Drain voltage and current waveforms of an ideal class AB PA (modified from Kazimierczuk, 2008)

The class AB PA facilitates a compromise between *PE* and linearity with respect the boundary conditions of class A and class B operation respectively.

2.5.1.4 Class C

When operating a PA in class C, the active device is biased into the cut-off region such that the RF input signal drives the active device into conduction. This allows the active device to conduct for a percentage of one half of the period of the RF input signal, determined by the designer, or ultimately, by the signal bandwidth of the channel being transmitted along. An illustration of this drain waveforms is provided in Figure 2.5.1.4

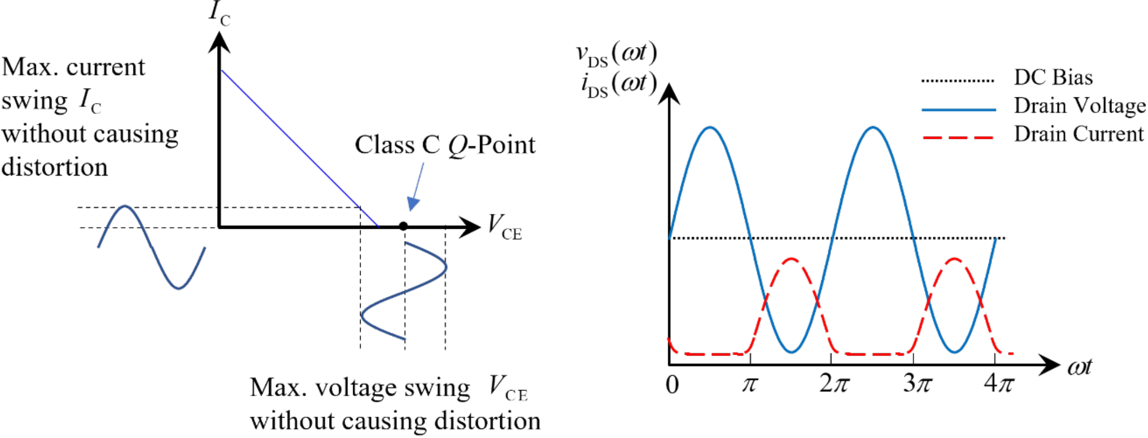

Figure 2.5.1.4: Drain voltage and current waveforms of an ideal class C PA (modified from Kazimierczuk, 2008)

This reduced conduction angle allows for achieving much greater *PE*s relative to class A and B PAs, due to the overlap between the drain voltage and drain current waveforms being considerably minimized. Class C PAs can ideally achieve *PE*s up 90%. However, for the same reason, due to the reduced conduction angle, the RF output power of a class C is constrained.

Class C amplifiers are vastly nonlinear and of a switching nature, however, certain texts still classify them as linear class amplifiers.

2.5.2 Synopsis of Linear Power Amplifiers

In summarising and with reference to Figure 2.5.2, we compare the different classes that constitute linear PAs with respect to RF output power and power efficiency as a function of the conduction angle of the active device [11, p. 46].

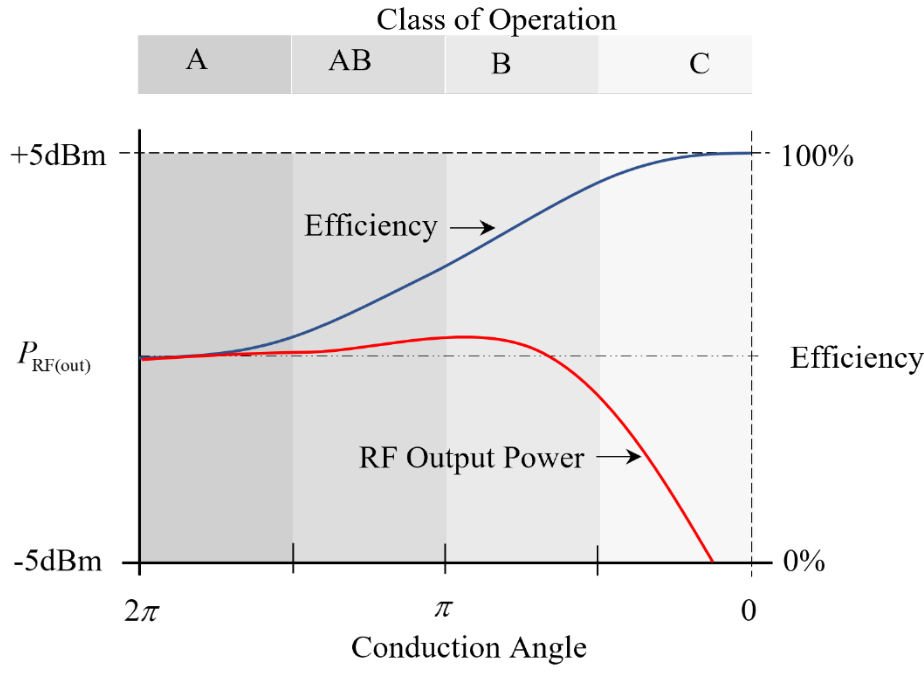

Figure 2.5.2: Comparison of linear class PAs

As illustrated, the RF output power achievable by the respective PA classes A, AB and B are similar. However, the *PE* increases due to the reduced conduction angle of the active device. The maximum achievable *PE* of a class C is substantially greater than classes A, AB and B, respectively, but the RF output power is considerably compromised when high *PE*s are trying to be achieved or implemented.

The *PE* of linear PAs varies with the respective classes (A, AB, B and C), some inferior to others. Similarly, the linearity of the respective PA classes varies, some inferior to others. Depending on the linearity requirements, a compromised can be made in *PE* in order facilitate the linearity requirements.

2.5.3 Switching Class Power Amplifiers

As the name suggests, switching power amplifiers are exactly that. A PA where the active device is operated as a switch. Dependant on the wave-shaping technique implemented and the bias conditions of the active device, switching PAs can further be categorised into class D, E, F and inverse class F. The nonlinear operation of switching PAs is due to power in the harmonics at the output port being considerably increased in comparison to linear PAs. The nonlinear nature of switching PAs allow for superior *PE* and reduced signal bandwidth to be achieved. However, this does not exclude other PA classes from being designed for narrow band operation.

2.5.3.1 Class D

There are many variants that exist, though the fundamental make-up of a class D PA is that it utilizes two active devices (operating as a half-bridge) or four active devices (operating as a full bridge) and a resonant circuit (series or parallel). Furthermore, class D PAs are categorized into voltage-switching and/or current-switching PAs based on the type of resonant circuit implemented at the output port of the PA [7, p. 109].

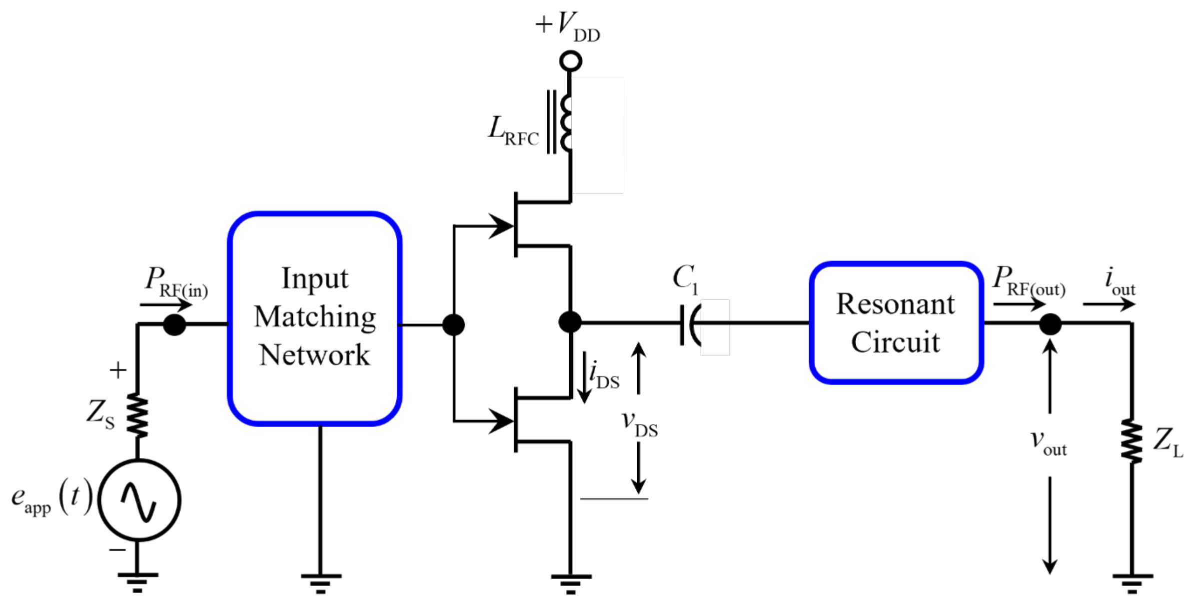

Figure 2.5.3.1: Simplified schematic of a class D PA with series resonant circuit

A simplified schematic of a class D PA with a series resonant circuit implemented at its output port, known as a voltage-mode class D (VMCD) is illustrated in Figure 2.5.3.1. Capacitor C_1 functions as a DC block.

A class D PA with a parallel resonant circuit implemented at its output port is known as current-mode Class D (CMCD). An illustration of such a PA is made in Figure 2.5.3.2. Capacitors, C_1 and C_2 function as DC blocking capacitors.

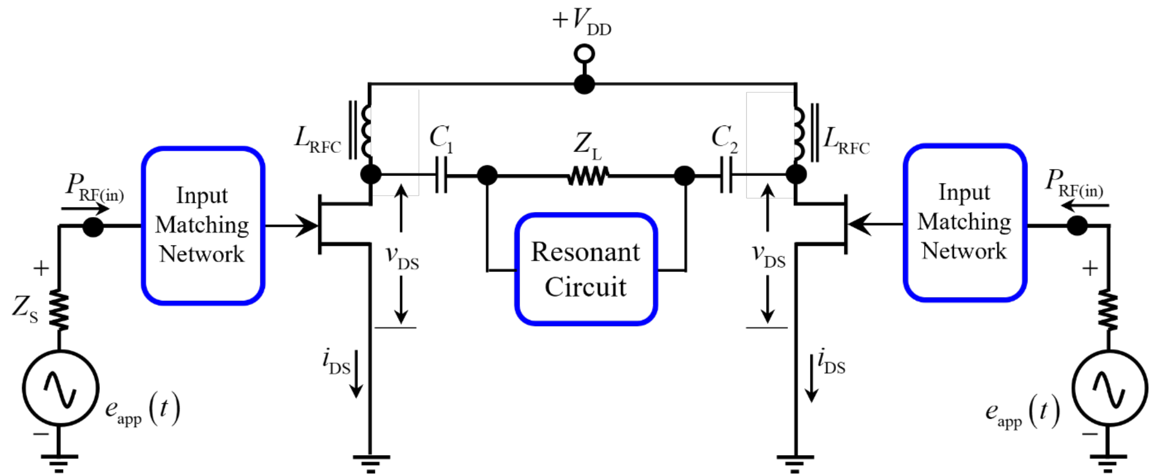

Figure 2.5.3.2: Simplified schematic of a current-mode class D (CMCD) PA

Theoretically, a *PE* of 100% is achievable with an ideal class D PA. With reference to Figure 2.5.3.3, zero overlap between the drain voltage and drain current waveforms of the active device allows for this resulting *PE* [9, p. 7] [13, p. 272].

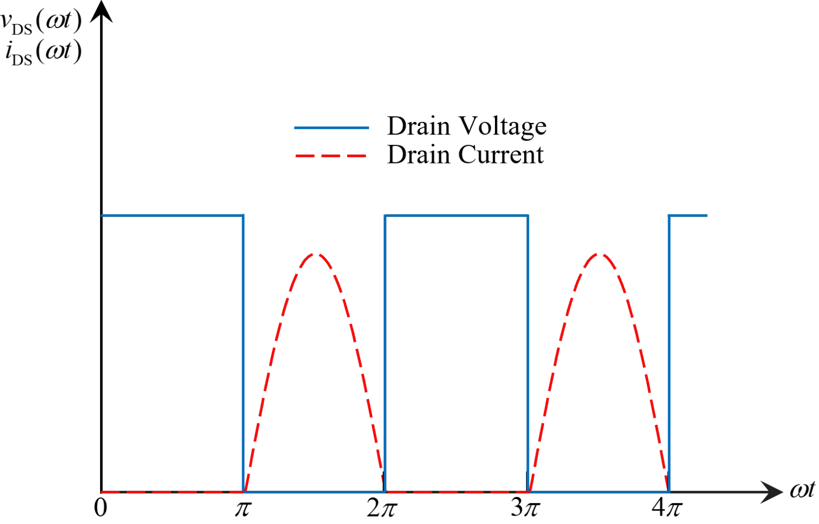

Figure 2.5.3.3: Drain voltage and current waveforms of an ideal class D PA (modified from)

One considerable advantage of the full bridge in comparison to the half bridge class D PA, is for the same given load impedance, Z_L, operating at the same frequency ratio, f/f_0 and operating at the same DC supply voltage, $+V_{DD}$, the RF output power is four times greater [7, p. 176].

2.5.3.2 Class E

An ideal class E PA offers a lot of simplicity with regards to circuit topology and allows an ease for analysis of operation when compared to other smitch-mode PAs. Furthermore, class E PAs are categorized as either a zero-voltage switching (ZVS) or a zero-current switching (ZCS) PA, based on when the active device is switched (with respect to zero drain voltage or zero drain current). An illustration of a simplified ideal class E PA is provided in Figure 2.5.3.4

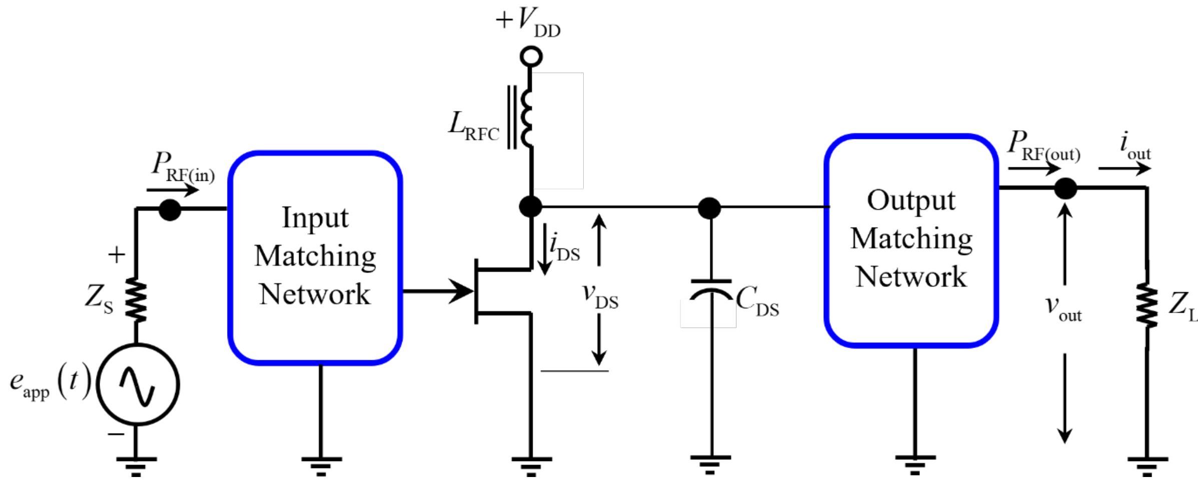

Figure 2.5.3.4: Simplified schematic of a class E PA

The drain-source capacitance, C_{DS}, connected in parallel with the drain of the active device, provides wave-shaping for the drain current. This drain-source capacitance, C_{DS}, is not to be mistaken with the intrinsic drain-source capacitance of the active device. The output matching network is effectively a series resonant circuit which terminates at harmonic frequencies, ensuring power transfer exclusively at the fundamental frequency. The intrinsic drain-source capacitance of the active device is a limitation on the maximum operating frequency of a class E PA.

The active device (switch) can be transitioned such that waveforms of the drain voltage and drain current have zero overlap. An example and illustration of this is provided in Figure 2.5.3.5 This reduces any switching losses experienced and minimizes power being dissipated into the active device and circuitry, resulting in higher power efficiency being obtainable [7, p. 180]. [8, p. 199].

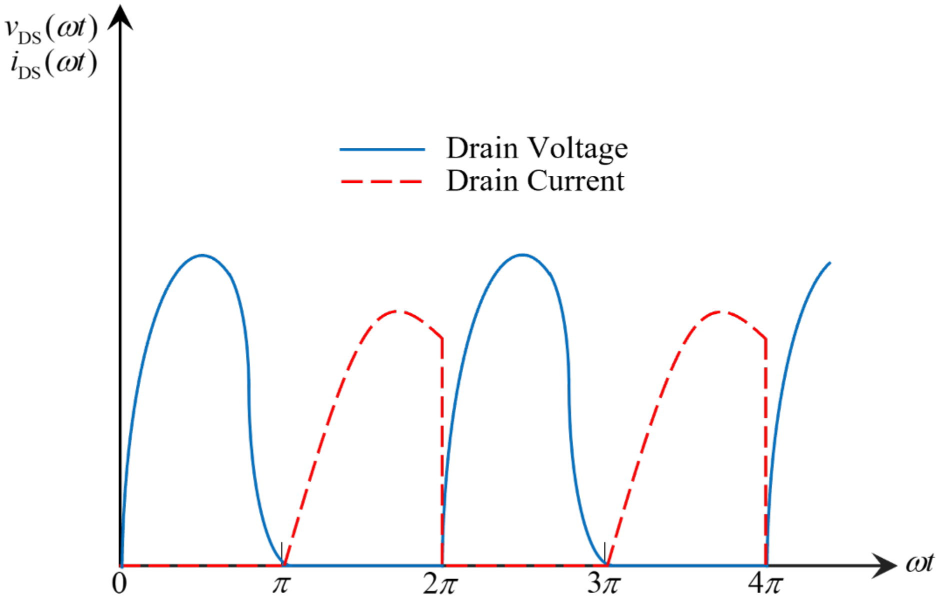

Figure 2.5.3.5: Drain voltage and current waveforms of an ideal class E PA (modified from)

2.5.3.3 Class F and Inverse Class F

The definition of a class F PA can be ambiguous since the DC bias conditions of the active device is effectively the same as class B. The fundamental difference between the two is the magnitude of the RF input signal, $P_{RF(in)}$. $P_{RF(in)}$ is substantially larger for class F than for class B, the result being power in the harmonic products can no longer be neglected. Figure 2.5.3.6 provides an illustration of a simplified class F PA.

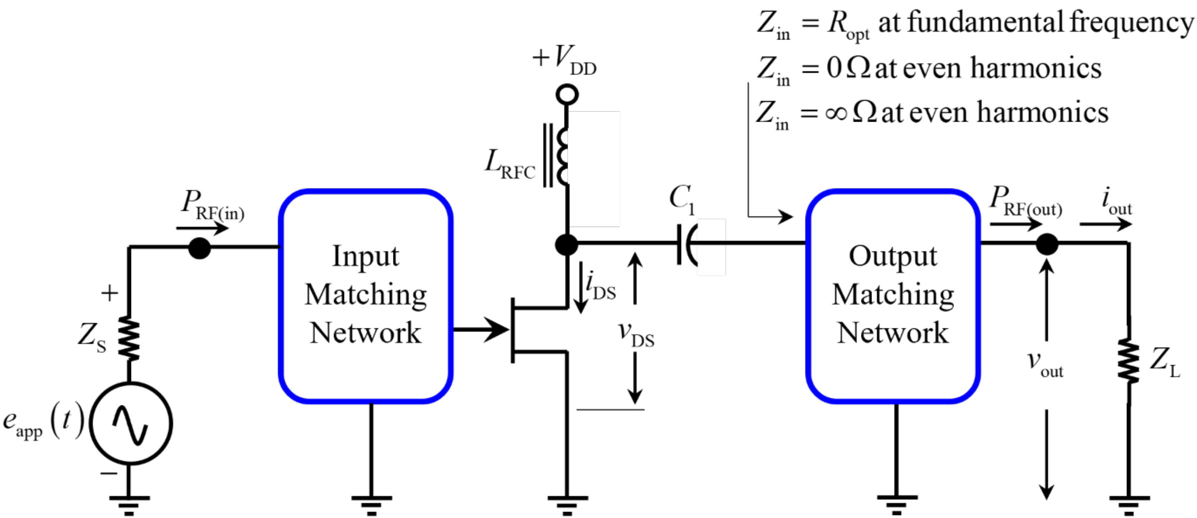

Figure 2.5.3.6: Simplified schematic of a class F PA

The drain waveforms of an ideal class F PA, as illustrated in Figure 2.5.3.7, comprises of an infinite number of the respective harmonic products. That is, the square-wave drain voltage comprises of an infinite number of odd harmonics and the half-sine wave drain current comprises of an infinite number of even harmonics [9] [10, pp. 51-53].

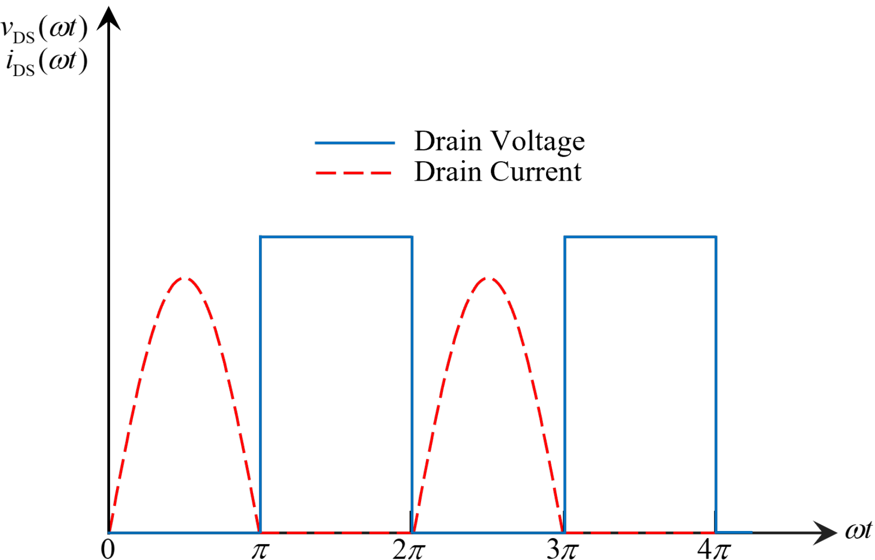

Figure 2.5.3.7: Drain voltage and current waveforms of an ideal class F PA (modified from)

The output network of a class F PA performs a duel function of wave-shaping for the drain waveforms, harmonic suppression for the harmonic products, impedance matching and phase correction for RF output signal, $P_{RF(out)}$ [8, p. 201]. The output network performing this duel

function is known as a “whip” network (wave-shaping, harmonic suppression, impedance matching and phase correction).

Class F and inverse class F PAs have an identical circuit topology other than the drain waveforms that are “inverse” to each other. That is, the drain voltage is a half-sine wave and the drain current is a square-wave for the inverse class F as opposed to the class F. The waveforms do not have the inverse magnitude of the other. The *PE* for both types of class F PAs is governed by the number of harmonics filtered by the output network, reaching more than 90% if the fifth harmonic is included.

2.5.4 Active Device Technology for RF Power Amplifiers

The choice of active device for any design of an RF PA is governed by the application and the design requirements. A given active device would be suitable for multiple applications, however the limitation of each device varies. For low to moderate output power applications, solid-state active devices are preferred to vacuum-tube amplifiers. Applications for high frequency operation requiring high output power from a single active device still prefer the use of vacuum tube amplifiers as opposed to solid-state devices [10, p. 16] [10, pp. 18-30].

It should be noted that the output power of multiple solid-state active devices operating at frequencies up to X-band, can be combined to achieve power levels that are equivalent to those achieved by vacuum tube devices. When considered within the boundary conditions of its operating frequency, the performance of a single active device can be measured with respect to the output power using the Pf^2 law. Figure 2.5.4. provides a comparison of various active devices suitable RF PAs implementing the Pf^2 law [4, p. 26].

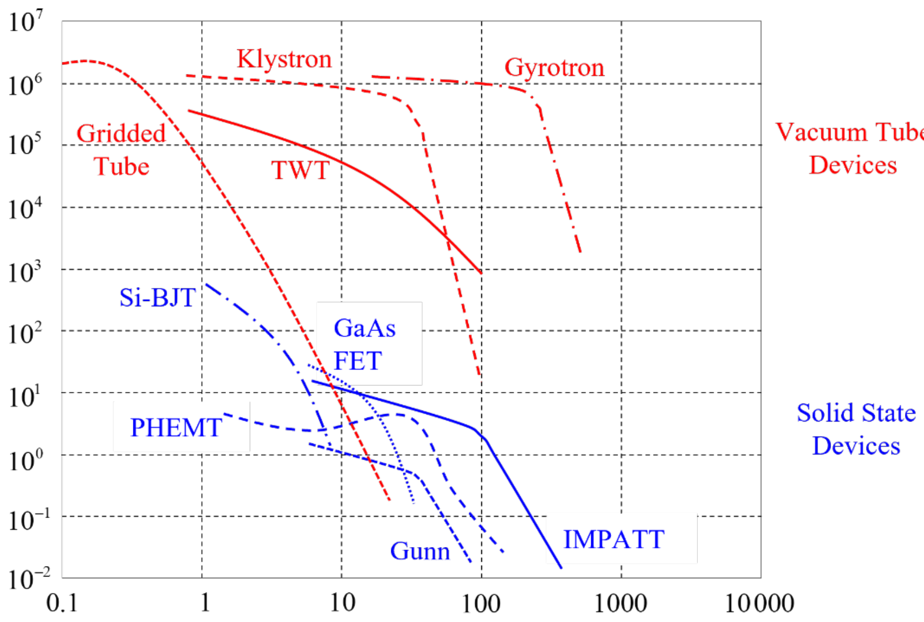

Figure 2.5.4: Output power of a single device as a function of frequency (modified from Colantonio *et al.*, 2008: 26)

Power amplifiers in satellite communication systems and base stations employ mainly four active device technologies. The two mature and established semiconductor technologies in this regard are GaAs FETs and silicone LDMOS FETs. GaN and SiC devices are no longer new semiconductor technologies and have gained considerable traction in RF PA design, in certain applications being favoured over GaAs and LDMOS devices [4, pp. 26-44].

Solid state active devices are designed with the intention of operating at either high frequency and low output power, or at low frequency and high output power, even more so with respect to RF and microwave applications. High frequency and high output power is difficult to achieve from a single solid state active device and vacuum tube devices are not very practical from a mobile or wireless perspective.

GaN HEMTs are widely used for the design of high efficiency PAs, predominantly from the switching class PAs since they are highly suitable for this function. While carrier mobility, current density and power density of GaN HEMTs are comparable with that of GaAs FETs, it is the high breakdown voltage of GaN HEMTs, the thermal dissipation and the dynamic range properties that make them favourable. Thus, they are highly suitable for PA design for satellite applications [14, p. 22]. Practically, a *PE* exceeding 80% is achievable with a switch-mode PA using a GaN active device, irrespective of the PA class [11, p. 172].

2.6 Performance Parameters of a Power Amplifier

The operation and performance of a PA can be defined and quantified by certain parameters. These parameters give us insight to the effectiveness of the amplification process relative to the power level of the input RF signal $P_{\mathrm{RF(in)}}$ .at a specific frequency, or within a frequency band, and is mathematically expressed as [4, p. 2]

$$P_{\mathrm{RF(in)}}(f) = \frac{1}{2}\mathrm{Re}\left\{V_{\mathrm{in}} I_{\mathrm{in}}^{*}\right\} \quad \mathrm{W} \tag{2.6}$$

2.6.1 Output Power

The output power of a PA, $P_{\mathrm{RF(out)}}$, is the power delivered to the external load. If the fundamental (operating) frequency and the resonant frequency of the output matching network are exactly the same (equal) then the load impedance is ideally 50 ohm, and is expressed as [4, p. 2] [7, p. 5],

$$P_{\mathrm{RF(out)}}(f) = \frac{1}{2}\mathrm{Re}\left\{V_{\mathrm{out}} I_{\mathrm{out}}^{*}\right\} \quad \mathrm{W} \tag{2.6.1}$$

2.6.2 Power Gain

The magnitude by which the input RF signal $P_{\mathrm{RF(in)}}$ has been amplified, regardless of the unit of measurement (W or dB), is referred to as the power gain. The power gain, which is a function of frequency, is expressed as [15, p. 312] [4, p. 2]

$$G(f) = \frac{P_{\mathrm{RF(out)}}(f)}{P_{\mathrm{RF(in)}}(f)} \tag{2.6.2}$$

The power gain G is a useful parameter when we consider linear amplifiers. That is, amplifiers where the active device operates within its linear “gain” region. The power gain of a PA is dependent on the power level of the RF input signal $P_{\mathrm{RF(in)}}$ and at low power levels (typically below 5 W, depending on the active device), PA’s exhibit linear behaviour. Therefore, these linear amplifiers are sometimes referred to as small-signal amplifiers, due to the low power level of the RF drive signal [16, p. 3] [4, p. 2]. This linear (small-signal) gain can be expressed as

$$G_{\text{L}}(f) = \lim_{P_{\text{RF(in)}} \to \infty} \left[G(f) \right] \tag{2.6.3}$$

By increasing the power level of $P_{\text{RF(in)}}$ such that the PA is driven into compression, $P_{\text{RF(out)}}$ tends to saturate and G tends to zero. This "gain compression or saturated gain" can be mathematically expressed as [4, p. 2] [14, p. 6]

$$\lim_{P_{\text{RF(in)}} \to \infty} \left[G(f) \right] = 0 \tag{2.6.4}$$

2.6.3 Power Conversion Efficiency

An important parameter to the overall performance of a PA, the *PE* of PA is a measure of the total applied DC power converted into RF output power. Depending on the active device, it is also referred to as the drain or collector efficiency, respectively. The *PE* can be mathematically expressed as [4, p. 4] [17, p. 2]

$$\eta = \frac{P_{\text{RF(out)}}}{P_{\text{DC}}} \times 100\% \tag{2.6.5}$$

In most transmission systems, and certainly with respect to portable devices (in this case a CubeSat), the PA is the fundamental consumer of DC power. The more efficient utilization of this resource will enable extended operation and battery lifetime and allows for consideration of a reduced power supply as a result of higher efficiency [4, p. 5].

2.6.4 Power Added Efficiency

Considering the typical performance of a PA as function of the input RF signal, yields Figure 2.6.4.

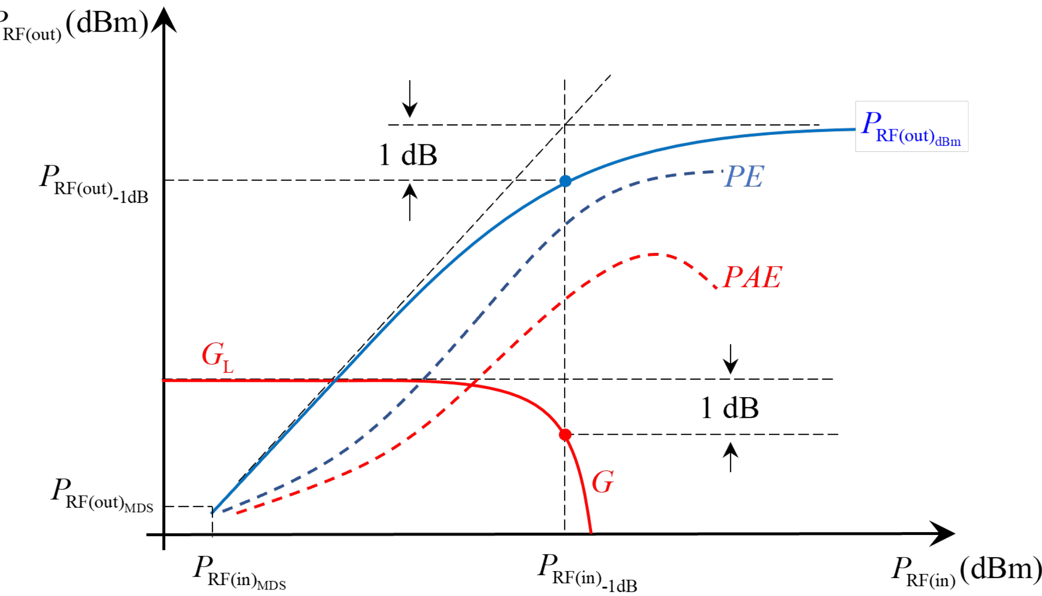

Figure 2.6.4: Performance of a PA as a function of RF input power (modified from Colantonio, 2009: 5)

For the linear region of the gain (i.e. where G remains constant and its magnitude is independent and unaffected by the magnitude of $P_{\text{RF(in)}}$), there is an exponential increase in the efficiency of the PA for any increase in $P_{\text{RF(in)}}$. However, due to the non-linear behaviour of any active device, there is a threshold where both G and P_{DC} are dependent on the magnitude of $P_{\text{RF(in)}}$. At this stage we will start experiencing gain compression and the efficiency of the PA will start saturating [4, p. 5].

Operating at microwave frequencies and above, a significant portion of the RF output power is directly as a result of the RF input power. For this reason, the RF input power, $P_{\text{RF(in)}}$, cannot be neglected when determining the overall efficiency of a PA. The net increase in the total signal power of a PA, considering the RF input signal is mathematically expressed as [16, p. 510]

$$PAE = \frac{P_{\text{add}}}{P_{\text{DC}}} = \frac{P_{\text{RF(out)}} - P_{\text{RF(in)}}}{P_{\text{DC}}} \qquad (2.6.6)$$

2.6.5 Linearity

Not to be confused with delineation. Defined by the following parameters, they all provide a measure of the linearity of the PA. The linearity of a PA is defined with respect to the range of

linear amplification of the system under test, where the RF output signal is experiences little to no distortion from mitigating factors.

2.6.5.1 Gain Compression (1 dB Compression)

The amplification process with respect to power amplifiers is extremely non-linear in its very nature, yet it is common to refer to the linear region the gain. It is this region where the RF output signal is an amplified replica of the RF input signal, and the magnitude is directly proportional to the magnitude of the RF input signal. An illustration of this is made in Figure 2.6.5.1. [18, p. 113].

The limitation of the active device causes the gain to saturate to a maximum value after the RF input signal power has been sufficiently increased. A measure to quantify the gain compression of a PA (and other amplifiers) is the 1dB compression point [8, p. 331]. With reference to the RF input power or the RF output power, the 1dB compression point is a measure where the gain G has saturated by 1dB from the linear amplification [19, p. 187] [14, p. 7].

The relation between $P_{\mathrm{RF(in)}_{\text{-1dB}}}$ and $P_{\mathrm{RF(out)}_{\text{-1dB}}}$ is governed by the linear power gain, G_{L}. Mathematically this relationship can be expressed as [4, p. 4]

$$P_{\mathrm{RF(out)}_{\text{-1dB}}} = (G_{\mathrm{L}} - 1\mathrm{dB}).P_{\mathrm{RF(in)}_{\text{-1dB}}} \tag{2.6.7}$$

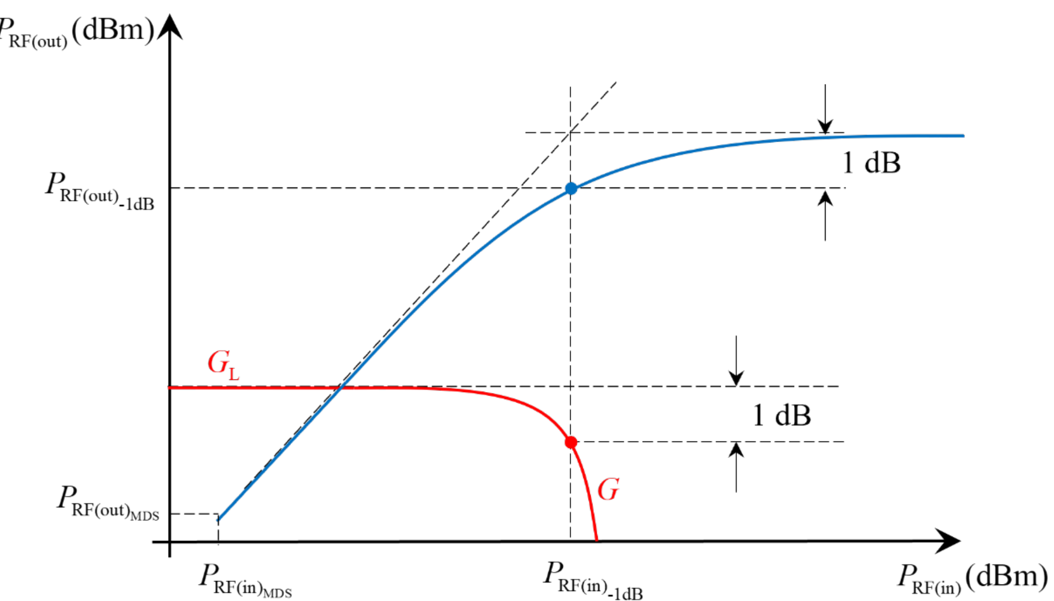

Figure 2.6.5.1: Illustration of the 1 dB compression point (modified from Colantonio *et al.*, 2009:3)

2.6.5.2 Third Order Intercept (TOI)

A hypothetical interception point where the power level of the ideal first order transfer function and the third order transfer function intersect. Well beyond the typical power level for drive signals for RF power amplifiers, the input power at the third-order intercept point allows for determining the level of intermodulation distortion (IMD) relative to the output signal of the PA [20, pp. 9-27].

The third order intercept (TOI) though hypothetical is crucial to determining the level of intermodulation distortion (IMD). The TIO occurs at the intersection of the first and third order transfer function power levels and used to determine an optimal power range in which the amplifier would not suffer any IMD. This power range is the difference between the output power of the PA at fundamental frequency and the IMD power level, known as the spurious-free dynamic range (SFDR).

A graphical representation of this is made in Figure 2.5.6.2

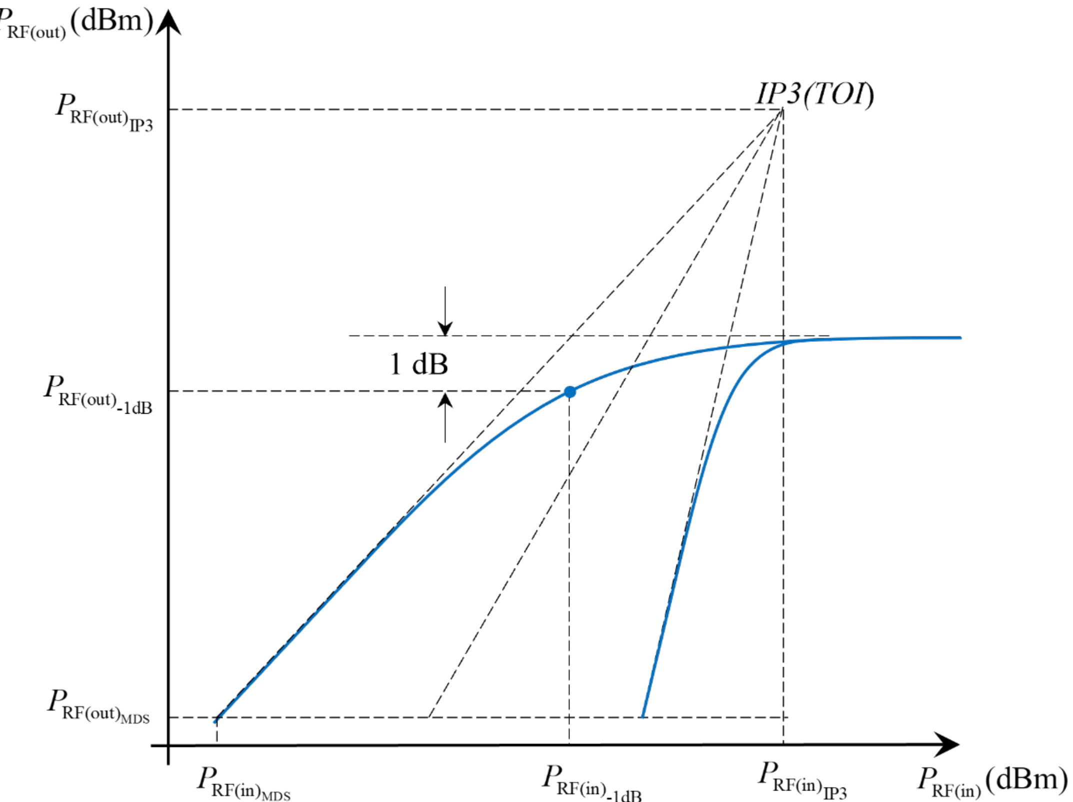

Figure 2.6.5.2: Illustration of the third-order intercept point (adapted from M. Golio et al., 2018: 9-25)

2.6.5.3 Carrier–to–Intermodulation Ratio

A measure of the power ratio between the output of the PA at the fundamental frequency and the power of the IMD products, the carrier-to-intermodulation ratio provides another measure of the linear behaviour of the PA. It is common to measure this quantity using logarithmic units, usually in decibels below the carrier (dBc) [4, p. 14] and is expressed as

$$C/I \,\square\, \frac{P_{\mathrm{RF(out)}}}{P_{\mathrm{IMD}}} \tag{2.6.8}$$

2.6.5.4 Spurious Free Dynamic Range (SFDR)

The dominant contributor to signal distortion in power amplifiers is the third-order intermodulation product. The range of linear operation of a PA can therefore be defined as the range for which $P_{\mathrm{RF(out)}}$ is unaffected by the magnitude of P_{IMD}. This variation of $P_{\mathrm{RF(in)}}$ for which the power level of the intermodulation distortion product P_{IMD} remains below the noise floor is known as the spurious free dynamic range [4, p. 15].

2.6.5.5 Adjacent Channel Power Ratio (ACPR)

As opposed to single-tone or two-tone linearity testing for power amplifiers, the adjacent channel power ratio (ACPR) accounts for a more real-world approach in the sense that the RF input to a PA substantially varies from a single-tone excitation. Modulation scheme, signal bandwidth and the bandwidth occupation may substantially vary from the single-tone counterpart. Numerous definitions exist for the adjacent channel power ratio, though it is with reference to the total ACPR that is standardised. This is the ratio between the total RF output power in the signal bandwidth and the total RF output power in the adjacent channels [4, p. 15].

2.6.5.6 Error Vector Magnitude (EVM)

Defined as the difference between the measured signal and an ideal reference signal, the EVM is a measure of the distortion to digital signals as a result of the PA. Graphically represented in Figure 2.6.5.6. Mainly dependant on the modulation scheme used as well as the standard followed, NADC and PDC are examples of modulation schemes that use the error vector magnitude. GSM modulation techniques make use of phase and frequency errors to measure the quality of modulated signals.

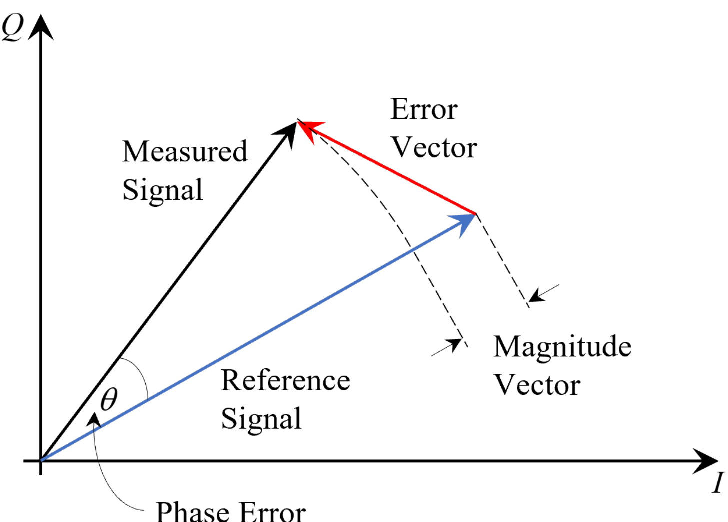

Figure 2.6.5.6: Error vector magnitude and dependant quantities (modified from Colantonio *et al.*, 2009:3)

2.7 Design Techniques and Principles

The technique and fundamental design tools implemented for any PA design is ultimately governed by the type of PA required. The tools and techniques applied may be identical in certain design cases and vastly different in others. Irrespective of the simplicity (or complexity) of the technique, the objective is to manipulate the nonlinear behaviour of the PA, resulting in the maximum achievable output power at some *PE*, or the maximum achievable *PE* at some output power level. It is important to note that these two parameters are not simultaneously achievable [21, pp. 12-16].

This inherently means within the linearity requirements of the modulation scheme utilized, without which, extraction of the information embedded within the signal cannot be successfully accomplished. A few fundamental techniques exist which provide a good basis for the design of a PA and provide insight to the limits of the active device under scrutiny [10, pp. 1-3].

2.7.1 Load-Line Theory

Pre-dating computer aided design (CAD) methods, load-line theory is a useful technique in predicting the performance of a linear PA. Not very suitable as a design technique for switch-mode PAs, and even with respect to linear PAs, the assumption is that the transistor is ideal [11, pp. 21-26].

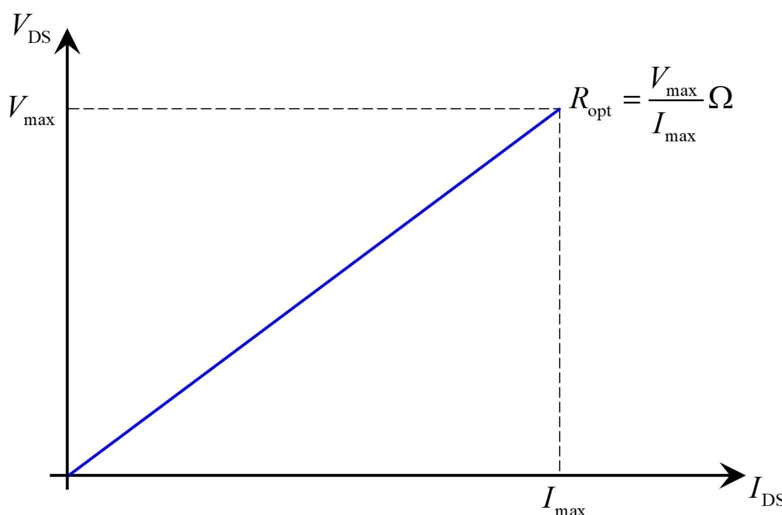

Figure 2.7.1: Illustration of the load-line technique (modified from MacPherson & Whaits, 2007: 14)

As illustrated in Figure 2.7.1, the optimum resistance of a given active device can be determined using the load-line theory. Maximum power will be transferred to the output port of an active device, granted that the output port of that device is terminated by its optimum resistance value [21, pp. 12-16].

The performance of a PA, in its most basic definition, generally refers to the output power level and the *PE* at a specific frequency, assuming an ideal active device. When making this assumption the knee voltage of the active device is equal to zero volts. Practically, this is not the case for most active devices. A good measure of the load-line theory and its effectiveness in estimating the performance of a given active device, is to evaluate the ratio of the knee voltage and the maximum drain voltage of that device [14, p. 21].

2.7.2 Load-Pull Technique

The load-pull technique, implemented in a few ways, is a method of determining the optimum impedance to be presented at the output port of the active device which enables optimum performance with respect to output power, *PE* or *PAE*. Maximum output power and maximum *PE* are not simultaneously achievable, however, a compromise can be made between the two parameters such that the design requirements are met. The load-pull method is a plot of the output power, the *PE* and the *PAE* at a selected operating frequency, while varying the output impedance.

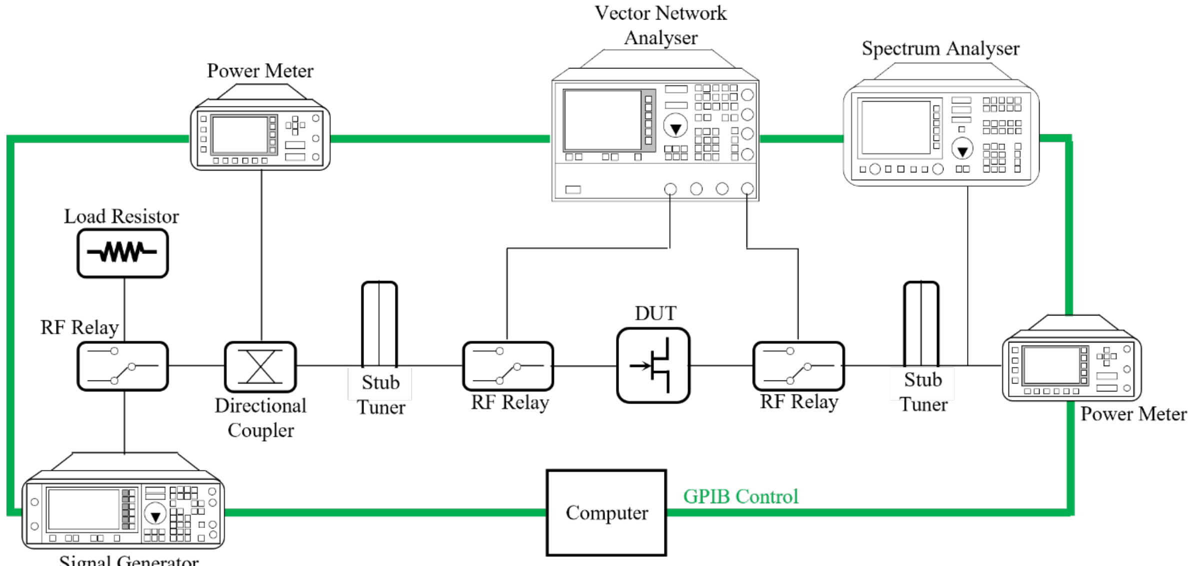

Figure 2.7.2: Load-pull measurement and equipment setup (modified from ...)

This allows for determining the impedance terminations which enables the maximum achievable *PE* or the maximum achievable output power, respectively. A measurement setup for the load-pull method is illustrated in Figure 2.7.2. This setup allows for direct measurement of the transistor and provides a full characterisation of the transistor in terms of *PE*, output power and all other parameters affecting the performance. In many ways regarded as the most effective way of testing a transistor, it eliminates any assumptions or extrapolations about the transistor. The limitation on implementing this technique is the cost and availability of the test equipment required. The testing procedure could be regarded as a complex one but by no means a limitation.

Another way of implementing the load-pull technique is by computer-aided design (CAD). Eliminating the need for expensive test equipment and with a measurement process less complex, this method does however compromise the accuracy of the measurements. The reason for this being, simulation of the load-pull data requires a large-signal model of the active device, as per manufacturer request. These transistor models differ vastly from a practical device, in the sense that, impedances for linear operation and impedances at large-signal operation are extrapolated (mathematically modelled and predicted) as opposed to physically being measured. This inconsistency may lead to a degradation in *PE* in a manufactured prototype, varying from the simulations [4, p. 191].

The load-pull data can also be obtained using a Smith-chart. By means of mathematical formulation, non-circular contours can be plotted on a Smith-chart and the impedance values for optimum operation can be determined. The nonlinear behaviour of the active device should be accounted for in the non-circular contours, making this method suitable for the design of nonlinear PAs [11, p. 221].

Nonlinear PAs consist of portions of the output power at harmonic frequencies, thus, the load-pull data at harmonic frequencies need to be measured in order to account for the optimum impedances required at these frequencies. Failure to do so will result in sub-optimum performance of the PA.

2.8 Conclusion

Comparing the various amplifier types and classes shows the capabilities and performance of each type of amplifier. Linear PAs are limited to a maximum *PE* dependant on the class of amplifier and the conduction angle of the active device but can achieve superior output power levels to its non-linear counterparts. Linear PAs are assumed to deliver negligible levels of power to the load at harmonic frequencies due to the transistor operating in its linear region. Reducing the conduction angle of the transistor improves the *PE*, however this affects the maximum achievable output power of the PA.

Non-linear PAs or switching PAs operate by using the transistor as a switch. This reduces the conduction angle of the transistor and limits the overlap between the voltage and current waveforms which decreases the power dissipated in the switch. This considerably increases the *PE* of the PA. However, switching PAs have limitations in terms of operating frequency and complexity of circuitry due to the requirement of harmonic suppression at integer multiples of the fundamental frequency.

The parameters that determine and measure the performance of a PA vary depending on the class and type of PA. For this reason, the performance parameters are discussed generally as opposed to focusing on the class-E only.

Chapter 3

Class-E Power Amplifiers with Shunt Capacitance

Class E PAs and many variants thereof, have been proposed and developed with the objective of improving *PE* and increasing RF output power. Applicable to many switch-mode PAs and different classes, class E power amplifiers satisfy the necessary criteria for achieving a maximum theoretical *PE*. A brief history and the evolution, the operation, the conditions required to facilitate optimum performance and a few variants of the class E will be discussed. Analysis and waveforms in this thesis are illustrated under the assumption a FET is used as the active device, but theory and operation is applicable other types of active devices too.

3.1 Introduction

One of the earliest proposals of the class E power amplifier was made by N. Sokal in 1975. Striving to achieve higher efficiencies from a single device, the proposed class E (Sokal) was fitting to the name switch-mode PA, in the sense that the active device is constantly being transitioned between the “on” and “off” states, operating as a switch. The output network fundamentally consisted of a shunt capacitor and a series resonant circuit resonating at the fundamental frequency. An illustration of the circuit is made in Figure 3.1 [22, p. 185].

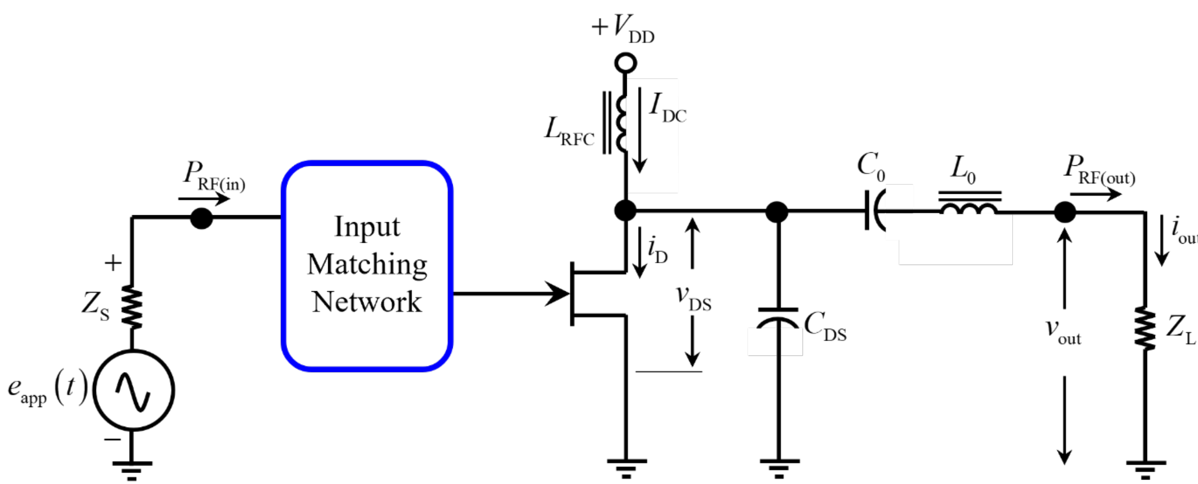

Figure 3.1: Schematic of a low-order class E PA (modified from Sokal, 2003: 31)

The high efficiency of the class E PA is attributed to the power dissipation within the active device being very low. The voltage across the FET and the current that flows through it for a given switching transient period, can be controlled by the designer. That is, both can have zero magnitude during the switching period [22, p. 180]. During the period of the RF input signal, the FET will be subject to high voltage and high current, though it can be ensured that these entities do not exist simultaneously. This is achieved through circuit manipulation such that the product of the two entities is low at each point during the RF period. Figure 3.2 graphically illustrates this concept [23, pp. 2-6].

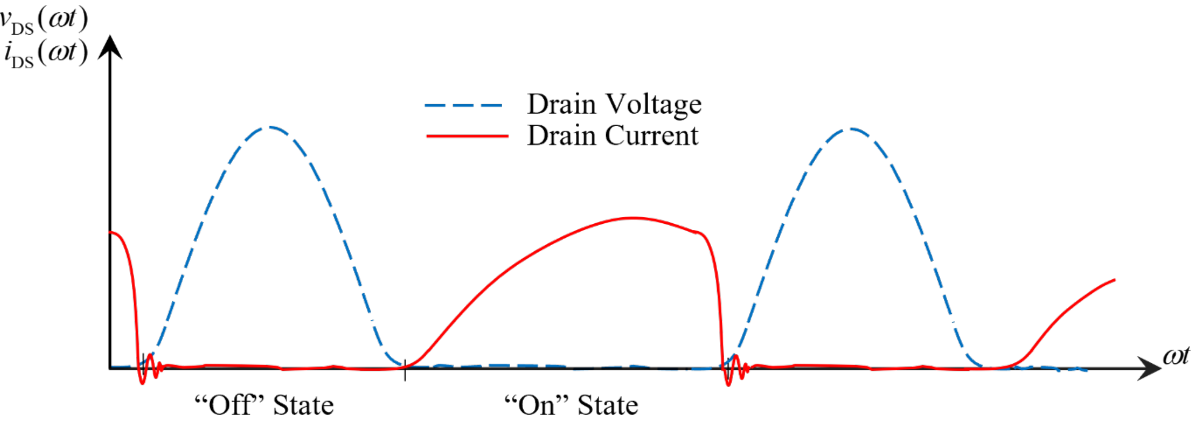

Figure 3.2: Drain waveforms of FET in low-order class E PA (modified from Sokal, 2003: 31)

3.2 Switching Transitions of the Active Device

Theoretical and practical analysis of the switching transitions of an active device are vastly different. In most cases, theoretical analysis assumes ideal conditions, a few of which are mentioned in 3.3. However, the practical limitations of the device should be considered when designing for high efficiency at RF and microwave frequencies [23, p. 3].

- The "On" State: The drain current rises to a maximum and decreases to a minimum while the drain voltage remains almost zero volt for the entire period the switch is conducting. The FET behaves as a low impedance "on" switch for the conduction period. This conduction period is only a small percentage of the RF signal period.
- The "Off" State: The drain voltage rises to a maximum and decreases to a minimum while the drain current remains almost zero ampere for the entire period the switch is open. The FET behaves like a high impedance "off" switch when the FET is not conducting [23, p. 3].

The parameters of the output network are obtained by applying the idealized conditions mentioned in 3.3, which are necessary for realizing an optimized operation of a class E with shunt capacitance. Bearing this in mind, the parameters are determined by considering the "on" and the "off" state of the FET in isolation to each other [22, p. 182].

3.3 Assumptions for Theoretical Analysis

Assuming some ideal conditions can greatly assist in presenting a circuit realizable or not, and theoretical analysis of a PA is less complex when these assumptions are introduced. With reference to switch-mode PAs [22, pp. 181-187]:

- It assumed that the FET is an ideal switch. That is, the saturation voltage, $V_{\text{sat}} = 0\,\text{V}$.
- The saturation resistance, $R_{\text{sat}} = 0\,\Omega$.
- In its "off" state, the resistance of the switch is infinite ohm.
- There are zero losses dissipated in the switch during the switching transition and that the switching action is instantaneous.
- All RF chokes have zero resistance and permit only a constant DC current.
- The shunt capacitance is independent of the source terminal of the FET and considered to be linear with respect to frequency.
- Circuit components exhibit zero losses and maximum power is transferred to the load.
- For realizing optimum operation of a class E PA, a duty cycle of 50% is assumed.

Presuming the above-mentioned is true, realizing a lossless amplifier requires some optimum and necessary conditions to exist. One such condition: *t=T* is the time moment the switch closes, where *T* is the RF period. At this moment [24, p. 3466],

$$v_{\text{DS}}(t)\big|_{t=T} = 0 \tag{3.3}$$

$v_{\text{DS}}(t)$ being the drain-source voltage of the FET with respect to time. Another such condition:

$$\left.\frac{dv_{\text{DS}}(t)}{dt}\right|_{t=T} = 0 \tag{3.4}$$

This implies that the drain-source capacitor has completely discharged and no increase in drain current will be experienced.

A lossless, optimum operation as described above is applicable to switch-mode PAs with any duty cycle (i.e. saturation time). However, the extent realizing such operation is governed by the loaded quality factor, Q_L of the "WHIP" network. Smaller duty cycles require larger values of Q_L to realise a sinusoidal drain current waveform [23, p. 5].

Illustrated to emphasise that even upon introducing these assumptions, the operation and output waveforms generated are non-ideal and design parameters should account for this. Considering the FET as an ideal switch and simulating at the operating frequency of 1 GHz, yields the following drain waveforms, as per Figure 3.3.

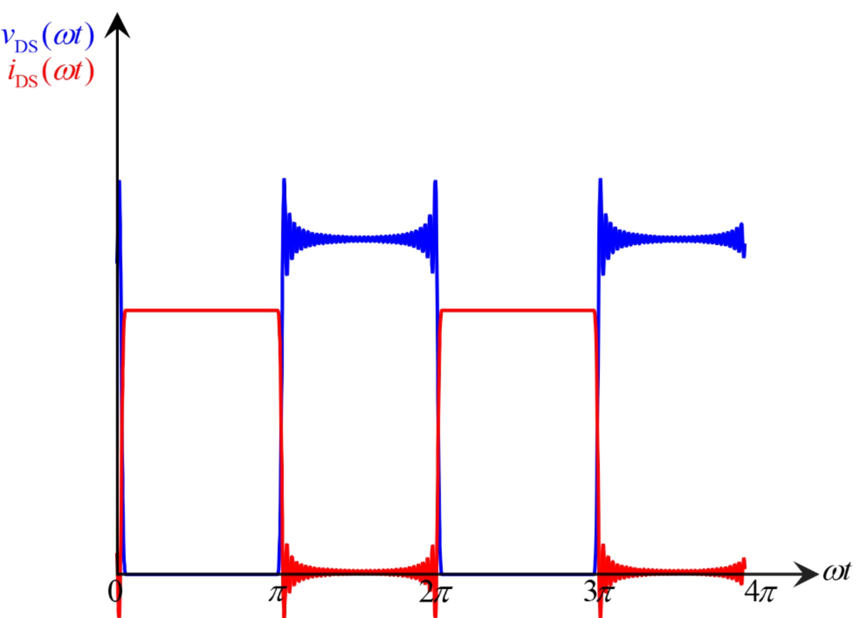

Figure 3.3: Waveforms of ideal switch model

3.4 Limitations on Maximum Achievable *PE*

Theoretically, a maximum drain efficiency of 100% is achievable with a class E PA, provided that the conditions mentioned in 3.3 are presented and fulfilled. Though these conditions are necessary, they are insufficient for achieving a *PE* of 100%. The limitation in this respect lies in the respective voltage and current harmonics not being exactly 90° out of phase [4, p. 225].

The parasitic components of a given active device, namely the drain-source capacitance (C_{DS}), lead inductance (L_{out}) and the impedance presented at the output port of the device also limit the maximum *PE* and this becomes more evident at higher operating frequencies. In addition to this, for some selected current value, the minimum voltage within the device is slightly above the knee voltage (V_{knee}) of that device, reducing the *PE* [14, p. 33].

3.5 Maximum Operating Frequency Before Experiencing Degradation

An optimum class-E PA is limited to a maximum frequency of operation to realize such before degradation in efficiency is realized. We therefore establish a relationship between certain circuit parameters $(f_{max}, C \text{ and } V_{DD})$ in order to determine up to which frequency we can extend this operation. We start establishing such a relationship by substituting equation (3.5) into equation (3.6), which results in [22, p. 190]. It is important to note that the maximum operating frequency will vary dependant on the choice of the active device. Degradation in PE will be experienced when operating above this frequency threshold, irrespective of the choice of active device

$$\omega CR = 0.1836 \tag{3.5}$$

$$\therefore R = \frac{0.1836}{\omega C}$$

$$I_0 = 0.5768\frac{V_{DD}}{R} \tag{3.6}$$

$$\begin{aligned} \therefore I_0 &= 0.5768\frac{V_{DD}}{\left(\frac{0.1836}{\omega C}\right)} \\ &= 0.5768\left(\frac{V_{DD}\omega C}{0.1836}\right) \\ &= \frac{0.5768}{0.1836}V_{DD}\omega C \\ &= 3.1414V_{DD}\omega C \end{aligned}$$

$$\therefore I_0 = \pi V_{DD}\omega C \tag{3.7}$$

Bearing in mind the relationship between I_0 and $I_{\max}$ (where I_0 = dc supply current and $I_{\max}$ = peak drain current) given in equation (5.28), the maximum operating frequency $f_{\max}$ for an optimum class-E with shunt capacitance can be determined as [22, p. 190],

$$f_{\max} = \frac{1}{\pi^2} \frac{1}{\sqrt{\pi^2+4}+2} \frac{I_{\max}}{C_{\text{out}} V_{\text{DD}}} = \frac{I_{\max}}{56.4995 C_{\text{out}} V_{\text{DD}}} \qquad (3.8)$$

where $C = C_{\text{out}}$ is the device output capacitance limiting the maximum operating frequency of an ideal class-E PA [25, p. 1393].

Using the relationship, we established between $f_{\max}$, C and V_{DD}, we determine I_0,

$$I_0 = \pi V_{\text{DD}} \omega C \qquad (3.7)$$

where $C = C_{\text{out}} = 1.3\,\text{pF}$, as per datasheet for the active device in this study.

$$I_{\max} = 2.8621 I_0 \qquad (3.9)$$

Thus, $f_{\max}$ is determined as,

$$f_{\max} = \frac{1}{\pi^2} \frac{1}{\sqrt{\pi^2+4}+2} \frac{I_{\max}}{C_{\text{out}} V_{\text{DD}}} \qquad (3.8)$$

Table 4.1 illustrates the degradation of efficiency for operation above $f_{\max}$. Theoretically, an efficiency of 100% is achievable for a large range of frequencies below $f_{\max}$.

$f/f_{\max}$	$\omega L/R$	$V_{\max}/V_{\text{DD}}$	$\eta_{\max}$ (%)
1.000	1.152	3.562	100
1.259	1.330	3.189	99.59
1.585	1.053	2.981	96.96
1.995	0.852	2.789	92.16
2.512	0.691	2.632	85.62
3.162	0.561	2.519	77.87

Table 3.5: Suboptimum operation of a class-E PA above $f_{\max}$ (adapted from Grebbenikov & Sokal, 2007:191)

3.6 Conclusion

The basic concept of being able to realize a functional class-E PA has been illustrated. As a switching PA and more specifically as a class-E PA with shunt capacitance, certain conditions are to be satisfied at the switching transitions of the active device to achieve the desired conduction period of the switch (based on the designers selected duty cycle) and maximum possible *PE*.

The condition of the voltage across the switch being equal to zero and the drain-to-source capacitance of the active device being completely discharged are fundamental factors to the operation of a class-E PA and to improving its *PE*.

The chapter concludes with the limitation of the class-E operation. If high efficiency is required at high frequency operation, the designer would want to consider other PA types or classes. If this is not achievable, a compromise would have to be made on power efficiency versus output power at the desired operating frequency.

Chapter 4

The Design of a Class-E PA with Shunt Capacitance

The primary objective (and hopefully in most cases) in PA design is to maximize the power added efficiency and power conversion efficiency. The design method concentrates on presenting the optimum loading conditions, both at the input port and output port of the active device

4.1 Specifications

The specifications for PA to be designed is as follows (revised from the class-E presented by [22]:

- $PE \geq 80\%$ at 1 GHz
- $PAE \geq 75\%$ at 1 GHz
- $P_{\mathrm{RF(out)}} \geq 35\,\mathrm{dBm}$ at 1 GHz

4.2 Choice of Active Device

The active device selected for this study is the Wolfspeed Cree CGH40010F GaN HEMT. The manufacturer has willingly provided linear and non-linear models for Advanced Design System (ADS) and samples of the active device upon request. A photograph of the active device is shown below, Figure 4.2.

Figure 4.2: The Wolfspeed Cree CGH40010F GaN HEMT

4.3 DC Biasing

For an ideal class-E operation, the active device should be biased near or into the cut-off region of the active device, depending on the input drive signal and the desired duty-cycle. In this study, the bias conditions were selected at a drain-to-source voltage $V_{DD} = 28\,\mathrm{V}$ and drain current $I_D = 202\,\mathrm{mA}$, as illustrated in Figure 4.3. The quiescent bias conditions are selected based on the maximum electrical characteristics of the active device as per datasheet as well as the typical performance as provided by the manufacturer.

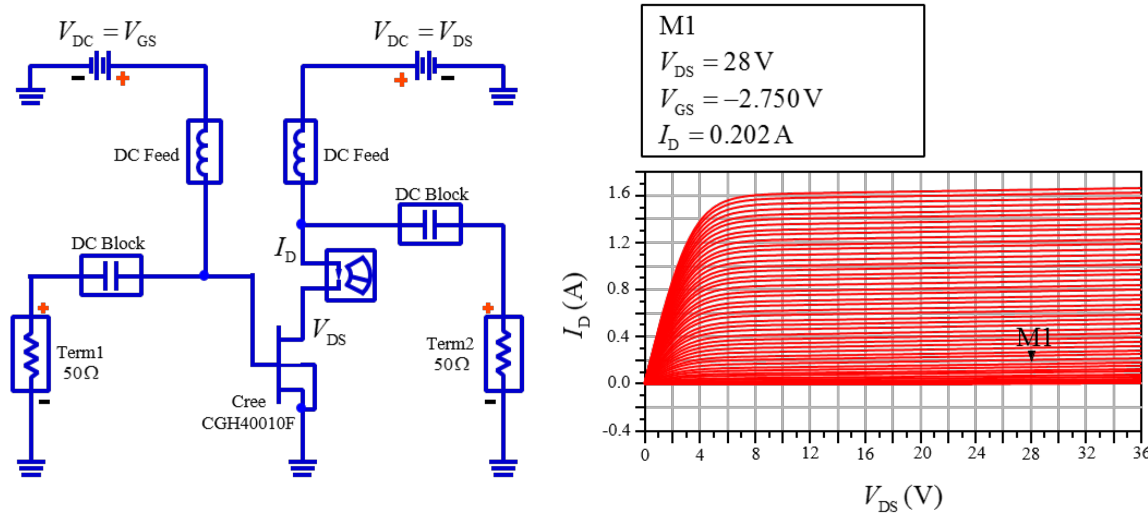

Figure 4.3: Choice of quiescent operating point

4.4 Design Procedure

The PA is designed using a lumped element proto-type and we then transform the lumped element circuit into a transmission-line equivalent. The design procedure includes but are not limited to the following steps [22, p. 215].

1. Determining the optimum load network conditions for an ideal class-E operation (optimum load impedance *R*, shunt capacitance *C* and series inductance *L*) bearing in mind that we design according to specific circuit parameters, V_{DD} .and $P_{RF(out)}$.
2. Design the output network (using lumped elements) to match the optimum load impedance *R* to the standard load impedance of $50\,\Omega$ at the fundamental frequency, at the same time providing sufficient harmonic suppression.
3. While carefully observing the impedances of the higher order harmonics, transform the lumped element circuit into a transmission-line equivalent.

4. Simulate the circuit design using ADS to analyse and validate the correct class-E operation.
5. Transform the transmission line equivalent circuit into a distributed microstrip layout.

4.4.1 Determining the Optimum Load Network Conditions

By applying the first condition to realize an ideal class-E operation, given by equation (3.3), we determine the phase angle as,

$$V_{\text{max}} = -2\pi\varphi V_{\text{DD}} \tag{4.4}$$

where,

$$\begin{aligned}\varphi &= \tan^{-1}\left(\frac{-2}{\pi}\right) \\ &= -32.482° \\ &= \left(-32.482°\right)\left(\frac{\pi}{180}\right) \\ &= -0.5669\,\text{radians}\end{aligned} \tag{4.5}$$

Thus,

$$\begin{aligned}V_{\text{max}} &= -2\pi\varphi V_{\text{DD}} \\ &= -2\pi(-0.5669)V_{\text{DD}} \\ &= 3.5619V_{\text{DD}}\end{aligned} \tag{4.6}$$

and

$$\begin{aligned}I_{\text{max}} &= \left(\frac{\sqrt{\pi^2+4}}{2}+1\right)I_0 \\ &= 2.8621I_0\end{aligned} \tag{4.7}$$

Now, considering the breakdown voltage of the active device $\left(V_{\text{BR}} = 120\,\text{V}\right)$, the maximum voltage will be limited to

$$\begin{aligned}V_{\text{max}} &= 3.5619V_{\text{DD}} \\ 120 &= 3.5619V_{\text{DD}} \\ \therefore V_{\text{DD(max)}} &= \frac{120}{3.5619} \\ &= 33.6899\,\text{V}\end{aligned} \tag{4.8}$$

Based on specific circuit parameters V_{DD} and $P_{\mathrm{RF(out)}}$, we determine the optimum load impedance *R* as follows,

$$R = \frac{8}{\pi^2 + 4} \cdot \frac{V_{\mathrm{DD}}^2}{P_{\mathrm{RF(out)}}} = 0.5768 \frac{V_{\mathrm{DD}}^2}{P_{\mathrm{RF(out)}}} \qquad (4.9)$$

To achieve the desired output power of 5 W, an ideal value of *R* is determined as

$$\begin{aligned} R &= \frac{8}{\pi^2 + 4} \cdot \frac{V_{\mathrm{DD}}^2}{P_{\mathrm{RF(out)}}} \\ &= 0.5768 \frac{V_{\mathrm{DD}}^2}{P_{\mathrm{RF(out)}}} \\ &= 0.5768 \left[\frac{(28)^2}{5} \right] \\ &= 90.4422\ \Omega \end{aligned} \qquad (4.9)$$

The optimum shunt capacitance C and series inductance L are determined using equations (4.10) and (4.11).

$$\frac{\omega L}{R} = \frac{V_{\mathrm{L}}}{V_{\mathrm{R}}} = 1.1525 \qquad (4.10)$$

$$\omega C R = \frac{\omega C}{I_{\mathrm{R}}} V_{\mathrm{R}} = 0.1836 \qquad (4.11)$$

Therefore, operating at a fundamental frequency of 1 GHz,

$$\begin{aligned} \frac{\omega L}{R} &= \frac{2\pi\left(1\times10^9\right)L}{90.4422} \\ &= 1.1525 \\ \therefore L &= \frac{(1.1525)(90.4422)}{2\pi(1\times10^9)} \\ &= 16.5886\,\mathrm{nH} \end{aligned}$$

An optimum class-E PA is limited to a maximum frequency of operation to realize such before degradation in efficiency is realized, as discussed in 3.5. Applying the device and circuit parameters for this study, we determine the maximum theoretical operating frequency for the selected active device.

$$\begin{aligned} f_{\max} &= \frac{1}{\pi^2} \frac{1}{\sqrt{\pi^2+4}+2} \frac{I_{\max}}{C_{\text{out}} V_{\text{DD}}} \\ &= \frac{I_{\max}}{56.4995 C_{\text{out}} V_{\text{DD}}} \end{aligned}$$

where $C = C_{\text{out}}$ is the device output capacitance limiting the maximum operating frequency of an ideal class-E PA [25, p. 1393]. Using the relationship, we established between $f_{\max}$, C and V_{DD}, we determine I_0,

$$\begin{aligned} I_0 &= \pi V_{\text{DD}} \omega C \\ &= \pi (28) 2\pi (1\times10^{9})(1.3\times10^{-12}) \\ &= 718.5072\,\text{mA} \end{aligned}$$

where $C = C_{\text{out}} = 1.3\,\text{pF}$, as per datasheet.

$$\begin{aligned} I_{\max} &= 2.8621 I_0 \\ &= (2.8621)(718.5072\times10^{-3}) \\ &= 2.0564\,\text{A} \end{aligned}$$

Thus, $f_{\max}$ is determined as,

$$\begin{aligned} f_{\max} &= \frac{1}{\pi^2} \frac{1}{\sqrt{\pi^2+4}+2} \frac{I_{\max}}{C_{\text{out}} V_{\text{DD}}} \\ &= (101.3212\times10^{-3})(174.6972\times10^{-3}) \left(\frac{2.0564}{(1.3\times10^{-12})(28)} \right) \\ &= 1\,\text{GHz} \end{aligned}$$

We are therefore operating at $f_{\max}$ (i.e. The fundamental frequency is equal to $f_{\max}$). Table 3.5 on page 41 illustrates the degradation of efficiency for operation above $f_{\max}$.

The optimum shunt capacitance C we calculate from equation (4.11),

$$\omega CR = 0.1836$$

$$\therefore C = \frac{0.1836}{\omega R}$$

$$= \frac{0.1836}{2\pi\left(1\times10^{9}\right)\left(226.1056\right)}$$

$$= 129.2354\,\text{fF}$$

4.4.2 Load Network Design

The output network is required to transform the optimum load impedance of $90.4422\ \Omega$ to the standard impedance of 50Ω at the fundamental frequency and provide sufficient harmonic suppression at integer multiples of the fundamental frequency. A π-matching network is decided upon due to the high loaded Q $\left(Q_{\text{L}}\right)$ requirement and three-element matching networks are suitable for high Q_{L} circuits, where $Q_{\text{L}} \geq 10$ [21, pp. 2-9]

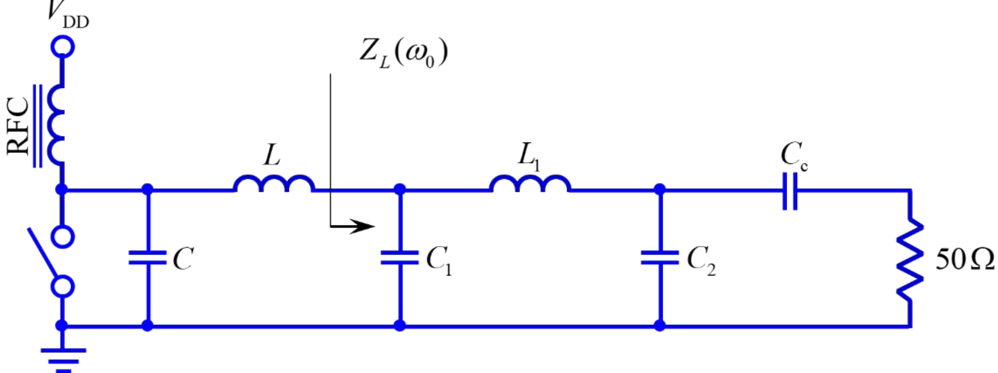

Figure 4.4.2.1: Class-E equivalent circuit

We start designing the π-network by splitting the circuit into two back-to-back L-networks with aid of a virtual resistor, R_{V}, as illustrated in Figure 4.4.2.2.

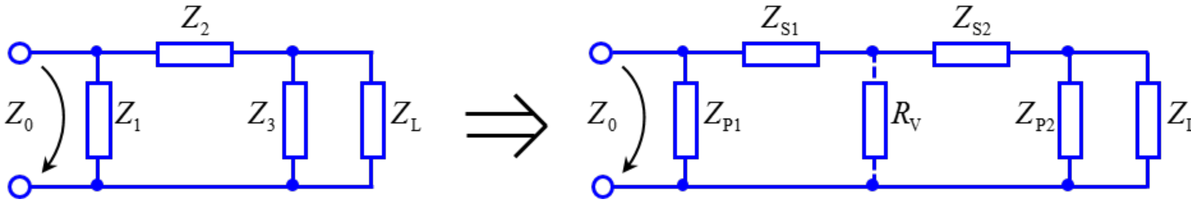

Figure 4.4.2.2: Splitting the pi-network

We design for $Q_L = 10$. R_V is determined from the L-section on the load side using equation (2.1),

$$Q_L = \sqrt{\frac{R_L}{R_V} - 1} \qquad (4.12)$$

$$\therefore 10 = \sqrt{\frac{90.4422}{R_V} - 1}$$

$$\therefore (10)^2 = \frac{90.4422}{R_V} - 1$$

$$\therefore R_V = \frac{90.4422}{101} = 0.8955\,\Omega$$

The magnitudes of Z_{S2} and Z_{P2} are determined as follows,

$$\begin{aligned} |Z_{S2}| &= Q_L . R_V \\ &= (10)(0.8955) \\ &= 8.9547\,\Omega \end{aligned} \qquad (4.13)$$

and

$$\begin{aligned} |Z_{P2}| &= \frac{R_L}{Q_L} \\ &= \frac{90.4422}{10} \\ &= 9.0442\,\Omega \end{aligned} \qquad (4.14)$$

We apply the same procedure to the source section, where

$$\begin{aligned} Q_S &= \sqrt{\frac{R_S}{R_V} - 1} \\ &= \sqrt{\frac{50}{0.8955} - 1} = 7.4050 \end{aligned} \qquad (4.15)$$

The magnitudes of Z_{S1} and Z_{P1} are determined as follows,

$$\begin{aligned} |Z_{S1}| &= Q_S . R_V \\ &= (7.4050)(0.8955) \\ &= 6.6312\,\Omega \end{aligned} \qquad (4.16)$$

and

$$|Z_{P1}| = \frac{R_S}{Q_S} = \frac{50}{7.4050} = 6.7522\,\Omega \quad (4.17)$$

For a low-pass configuration, combining the two series inductive reactance values, the π-network can be represented as per Figure 4.4.2.3.

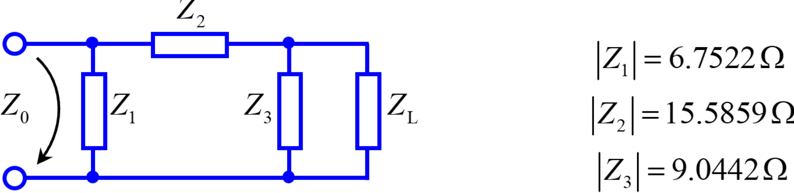

Figure 4.4.2.3: Pi-network with relevant reactance values

Determining the component values from the corresponding reactance values calculated above, the equivalent class-E circuit can be realized and is illustrated in Figure 4.4.2.4.

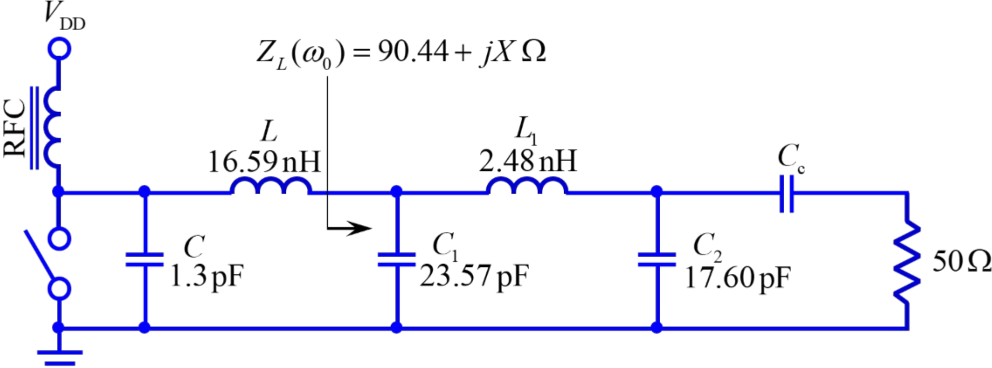

Figure 4.4.2.4: Realizable class-E amplifier

The following step in the design procedure is to convert the lumped element circuit into a transmission-line equivalent.

4.5 Load Network Simulation Results

The input and output return loss of the designed load is simulated by S-parameter simulation using Advanced Design Systems (ADS) by Agilent. The simulation is run over a frequency sweep from 0 - 5 GHz, illustrating the power transfer at the fundamental frequency. The simulation results show a good match between the optimum impedance presented to the output of the active device and the actual load impedance of 50 ohm.

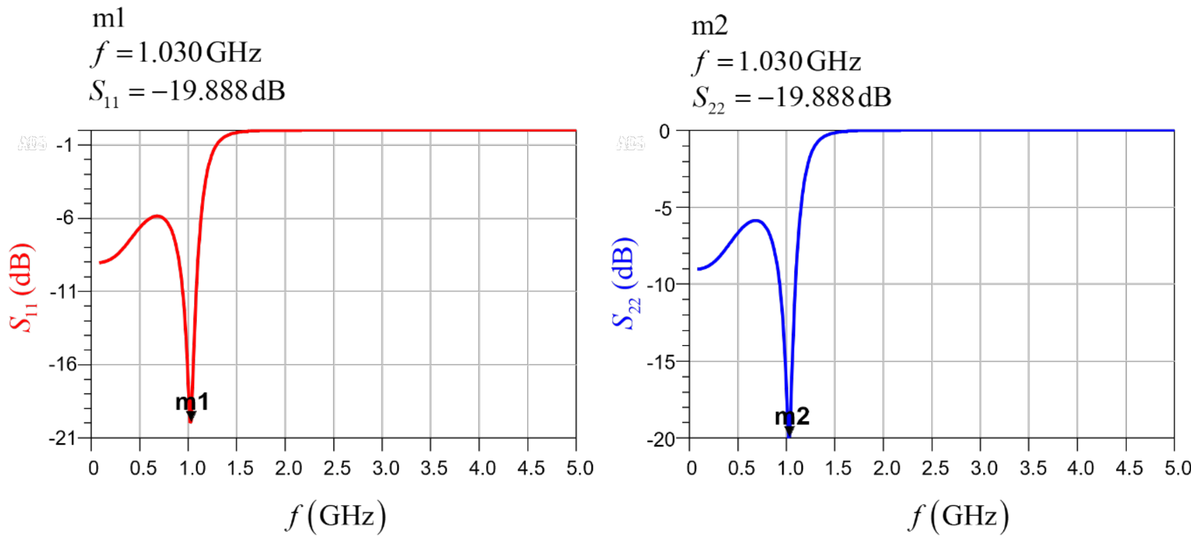

Figure 4.5: Input and output return loss of the load network

4.6 Lumped Component Class-E PA

The entire PA circuit is simulated, sweeping the RF input signal from 0 dBm to 35 dBm. The optimum drive power yielding the best power conversion efficiency is at 28 dBm. The ideal RF chokes are replaced by 500 nH inductors. The input matching is designed and implemented at the input port of the PA, matching the input impedance of the PA to the source impedance of 50 ohm.

The component values of the PA circuit are tuned using ADS optimiser such that the *PE* can be maximised at the fundamental frequency. Optimisation is also required as result of ideal lumped components behaving considerably different to real design models of the same component. An illustration of the PA schematic is provided in Figure 4.6, showing the tuned values of the components.

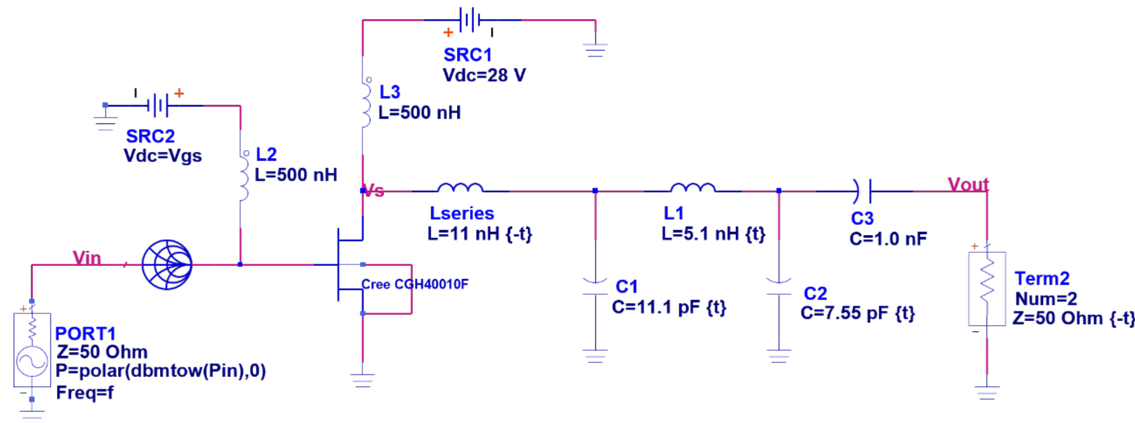

Figure 4.6: Lumped circuit schematic of designed class-E PA

4.6.1 Simulation Results of Lumped Component Class-E

The component values are tuned as previously mentioned, however the variance required from the calculated component values were minimal and this is a very satisfactory result. The expected performance of the PA as defined in the specification was exceeded, although degradation is expected from simulation to prototype measurement results. The simulation results illustrated in Figure 4.6.1 was measured for simulation at the fundamental frequency of 1 GHz, with the RF input drive power at 26 dBm. The transient response of the drain-source voltage across the switch and drain current flowing through the switch is shown, illustrating the voltage being at a maximum magnitude when the drain current is near zero and the maximum drain current flowing when the drain voltage is at a minimum.

By controlling the switching transition of the FET as well as the phase shift between the drain voltage and current waveforms, the power efficiency of the PA can be maximised. The tuned lumped component PA yielded a *PE* of 91.3% and *PAE* of 90.3%, shown in Figure 4.6.3.

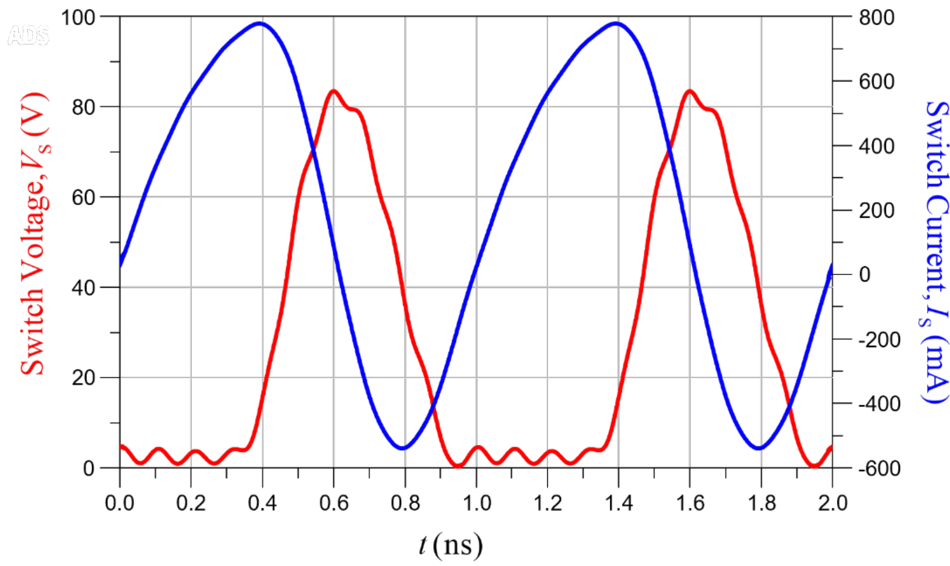

Figure 4.6.2: Simulated drain voltage and current waveforms

The analysis for an idealised class-E PA as proposed by Raab and later implemented by Sokal [23], assumes infinite load impedance at harmonic frequencies. The output network for this design follows a tuned approach similar to that adapted by Wilkinson [26]. The circuit parameters of the load network were tuned to achieve zero switching voltage of the active device.

A simulation of the complete lumped circuit PA as per Figure 4.6 was performed, sweeping the RF input power from 0 dBm to 35 dBm. It is important to mention that the simulation of the lumped circuit PA was perform with the tuned component values as illustrated, using ideal component models, as it is the intention to manufacture a microstrip equivalent of the circuit.

The lumped circuit design is for realising correct operation of the class-E PA before continuing to the design step. The simulation results are displayed in Figure 4.6.3. The power efficiency (*PE*), also known as the drain efficiency (*DE*) as well as the power added efficiency (*PAE*) are displayed with respect to the change in RF input power, measured on the left *y*-axis. The output power ($P_{\mathrm{RF(out)}}$) is measured for the same simulation and is recorded on the right *y*-axis of the plot.

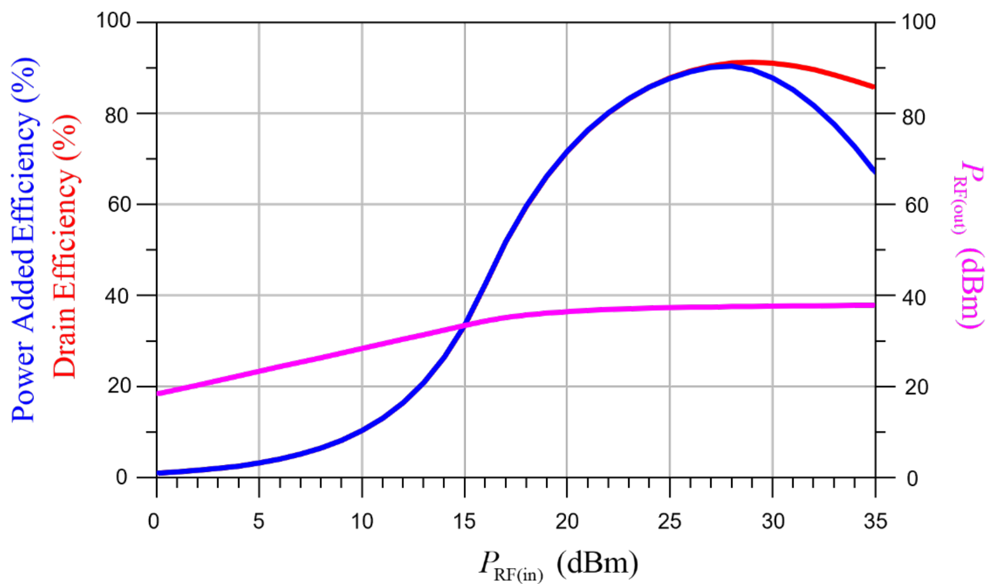

Figure 4.6.3: Simulated performance parameters of the lumped circuit PA.

The results of the ideal lumped component class-E PA are satisfactory and confirm realisation and operation of the amplifier. However, the results will change considerably when the parasitic capacitance, resistance and/or inductance of the components are included in the simulation. These parasitic elements cause the components to behave far from an ideal case.

Bearing mind that the intention is to design a microstrip equivalent of the circuit, and not a functional lumped component PA. Though this has been completed outside the scope of this thesis, the parasitic elements of each individual component is of little regard or assistance in the conversion process.

Before this can be achieved, we need to realise a transmission line equivalent of the circuit first. Once this achieved, the transmission line equivalent of the circuit can be transformed into a microstrip equivalent of the circuit.

4.7 Ideal Transmission Line Class-E

Following the satisfying results of the ideal lumped circuit PA, it is transformed into a transmission line equivalent. That is, each capacitor and inductor is transformed into a transmission equivalent of its respective lumped counterpart. The conversion is performed using the following equations: for each inductance,

$$L = \frac{(Z_0 EL)}{(f360)} \qquad (4.18)$$

where Z_0 is the characteristic impedance of the transmission line, f is the fundamental frequency and EL is the electrical length of the transmission line in degrees [26, p. 1204].

Similarly, each capacitor is transformed by

$$C = \frac{(EL)}{(Z_0 f360)} \qquad (4.19).$$

The complete transmission line equivalent circuit is shown in Figure 4.7.1. The two capacitors of the output network (C_1 and C_2, as illustrated in Figure 4.6) are each split into a parallel combination of two capacitors. In doing so, upon the transformation into transmission line sections, ideal short circuit and open circuit conditions can be created for the RF power at harmonic frequencies which substantially increase the power efficiency of the PA.

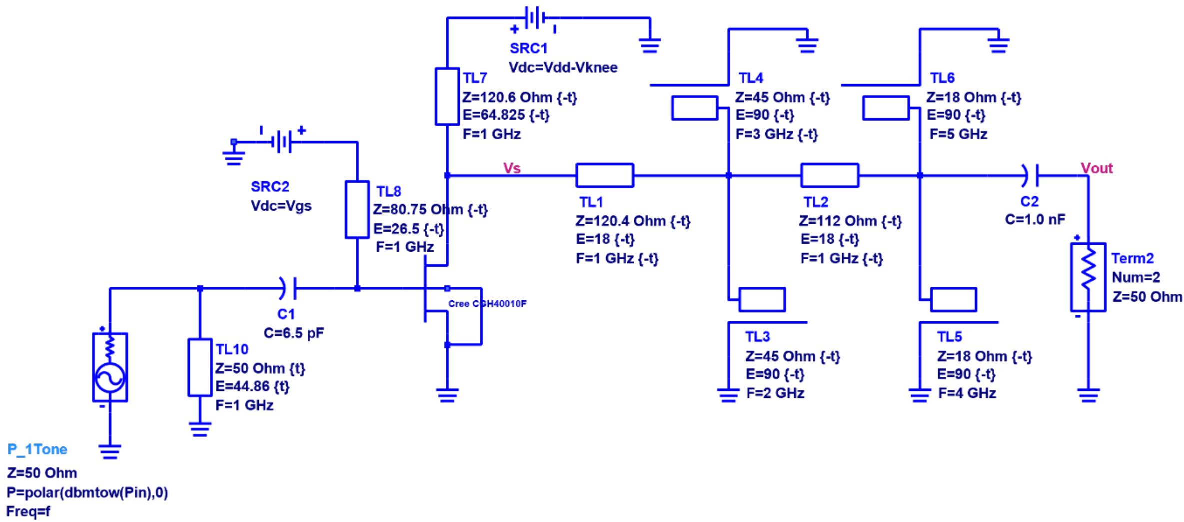

Figure 4.7.1: Transmission line equivalent of the class-E PA

A simulation of the transmission line equivalent PA is performed at the fundamental frequency of 1 GHz and an RF input power level of 28 dBm. The RF input power level is selected to be sufficiently high such that the power generated at harmonic frequencies is sufficiently large. This enables the verification of the design technique implemented and correct class-E operation.

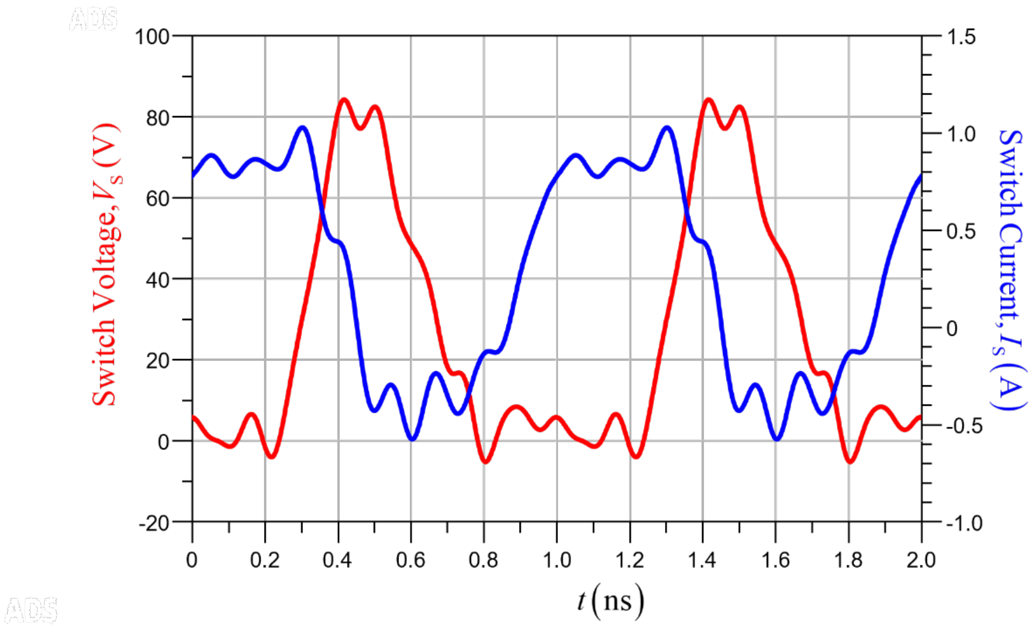

Figure 4.7.2: Drain voltage and current waveforms of the transmission line topology.

Illustrated in Figure 4.7.2 are the simulated drain-to-source voltage, v_{DS} and the drain current, i_D waveforms of the active device of the PA. The shape of the waveforms are as expected, exhibiting minimum overlap between the drain-source voltage and the drain current.

It is important to note that conversion from the lumped component class-E to its transmission line equivalent may require tuning and optimisation. Merely performing the conversion may not necessarily be sufficient to ensure correct class-E operation or exhibit the expected parameters.

An S-parameter simulation was performed over a frequency range of 1-10 GHz. A plot of the simulation results as shown in figure 4.6.2 illustrates the suppression of RF power at harmonic frequencies, thereby confirming operation of the output network. Significant attenuation is exhibited at even and odd harmonic frequencies, which is the desired result. This means minimal RF power is being delivered to the load at these frequencies. Equally important to note is that approximately 0 dB attenuation is experienced at the fundamental frequency of 1 GHz. This implies that maximum power will be delivered to the load at 1 GHz.

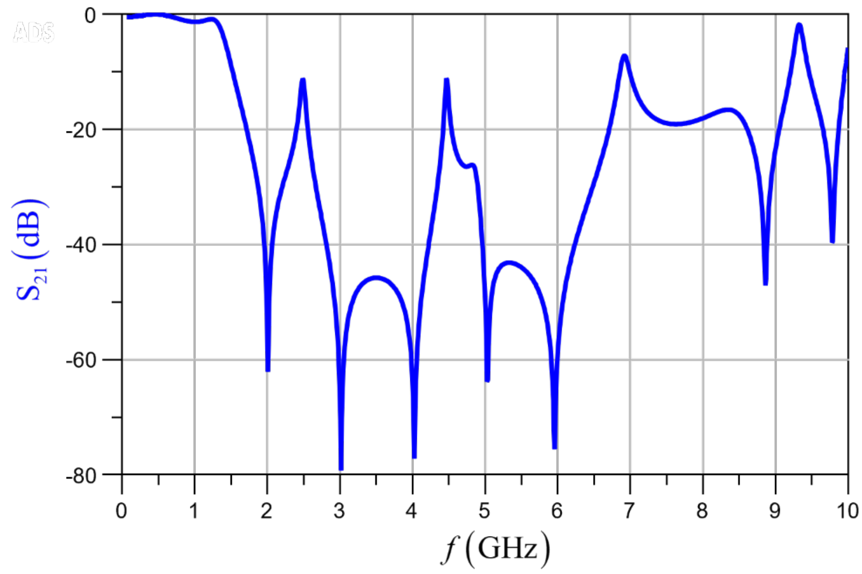

Figure 4.6.2: Simulated S_{21} response of the output network

4.8 Microstrip Class-E PA Simulation Results

A distinguishing factor between the ideal transmission line PA and its microstrip equivalent is the practical implication and required compensation of the interconnecting and added transmission line sections. The results obtained in Chapter 4.7 assume ideal simulation conditions and these cannot practically be replicated. Practically implementing this concept requires interconnecting transmission line sections, that is, PCB traces that physically connect the transmission line sections making up the wave-shaping network and input matching network.

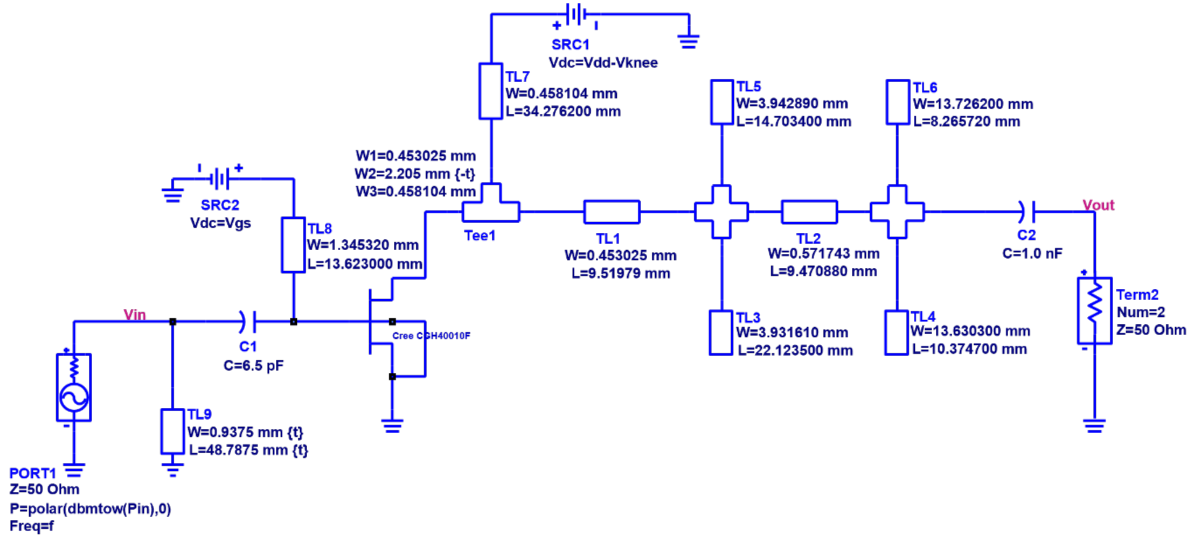

Figure 4.8.1: Microstrip schematic of designed class-E PA

In addition to the abovementioned, non-linear component models are required for any capacitors or inductors required for the circuit design. In the case where non-ferrite components are used the linear model of that component may suffice for the simulation. The added interconnecting sections and the parasitic elements of the required components will affect the behaviour of both, the wave-shaping network and input matching network. It may be necessary to optimize the PA design once these additions have been made.

The physical widths and lengths of each transmission line section of the PA, including the interconnecting sections are synthesized using LineCalc. LineCalc is an ADS tool meant for this very function. This allows the simulation of the PA to exhibit the results including the effects of the added sections.

The drain-source voltage and drain current waveforms of the mictrostrip PA are shown in Figure 4.8.2. Results of this simulation is inclusive of the vendor spice models and the effects of the added PCB trace sections.

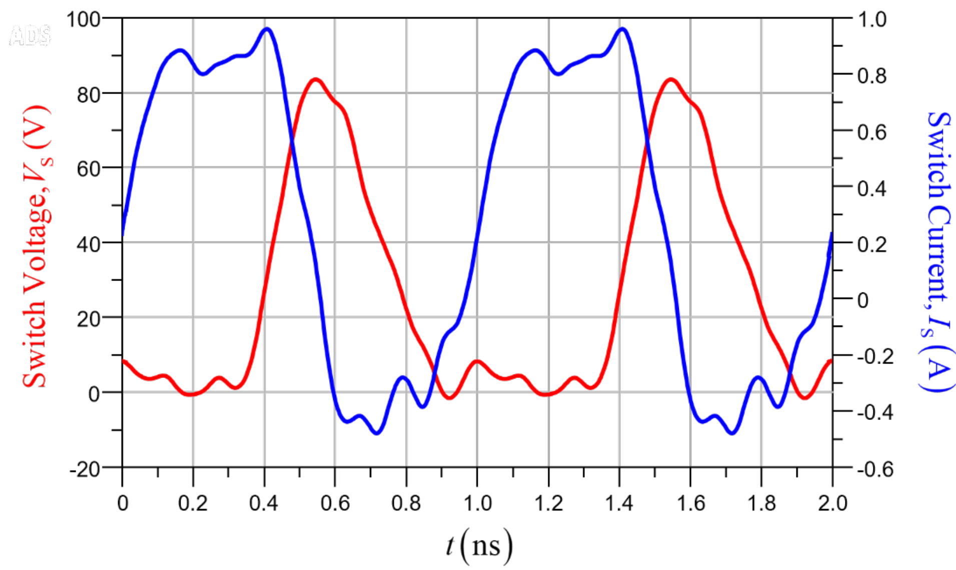

Figure 4.8.2: Drain voltage and current waveforms of microstrip class-E PA

The shape of the waveforms definitely illustrates correct class-E operation, exhibiting minimum overlap between the two waveforms. The peak drain voltage is 84 V, which is greater than the DC supply voltage by three times, exhibiting good voltage gain of the class-E PA.

4.9 Optimised Class-E PA Simulation Results

The microstrip PA above was simulated without performing any optimization to the circuit. The circuit represents a direct transformation from the ideal transmission line PA to its microstrip equivalent. Optimization of the microstrip PA was implemented and the simulation of the PA was performed yielding the results shown in Figure 4.9.1 to Figure 4.9.5.

The PA performance is measured against the variation of the RF input power, $P_{\mathrm{RF(in)}}$ at the fundamental frequency of 1 GHz. The DC bias conditions is set at $V_{\mathrm{DD}} = 28\,\mathrm{V}$ and $V_{\mathrm{GS}} = -2.75\,\mathrm{V}$.

The transient response of the drain voltage across the switch and drain current flowing through the switch is shown, illustrating the voltage being at a maximum magnitude when the drain current is near zero and the maximum drain current flowing when the drain voltage is at a minimum.

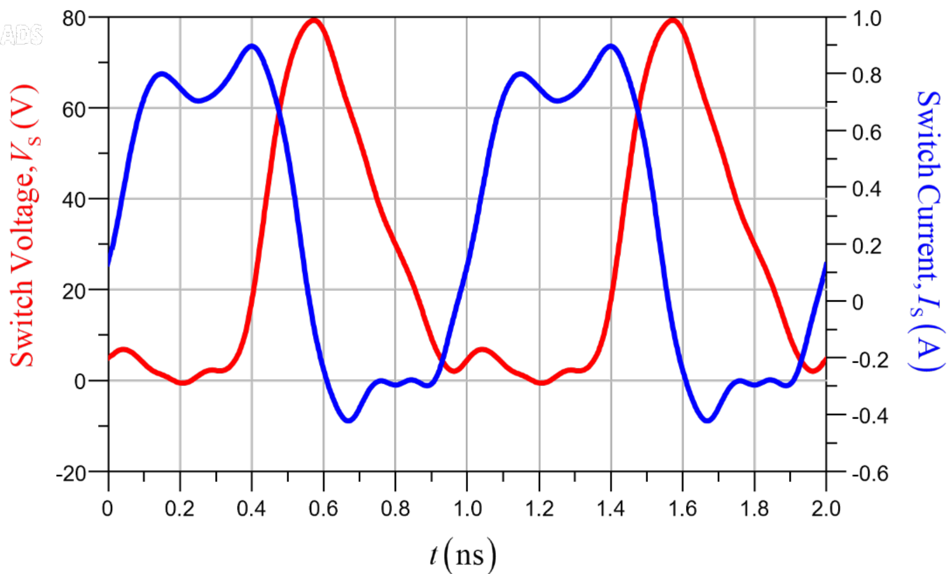

Figure 4.9.1: Drain voltage and current waveforms of optimized microstrip circuit.

Figure 4.9.2 shows the *PE* and the *PAE* (measured on the left y-axis) and the RF output power, $P_{\mathrm{RF(out)}}$ (measured on the right y-axis). The maximum *PE* achieved is measured at marker 1 as 91% with the magnitude of RF output power measured at 37.899 dBm. The maximum *PAE*, measured at marker 2 is 90%. This is achieved at an RF input power magnitude of 26 dBm.

The maximum RF output power, $P_{\mathrm{RF(out)}}$ is measured at marker 3 as 39 dBm. This is measured at $P_{\mathrm{RF(in)}}$ of 35 dBm. It is important to note that despite the maximum output power being achieved at the input power level of 35 dBm, the maximum *PE* is achieved at $P_{\mathrm{RF(in)}}$ 26 dBm. That is, 91% of the applied DC power is transformed into RF output power meaning only 9% is being dissipated or radiated as heat. This is a good result given the power limitation and radiation factors experienced in a CubeSat environment, especially when compared to the current solution.

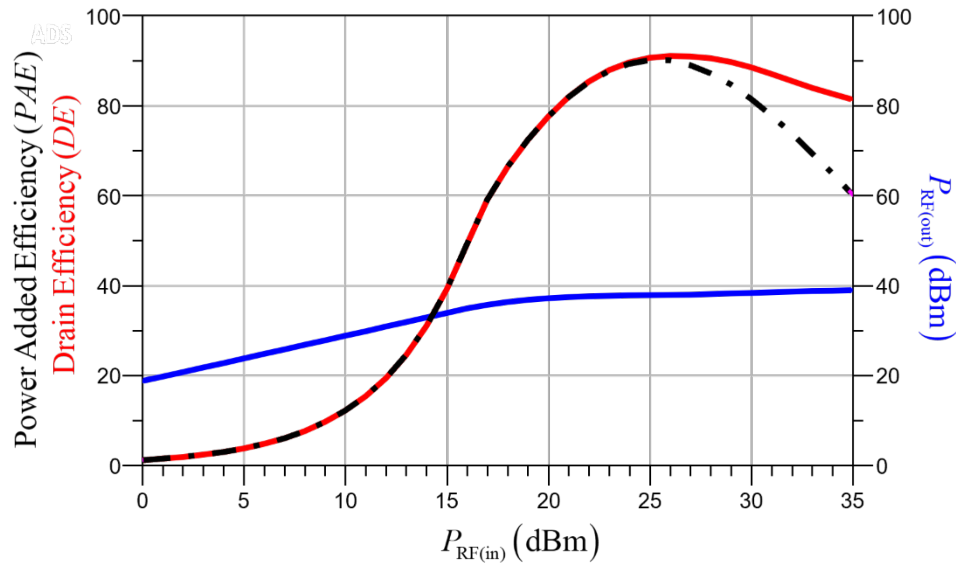

Figure 4.9.2: Simulated performance of PA with respect to input power

The optimized microstrip PA was measured against the drain supply voltage, V_{DD} subjecting the PA to conditions where any variations in the supply voltage may occur. This is a common scenario in CubeSats. The results show that this PA maintains a *PE* above 90% for V_{DD} swept from 15 V to 32 V. The *PAE* is maintained above 87% for the same simulation sweep of V_{DD}. This simulation is performed at the fundamental frequency of 1 GHz. A comparison is made with the performance of passed designs of high efficiency class-E PAs.

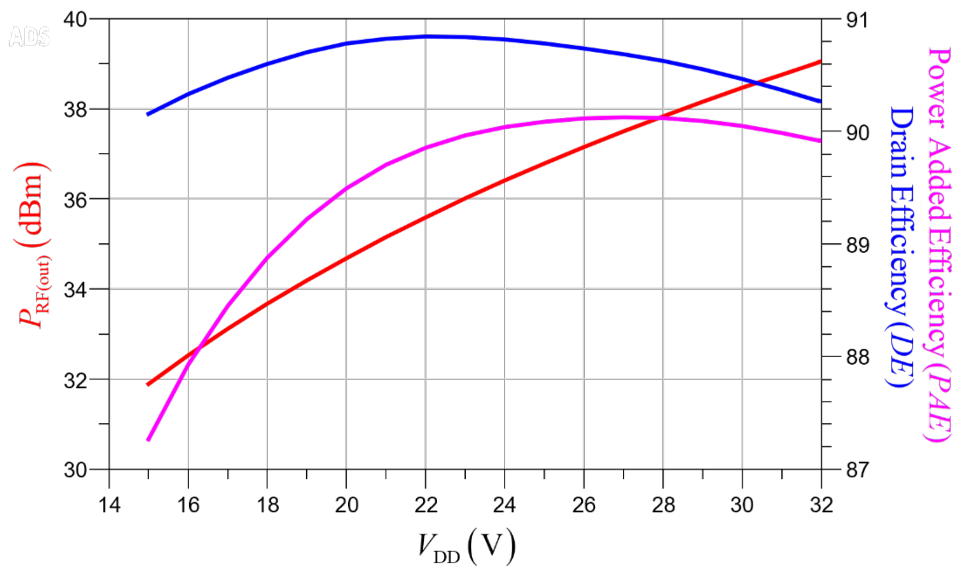

Figure 4.9.3: Simulated performance of PA with respect to DC supply voltage

The PAs instantaneous *PAE*, simulated at $V_{DD} = 28\,V$ is plotted in Figure 4.9.5 showing the degradation of the PAE at lower levels of RF output power. This simulation is done without the implementation of quasi-static envelope tracking, as employed by Mugisho *et al*. [24, p. 3472].

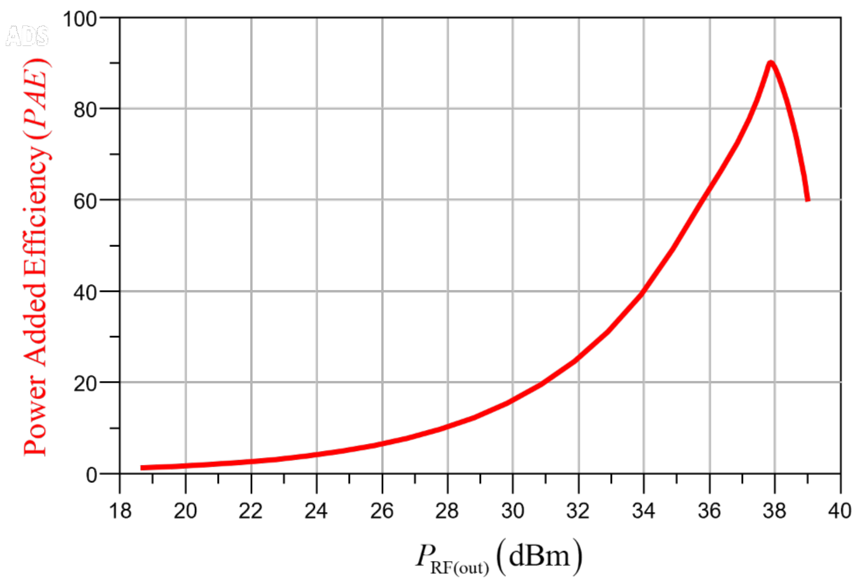

Figure 4.9.4: Simulated PAE with respect to output power

A comparison between the designed PA in this thesis is made to previously designed high efficiency class-E PAs. The performance of the various class-E designs are summarized in Table 4.2. Degradation in performance is expected upon the manufacturing of a prototype.

Ref	Freq (GHz)	(V)	*PE* *(%)*	*PAE* (%)	(dBm)	Gain (dB)
[56]	2	28	84.6	80.1	40.7	12.7
[52]	1.9	30	63	57	37	10
[53]	1.5	28	85	81	42	13.1
[23]	1.37	28	90.2	82.7	39.8	11.5
[55]	1	25	78.8	77.7	37	18.5
[57	1	28	77.5	74.2	39.8	13.7
This work	1	28	91	90.3	37.89	11.8

Table 4.9: Comparison of Class-E Power Amplifiers

Chapter 5

Conclusion, Recommendations and Future Work

The final chapter discusses conclusions of the class-E PA designed using a theoretical approach and an optimization tuning technique. The development of the design and the results has yielded recommendations for further improvement and feeds into concepts for exciting future work.

5.1 Conclusion

The generalized analysis of a class-E PA has theoretically been investigated and presented. The analysis is representative to class-E PAs with shunt capacitance operating with a duty-cycle of 50%. The design method is inclusive of a lumped circuit class-E PA design including explicit design equations for presenting optimum conditions to realize correct class-E operation.

The high efficiency class-E PA was designed for operation in a portion of the *L*-band used for uplink and downlink communications for satellite applications, making the proposed PA a very suitable option for nanosatellites and transmitters for ground stations.

The output network provides the required impedance transformation to the standardized $50\,\Omega$ load and simultaneously performs harmonic suppression by implementing quarter wavelength transmission line stubs at harmonic frequencies. Verification of correct class-E operation has been made through harmonic balance simulation and time domain analysis of the PA circuit. All the ZVS and ZVDS conditions required for correct class-E operation have been fulfilled and the theory and simulation results exhibit very good confirmation with each other.

The proposed design of the PA delivers a PE of 91% and PAE of 90% operating at a 1 GHz fundamental frequency. The optimum RF input power at which this achieved is 26 dBm. The RF output power delivered at this input power level is 37.899 dBm. All the design specifications were well exceeded, and performance of the PA is very satisfactory.

5.2 Recommendations

As is the case for most PAs, the power magnitude of the RF input signal is required to be considerably large. It is therefore advisable to consider the use of a preamplifier able to deliver at least 35 dBm at its output port to the achieve the input power level required by the PA.

This PA was designed for the Rogers FR4 RO4003C (0.406 mm thickness) substrate based availability. It might be beneficial using a thinner substrate or even a different substrate composite than Rogers FR4 RO4003C, especially at frequencies exceeding 2 GHz.

The results have shown that greater power efficiency can be achieved by reducing the DC supply voltage, V_{DD}. The improved PE comes at a loss of RF output power. If this is a compromise that can be made and justified, then it is a useful way to spend your resources.

Appendix

CGH40010

10 W, DC - 6 GHz, RF Power GaN HEMT

Cree's CGH40010 is an unmatched, gallium nitride (GaN) high electron mobility transistor (HEMT). The CGH40010, operating from a 28 volt rail, offers a general purpose, broadband solution to a variety of RF and microwave applications. GaN HEMTs offer high efficiency, high gain and wide bandwidth capabilities making the CGH40010 ideal for linear and compressed amplifier circuits. The transistor is available in both screw-down, flange and solder-down, pill packages.

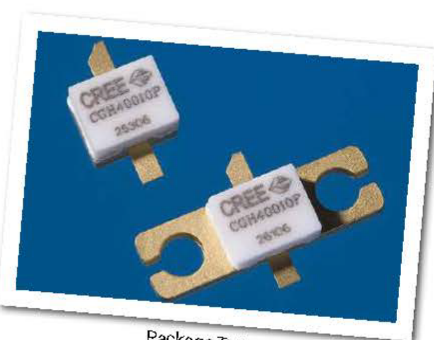

Package Types: 440166, & 440196
PN's: CGH40010F & CGH40010P

FEATURES

- Up to 6 GHz Operation
- 16 dB Small Signal Gain at 2.0 GHz
- 14 dB Small Signal Gain at 4.0 GHz
- 13 W typical P_{SAT}
- 65 % Efficiency at P_{SAT}
- 28 V Operation

APPLICATIONS

- 2-Way Private Radio
- Broadband Amplifiers
- Cellular Infrastructure
- Test Instrumentation
- Class A, AB, Linear amplifiers suitable for OFDM, W-CDMA, EDGE, CDMA waveforms

Rev 4.0 – May 2015

Large Signal Models Available for ADS and MWO

Subject to change without notice.
www.cree.com/wireless

Absolute Maximum Ratings (not simultaneous) at 25˚C Case Temperature

Parameter	Symbol	Rating	Units	Conditions
Drain-Source Voltage	V_{DSS}	84	Volts	25˚C
Gate-to-Source Voltage	V_{GS}	-10, +2	Volts	25˚C
Storage Temperature	T_{STG}	-65, +150	˚C	
Operating Junction Temperature	T_J	225	˚C	
Maximum Forward Gate Current	I_{GMAX}	4.0	mA	25˚C
Maximum Drain Current[1]	I_{DMAX}	1.5	A	25˚C
Soldering Temperature[2]	T_S	245	˚C	
Screw Torque	τ	60	in-oz	
Thermal Resistance, Junction to Case[3]	$R_{\theta JC}$	8.0	˚C/W	85˚C
Case Operating Temperature[3,4]	T_C	-40, +150	˚C	

Note:
[1] Current limit for long term, reliable operation
[2] Refer to the Application Note on soldering at www.cree.com/RF/Document-Library
[3] Measured for the CGH40010F at P_{DISS} = 14 W.
[4] See also, the Power Dissipation De-rating Curve on Page 6.

Electrical Characteristics (T_C = 25˚C)

Characteristics	Symbol	Min.	Typ.	Max.	Units	Conditions
DC Characteristics[1]						
Gate Threshold Voltage	$V_{GS(th)}$	-3.8	-3.0	-2.3	V_{DC}	V_{DS} = 10 V, I_D = 3.6 mA
Gate Quiescent Voltage	$V_{GS(Q)}$	–	-2.7	–	V_{DC}	V_{DS} = 28 V, I_D = 200 mA
Saturated Drain Current	I_{DS}	2.9	3.5	–	A	V_{DS} = 6.0 V, V_{GS} = 2.0 V
Drain-Source Breakdown Voltage	V_{BR}	120	–	–	V_{DC}	V_{GS} = -8 V, I_D = 3.6 mA
RF Characteristics[2] (T_C = 25˚C, F_0 = 3.7 GHz unless otherwise noted)						
Small Signal Gain	G_{SS}	12.5	14.5	–	dB	V_{DD} = 28 V, I_{DQ} = 200 mA
Power Output[3]	P_{SAT}	10	12.5	–	W	V_{DD} = 28 V, I_{DQ} = 200 mA
Drain Efficiency[4]	η	55	65	–	%	V_{DD} = 28 V, I_{DQ} = 200 mA, P_{SAT}
Output Mismatch Stress	VSWR	–	–	10 : 1	Ψ	No damage at all phase angles, V_{DD} = 28 V, I_{DQ} = 200 mA, P_{OUT} = 10 W CW
Dynamic Characteristics						
Input Capacitance	C_{GS}	–	4.5	–	pF	V_{DS} = 28 V, V_{gs} = -8 V, f = 1 MHz
Output Capacitance	C_{DS}	–	1.3	–	pF	V_{DS} = 28 V, V_{gs} = -8 V, f = 1 MHz
Feedback Capacitance	C_{GD}	–	0.2	–	pF	V_{DS} = 28 V, V_{gs} = -8 V, f = 1 MHz

Notes:
[1] Measured on wafer prior to packaging.
[2] Measured in CGH40010-AMP.
[3] P_{SAT} is defined as I_G = 0.36 mA.
[4] Drain Efficiency = P_{OUT} / P_{DC}

Copyright © 2006-2015 Cree, Inc. All rights reserved. The information in this document is subject to change without notice. Cree and the Cree logo are registered trademarks of Cree, Inc.

Cree, Inc.
4600 Silicon Drive
Durham, North Carolina, USA 27703
USA Tel: +1.919.313.5300
Fax: +1.919.869.2733
www.cree.com/rf

Typical Performance

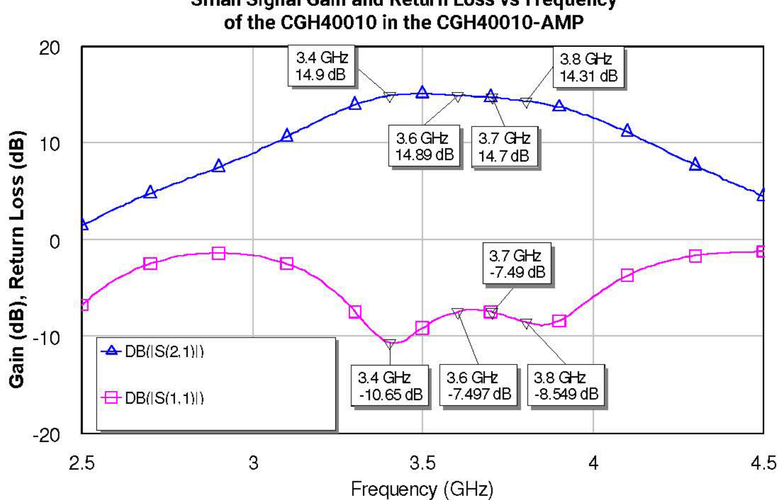

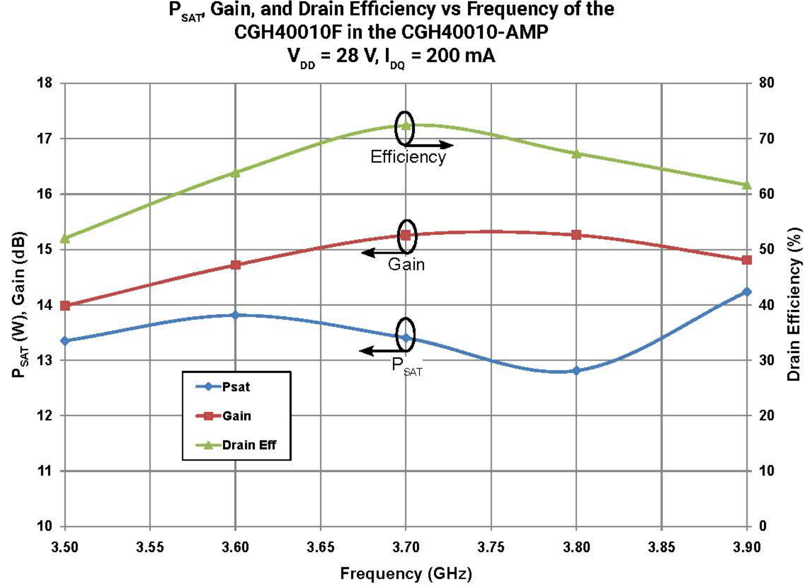

Copyright © 2006-2015 Cree, Inc. All rights reserved. The information in this document is subject to change without notice. Cree and the Cree logo are registered trademarks of Cree, Inc.

Cree, Inc.
4600 Silicon Drive
Durham, North Carolina, USA 27703
USA Tel: +1.919.313.5300
Fax: +1.919.869.2733
www.cree.com/rf

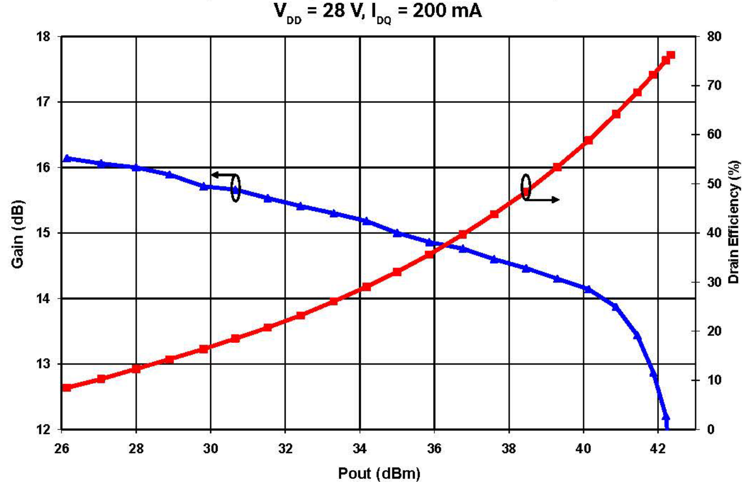

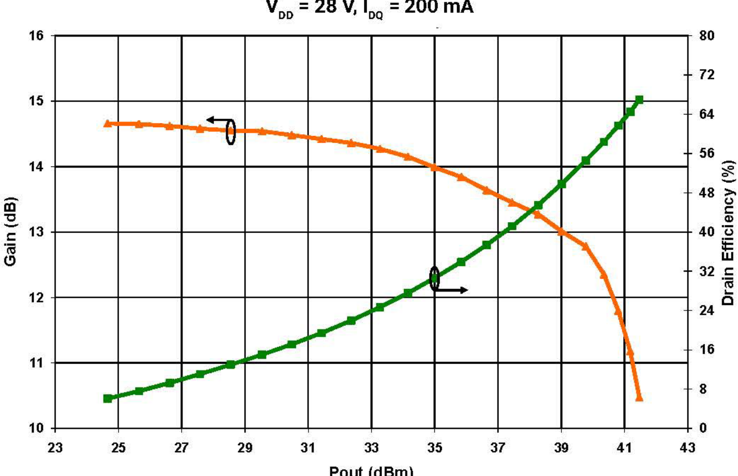

Copyright © 2006-2015 Cree, Inc. All rights reserved. The information in this document is subject to change without notice. Cree and the Cree logo are registered trademarks of Cree, Inc.

Cree, Inc.
4600 Silicon Drive
Durham, North Carolina, USA 27703
USA Tel: +1.919.313.5300
Fax: +1.919.869.2733
www.cree.com/rf

Typical Performance

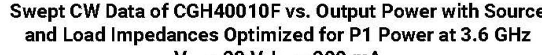

Swept CW Data of CGH40010F vs. Output Power with Source and Load Impedances Optimized for P1 Power at 3.6 GHz
V_{DD} = 28 V, I_{DQ} = 200 mA

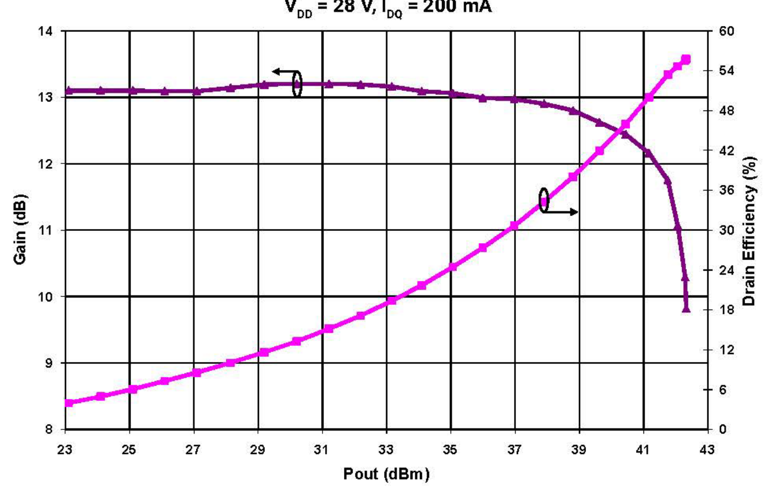

Simulated Maximum Available Gain and K Factor of the CGH40010F
V_{DD} = 28 V, I_{DQ} = 200 mA

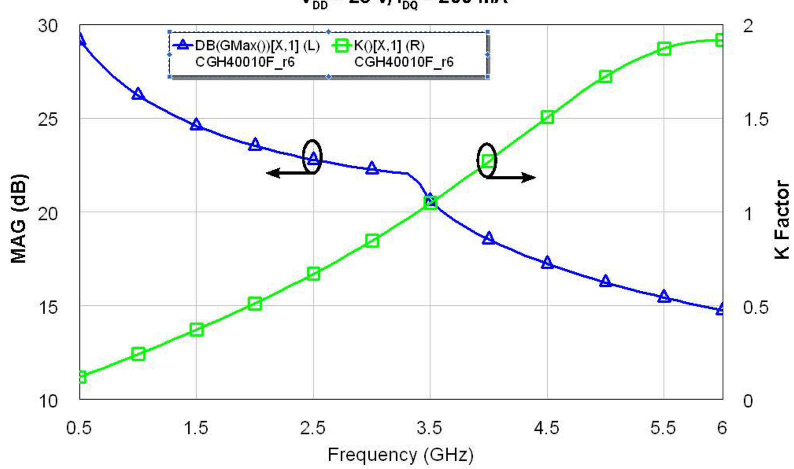

Copyright © 2006-2015 Cree, Inc. All rights reserved. The information in this document is subject to change without notice. Cree and the Cree logo are registered trademarks of Cree, Inc.

Cree, Inc.
4600 Silicon Drive
Durham, North Carolina, USA 27703
USA Tel: +1.919.313.5300
Fax: +1.919.869.2733
www.cree.com/rf

Typical Noise Performance

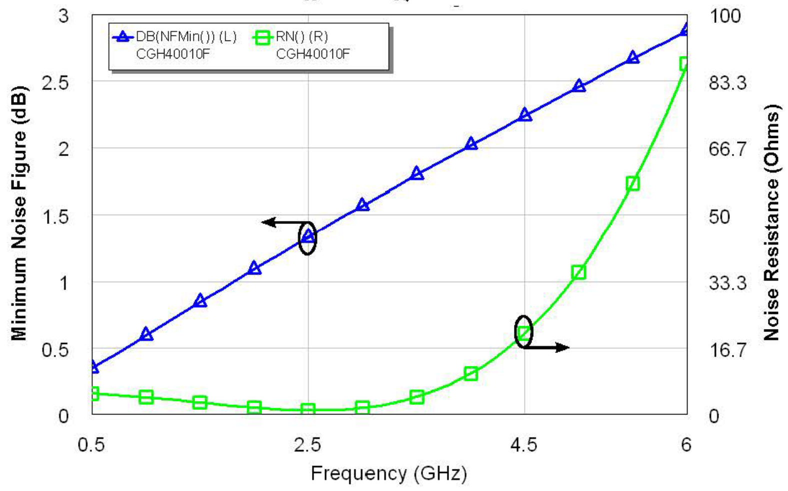

Electrostatic Discharge (ESD) Classifications

Parameter	Symbol	Class	Test Methodology
Human Body Model	HBM	1A > 250 V	JEDEC JESD22 A114-D
Charge Device Model	CDM	1 < 200 V	JEDEC JESD22 C101-C

Copyright © 2006-2015 Cree, Inc. All rights reserved. The information in this document is subject to change without notice. Cree and the Cree logo are registered trademarks of Cree, Inc.

Cree, Inc.
4600 Silicon Drive
Durham, North Carolina, USA 27703
USA Tel: +1.919.313.5300
Fax: +1.919.869.2733
www.cree.com/rf

Source and Load Impedances

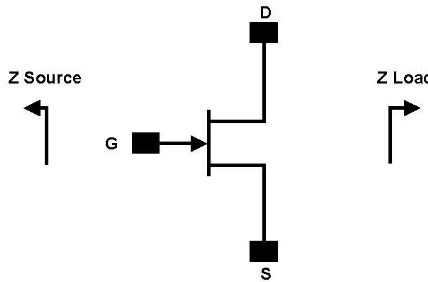

Frequency (MHz)	Z Source	Z Load
500	20.2 + j16.18	51.7 + j15.2
1000	8.38 + j9.46	41.4 + j28.5
1500	7.37 + j0	28.15 + j29
2500	3.19 - j4.76	19 + j9.2
3500	3.18 - j13.3	14.6 + j7.46

Note 1. V_{DD} = 28V, I_{DQ} = 200mA in the 440166 package.
Note 2. Optimized for power, gain, P_{SAT} and PAE.
Note 3. When using this device at low frequency, series resistors should be used to maintain amplifier stability.

CGH40010 Power Dissipation De-rating Curve

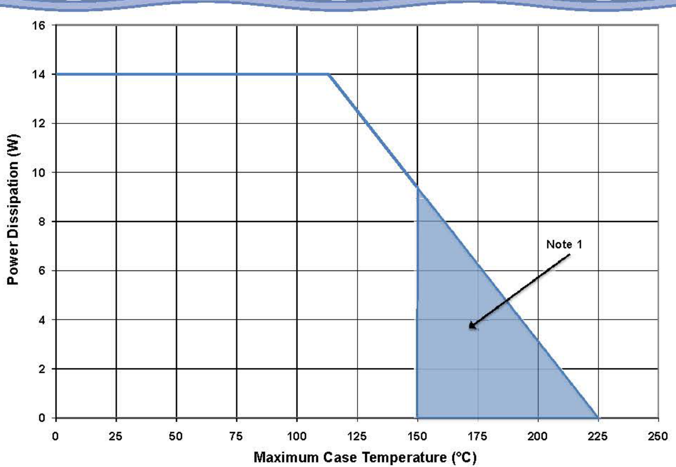

Note 1. Area exceeds Maximum Case Operating Temperature (See Page 2).

Copyright © 2006-2015 Cree, Inc. All rights reserved. The information in this document is subject to change without notice. Cree and the Cree logo are registered trademarks of Cree, Inc.

Cree, Inc.
4600 Silicon Drive
Durham, North Carolina, USA 27703
USA Tel: +1.919.313.5300
Fax: +1.919.869.2733
www.cree.com/rf

CGH40010-AMP Demonstration Amplifier Circuit Bill of Materials

Designator	Description	Qty
R1,R2	RES,1/16W,0603,1%,0 OHMS	1
R3	RES,1/16W,0603,1%,47 OHMS	1
R4	RES,1/16W,0603,1%,100 OHMS	1
C6	CAP, 470PF, 5%,100V, 0603	1
C17	CAP, 33 UF, 20%, G CASE	1
C16	CAP, 1.0UF, 100V, 10%, X7R, 1210	1
C8	CAP 10UF 16V TANTALUM	1
C14	CAP, 100.0pF, +/-5%, 0603	1
C1	CAP, 0.5pF, +/-0.05pF, 0603	1
C2	CAP, 0.7pF, +/-0.1pF, 0603	1
C10,C11	CAP, 1.0pF, +/-0.1pF, 0603	2
C4,C12	CAP, 10.0pF,+/-5%, 0603	2
C5,C13	CAP, 39pF, +/-5%, 0603	2
C7,C15	CAP,33000PF, 0805,100V, X7R	2
J3,J4	CONN SMA STR PANEL JACK RECP	1
J2	HEADER RT>PLZ.1CEN LK 2 POS	1
J1	HEADER RT>PLZ .1CEN LK 5POS	1
-	PCB, RO4350B, Er = 3.48, h = 20 mil	1
Q1	CGH40010F or CGH40010P	1

CGH40010-AMP Demonstration Amplifier Circuit

Copyright © 2006-2015 Cree, Inc. All rights reserved. The information in this document is subject to change without notice. Cree and the Cree logo are registered trademarks of Cree, Inc.

Cree, Inc.
4600 Silicon Drive
Durham, North Carolina, USA 27703
USA Tel: +1.919.313.5300
Fax: +1.919.869.2733
www.cree.com/rf

CGH40010-AMP Demonstration Amplifier Circuit Schematic

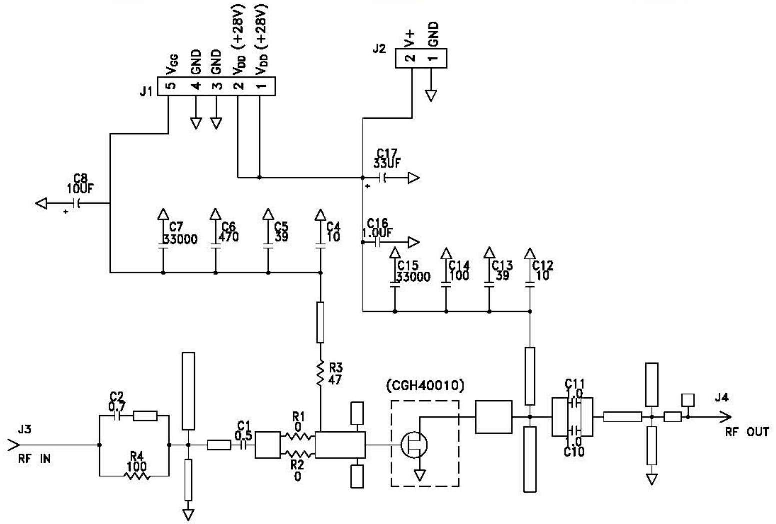

CGH40010-AMP Demonstration Amplifier Circuit Outline

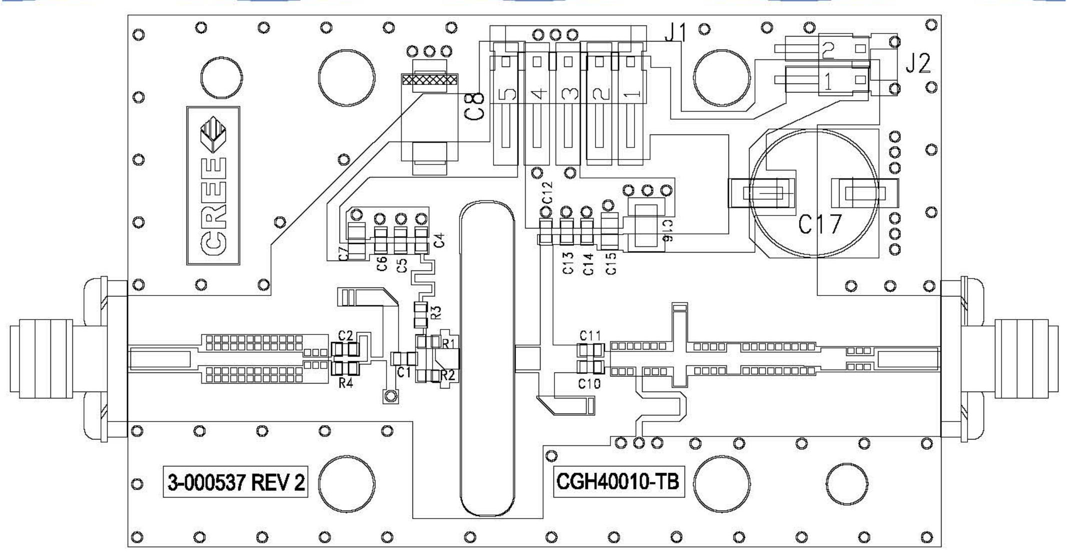

Copyright © 2006-2015 Cree, Inc. All rights reserved. The information in this document is subject to change without notice. Cree and the Cree logo are registered trademarks of Cree, Inc.

Cree, Inc.
4600 Silicon Drive
Durham, North Carolina, USA 27703
USA Tel: +1.919.313.5300
Fax: +1.919.869.2733
www.cree.com/rf

Typical Package S-Parameters for CGH40010
(Small Signal, V_{DS} = 28 V, I_{DQ} = 100 mA, angle in degrees)

Frequency	Mag S11	Ang S11	Mag S21	Ang S21	Mag S12	Ang S12	Mag S22	Ang S22
500 MHz	0.909	-123.34	17.19	108.22	0.027	21.36	0.343	-90.81
600 MHz	0.902	-133.06	14.86	101.82	0.028	15.60	0.329	-98.65
700 MHz	0.897	-140.73	13.04	96.45	0.028	10.87	0.321	-104.84
800 MHz	0.894	-146.96	11.58	91.78	0.029	6.84	0.317	-109.84
900 MHz	0.891	-152.16	10.41	87.61	0.029	3.33	0.316	-113.95
1.0 GHz	0.890	-156.60	9.43	83.82	0.029	0.19	0.318	-117.42
1.1 GHz	0.889	-160.47	8.62	80.31	0.029	-2.66	0.321	-120.40
1.2 GHz	0.888	-163.90	7.93	77.02	0.029	-5.28	0.326	-123.02
1.3 GHz	0.887	-166.99	7.34	73.90	0.029	-7.72	0.332	-125.36
1.4 GHz	0.887	-169.80	6.82	70.92	0.029	-10.01	0.338	-127.51
1.5 GHz	0.887	-172.39	6.38	68.05	0.029	-12.18	0.345	-129.50
1.6 GHz	0.887	-174.80	5.98	65.28	0.028	-14.24	0.353	-131.37
1.7 GHz	0.887	-177.07	5.63	62.59	0.028	-16.21	0.360	-133.15
1.8 GHz	0.887	-179.22	5.32	59.97	0.028	-18.09	0.369	-134.87
1.9 GHz	0.887	178.73	5.04	57.41	0.028	-19.91	0.377	-136.54
2.0 GHz	0.888	176.76	4.78	54.89	0.027	-21.66	0.385	-138.17
2.1 GHz	0.888	174.86	4.55	52.42	0.027	-23.35	0.393	-139.77
2.2 GHz	0.888	173.02	4.34	49.99	0.027	-24.98	0.402	-141.34
2.3 GHz	0.888	171.23	4.15	47.60	0.026	-26.56	0.410	-142.90
2.4 GHz	0.889	169.48	3.97	45.24	0.026	-28.08	0.418	-144.45
2.5 GHz	0.889	167.76	3.81	42.90	0.026	-29.55	0.426	-145.99
2.6 GHz	0.890	166.07	3.66	40.59	0.025	-30.98	0.434	-147.53
2.7 GHz	0.890	164.39	3.53	38.30	0.025	-32.36	0.442	-149.06
2.8 GHz	0.890	162.74	3.40	36.03	0.025	-33.69	0.450	-150.59
2.9 GHz	0.891	161.10	3.28	33.78	0.024	-34.97	0.458	-152.12
3.0 GHz	0.891	159.46	3.17	31.55	0.024	-36.20	0.465	-153.65
3.2 GHz	0.892	156.21	2.97	27.12	0.023	-38.51	0.479	-156.72
3.4 GHz	0.893	152.96	2.79	22.73	0.022	-40.63	0.493	-159.80
3.6 GHz	0.893	149.69	2.64	18.38	0.022	-42.52	0.505	-162.90
3.8 GHz	0.894	146.38	2.50	14.05	0.021	-44.17	0.517	-166.03
4.0 GHz	0.894	143.03	2.38	9.72	0.020	-45.56	0.527	-169.19
4.2 GHz	0.894	139.61	2.28	5.40	0.019	-46.67	0.537	-172.39
4.4 GHz	0.895	136.11	2.18	1.07	0.019	-47.46	0.546	-175.64
4.6 GHz	0.895	132.53	2.09	-3.29	0.018	-47.90	0.554	-178.95
4.8 GHz	0.895	128.85	2.01	-7.68	0.017	-47.96	0.561	177.69
5.0 GHz	0.895	125.06	1.94	-12.10	0.017	-47.61	0.568	174.25
5.2 GHz	0.895	121.15	1.88	-16.58	0.016	-46.84	0.573	170.72
5.4 GHz	0.895	117.11	1.82	-21.12	0.016	-45.67	0.578	167.10
5.6 GHz	0.895	112.94	1.77	-25.73	0.015	-44.12	0.582	163.38
5.8 GHz	0.895	108.62	1.72	-30.42	0.015	-42.30	0.586	159.54
6.0 GHz	0.895	104.15	1.68	-35.20	0.015	-40.33	0.589	155.56

To download the s-parameters in s2p format, go to the CGH40010 Product page and click on the documentation tab.

Copyright © 2006-2015 Cree, Inc. All rights reserved. The information in this document is subject to change without notice. Cree and the Cree logo are registered trademarks of Cree, Inc.

Cree, Inc.
4600 Silicon Drive
Durham, North Carolina, USA 27703
USA Tel: +1.919.313.5300
Fax: +1.919.869.2733
www.cree.com/rf

Typical Package S-Parameters for CGH40010
(Small Signal, V_{DS} = 28 V, I_{DQ} = 200 mA, angle in degrees)

Frequency	Mag S11	Ang S11	Mag S21	Ang S21	Mag S12	Ang S12	Mag S22	Ang S22
500 MHz	0.911	-130.62	18.41	105.41	0.022	19.44	0.303	-112.24
600 MHz	0.906	-139.65	15.80	99.47	0.023	14.31	0.299	-119.83
700 MHz	0.902	-146.70	13.80	94.50	0.023	10.17	0.298	-125.50
800 MHz	0.899	-152.41	12.22	90.19	0.023	6.68	0.299	-129.85
900 MHz	0.898	-157.17	10.96	86.34	0.024	3.67	0.302	-133.28
1.0 GHz	0.896	-161.24	9.92	82.82	0.024	0.99	0.305	-136.05
1.1 GHz	0.896	-164.79	9.06	79.56	0.024	-1.41	0.309	-138.34
1.2 GHz	0.895	-167.95	8.33	76.49	0.024	-3.62	0.314	-140.30
1.3 GHz	0.895	-170.80	7.70	73.57	0.023	-5.66	0.320	-142.01
1.4 GHz	0.894	-173.41	7.17	70.78	0.023	-7.56	0.326	-143.54
1.5 GHz	0.894	-175.82	6.70	68.08	0.023	-9.35	0.332	-144.94
1.6 GHz	0.894	-178.09	6.28	65.47	0.023	-11.05	0.338	-146.24
1.7 GHz	0.894	179.78	5.92	62.92	0.023	-12.66	0.345	-147.48
1.8 GHz	0.894	177.75	5.59	60.43	0.023	-14.19	0.352	-148.68
1.9 GHz	0.894	175.81	5.30	57.99	0.023	-15.65	0.358	-149.84
2.0 GHz	0.894	173.94	5.04	55.59	0.022	-17.05	0.365	-150.99
2.1 GHz	0.894	172.13	4.80	53.23	0.022	-18.39	0.372	-152.12
2.2 GHz	0.894	170.37	4.58	50.91	0.022	-19.67	0.379	-153.26
2.3 GHz	0.895	168.65	4.38	48.61	0.022	-20.90	0.386	-154.39
2.4 GHz	0.895	166.96	4.20	46.33	0.021	-22.08	0.393	-155.54
2.5 GHz	0.895	165.30	4.03	44.08	0.021	-23.20	0.400	-156.69
2.6 GHz	0.895	163.66	3.88	41.84	0.021	-24.27	0.407	-157.85
2.7 GHz	0.895	162.04	3.74	39.63	0.021	-25.28	0.414	-159.03
2.8 GHz	0.895	160.43	3.60	37.43	0.020	-26.25	0.420	-160.22
2.9 GHz	0.896	158.83	3.48	35.24	0.020	-27.16	0.427	-161.42
3.0 GHz	0.896	157.24	3.37	33.06	0.020	-28.02	0.433	-162.64
3.2 GHz	0.896	154.06	3.16	28.74	0.019	-29.57	0.446	-165.13
3.4 GHz	0.896	150.87	2.98	24.44	0.019	-30.88	0.457	-167.69
3.6 GHz	0.896	147.66	2.82	20.16	0.018	-31.95	0.468	-170.31
3.8 GHz	0.897	144.41	2.68	15.89	0.018	-32.76	0.478	-173.00
4.0 GHz	0.897	141.10	2.56	11.61	0.017	-33.30	0.488	-175.77
4.2 GHz	0.897	137.72	2.45	7.33	0.017	-33.55	0.497	-178.61
4.4 GHz	0.897	134.26	2.35	3.03	0.017	-33.50	0.505	178.47
4.6 GHz	0.897	130.71	2.26	-1.31	0.016	-33.18	0.512	175.46
4.8 GHz	0.896	127.06	2.17	-5.68	0.016	-32.58	0.518	172.36
5.0 GHz	0.896	123.30	2.10	-10.09	0.016	-31.74	0.524	169.16
5.2 GHz	0.896	119.42	2.04	-14.57	0.016	-30.72	0.529	165.86
5.4 GHz	0.896	115.41	1.98	-19.10	0.016	-29.60	0.534	162.44
5.6 GHz	0.896	111.26	1.92	-23.71	0.016	-28.46	0.537	158.89
5.8 GHz	0.895	106.97	1.87	-28.40	0.017	-27.41	0.540	155.20
6.0 GHz	0.895	102.53	1.82	-33.19	0.017	-26.54	0.543	151.36

To download the s-parameters in s2p format, go to the CGH40010 Product Page and click on the documentation tab.

Copyright © 2006-2015 Cree, Inc. All rights reserved. The information in this document is subject to change without notice. Cree and the Cree logo are registered trademarks of Cree, Inc.

Cree, Inc.
4600 Silicon Drive
Durham, North Carolina, USA 27703
USA Tel: +1.919.313.5300
Fax: +1.919.869.2733
www.cree.com/rf

Typical Package S-Parameters for CGH40010
(Small Signal, V_{DS} = 28 V, I_{DQ} = 500 mA, angle in degrees)

Frequency	Mag S11	Ang S11	Mag S21	Ang S21	Mag S12	Ang S12	Mag S22	Ang S22
500 MHz	0.914	-135.02	18.58	103.70	0.020	18.36	0.300	-126.80
600 MHz	0.909	-143.57	15.88	98.05	0.020	13.67	0.302	-133.51
700 MHz	0.906	-150.23	13.83	93.33	0.021	9.90	0.304	-138.40
800 MHz	0.904	-155.61	12.23	89.23	0.021	6.77	0.307	-142.08
900 MHz	0.903	-160.09	10.95	85.56	0.021	4.08	0.311	-144.94
1.0 GHz	0.902	-163.93	9.91	82.21	0.021	1.71	0.314	-147.23
1.1 GHz	0.901	-167.29	9.04	79.09	0.021	-0.41	0.319	-149.10
1.2 GHz	0.901	-170.29	8.31	76.15	0.021	-2.35	0.323	-150.69
1.3 GHz	0.900	-173.00	7.69	73.35	0.021	-4.12	0.328	-152.07
1.4 GHz	0.900	-175.50	7.15	70.66	0.021	-5.78	0.333	-153.29
1.5 GHz	0.900	-177.81	6.69	68.07	0.021	-7.32	0.338	-154.41
1.6 GHz	0.900	-179.98	6.27	65.54	0.021	-8.77	0.344	-155.44
1.7 GHz	0.900	177.96	5.91	63.08	0.020	-10.15	0.349	-156.43
1.8 GHz	0.899	176.00	5.59	60.67	0.020	-11.45	0.355	-157.38
1.9 GHz	0.899	174.12	5.30	58.30	0.020	-12.68	0.361	-158.30
2.0 GHz	0.899	172.31	5.04	55.97	0.020	-13.85	0.366	-159.22
2.1 GHz	0.899	170.54	4.80	53.67	0.020	-14.96	0.372	-160.14
2.2 GHz	0.900	168.83	4.58	51.40	0.020	-16.01	0.378	-161.06
2.3 GHz	0.900	167.15	4.39	49.16	0.019	-17.01	0.384	-161.99
2.4 GHz	0.900	165.49	4.21	46.94	0.019	-17.95	0.390	-162.93
2.5 GHz	0.900	163.87	4.04	44.73	0.019	-18.85	0.396	-163.88
2.6 GHz	0.900	162.26	3.89	42.54	0.019	-19.69	0.402	-164.86
2.7 GHz	0.900	160.66	3.75	40.37	0.019	-20.48	0.407	-165.85
2.8 GHz	0.900	159.08	3.62	38.21	0.019	-21.21	0.413	-166.86
2.9 GHz	0.900	157.51	3.50	36.05	0.018	-21.89	0.418	-167.89
3.0 GHz	0.900	155.93	3.39	33.91	0.018	-22.52	0.424	-168.95
3.2 GHz	0.900	152.79	3.18	29.65	0.018	-23.61	0.435	-171.12
3.4 GHz	0.900	149.64	3.00	25.40	0.017	-24.48	0.445	-173.38
3.6 GHz	0.900	146.45	2.85	21.17	0.017	-25.11	0.454	-175.73
3.8 GHz	0.900	143.23	2.71	16.93	0.017	-25.51	0.463	-178.17
4.0 GHz	0.900	139.94	2.58	12.69	0.017	-25.67	0.471	179.30
4.2 GHz	0.900	136.58	2.47	8.43	0.016	-25.60	0.479	176.67
4.4 GHz	0.899	133.14	2.38	4.15	0.016	-25.32	0.486	173.94
4.6 GHz	0.899	129.61	2.29	-0.17	0.016	-24.85	0.492	171.12
4.8 GHz	0.899	125.97	2.21	-4.53	0.016	-24.24	0.498	168.18
5.0 GHz	0.898	122.23	2.13	-8.94	0.016	-23.54	0.503	165.13
5.2 GHz	0.898	118.36	2.07	-13.41	0.016	-22.80	0.507	161.96
5.4 GHz	0.898	114.36	2.01	-17.95	0.017	-22.11	0.511	158.66
5.6 GHz	0.897	110.22	1.95	-22.56	0.017	-21.54	0.514	155.22
5.8 GHz	0.897	105.94	1.90	-27.26	0.018	-21.16	0.517	151.63
6.0 GHz	0.897	101.51	1.86	-32.04	0.019	-21.04	0.519	147.87

To download the s-parameters in s2p format, go to the CGH40010 Product Page and click on the documentation tab.

Copyright © 2006-2015 Cree, Inc. All rights reserved. The information in this document is subject to change without notice. Cree and the Cree logo are registered trademarks of Cree, Inc.

Cree, Inc.
4600 Silicon Drive
Durham, North Carolina, USA 27703
USA Tel: +1.919.313.5300
Fax: +1.919.869.2733
www.cree.com/rf

Product Dimensions CGH40010F (Package Type — 440166)

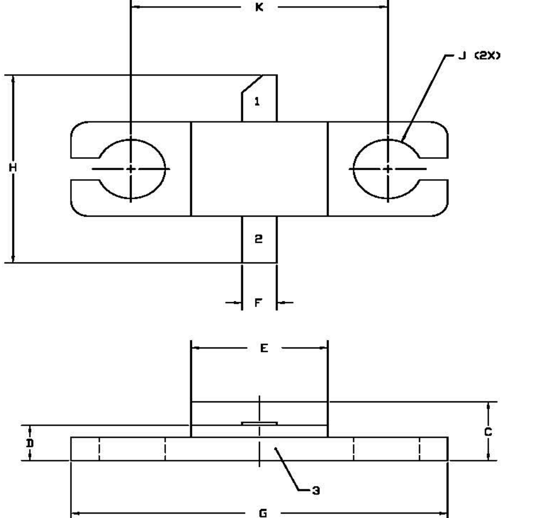

NOTES:

1. DIMENSIONING AND TOLERANCING PER ANSI Y14.5M, 1982.
2. CONTROLLING DIMENSION: INCH.
3. ADHESIVE FROM LID MAY EXTEND A MAXIMUM OF 0.020" BEYOND EDGE OF LID.
4. LID MAY BE MISALIGNED TO THE BODY OF THE PACKAGE BY A MAXIMUM OF 0.008" IN ANY DIRECTION.
5. ALL PLATED SURFACES ARE NI/AU

DIM	INCHES		MILLIMETERS	
	MIN	MAX	MIN	MAX
A	0.155	0.165	3.94	4.19
B	0.004	0.006	0.10	0.15
C	0.115	0.135	2.92	3.43
D	0.057	0.067	1.45	1.70
E	0.195	0.205	4.95	5.21
F	0.045	0.055	1.14	1.40
G	0.545	0.555	13.84	14.09
H	0.280	0.360	7.11	9.14
J	ø .100		2.54	
K	0.375		9.53	

PIN 1. GATE
PIN 2. DRAIN
PIN 3. SOURCE

Product Dimensions CGH40010P (Package Type — 440196)

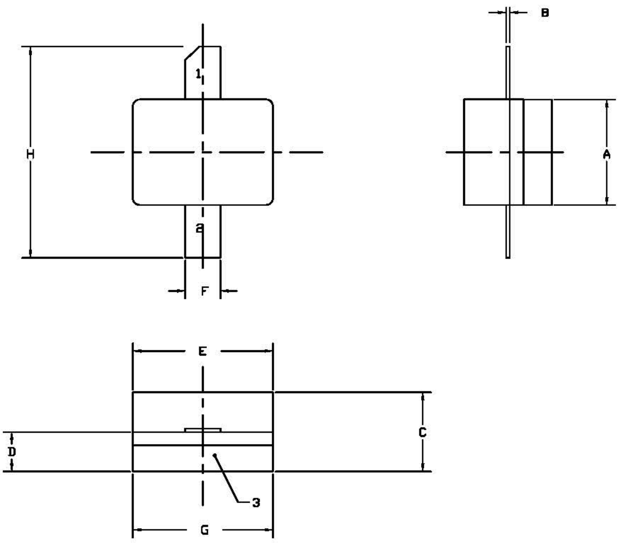

NOTES:

1. DIMENSIONING AND TOLERANCING PER ANSI Y14.5M, 1982.
2. CONTROLLING DIMENSION: INCH.
3. ADHESIVE FROM LID MAY EXTEND A MAXIMUM OF 0.020" BEYOND EDGE OF LID.
4. LID MAY BE MISALIGNED TO THE BODY OF THE PACKAGE BY A MAXIMUM OF 0.008" IN ANY DIRECTION.
5. ALL PLATED SURFACES ARE NI/AU

DIM	INCHES		MILLIMETERS	
	MIN	MAX	MIN	MAX
A	0.155	0.165	3.94	4.19
B	0.003	0.006	0.10	0.15
C	0.115	0.135	2.92	3.17
D	0.057	0.067	1.45	1.70
E	0.195	0.205	4.95	5.21
F	0.045	0.055	1.14	1.40
G	0.195	0.205	4.95	5.21
H	0.280	0.360	7.11	9.14

PIN 1. GATE
PIN 2. DRAIN
PIN 3. SOURCE

Copyright © 2006-2015 Cree, Inc. All rights reserved. The information in this document is subject to change without notice. Cree and the Cree logo are registered trademarks of Cree, Inc.

Cree, Inc.
4600 Silicon Drive
Durham, North Carolina, USA 27703
USA Tel: +1.919.313.5300
Fax: +1.919.869.2733
www.cree.com/rf

Product Ordering Information

Order Number	Description	Unit of Measure	Image
CGH40010F	GaN HEMT	Each	
CGH40010P	GaN HEMT	Each	
CGH40010F-TB	Test board without GaN HEMT	Each	
CGH40010F-AMP	Test board with GaN HEMT installed	Each	

Copyright © 2006-2015 Cree, Inc. All rights reserved. The information in this document is subject to change without notice. Cree and the Cree logo are registered trademarks of Cree, Inc.

Cree, Inc.
4600 Silicon Drive
Durham, North Carolina, USA 27703
USA Tel: +1.919.313.5300
Fax: +1.919.869.2733
www.cree.com/rf

Disclaimer

Specifications are subject to change without notice. Cree, Inc. believes the information contained within this data sheet to be accurate and reliable. However, no responsibility is assumed by Cree for any infringement of patents or other rights of third parties which may result from its use. No license is granted by implication or otherwise under any patent or patent rights of Cree. Cree makes no warranty, representation or guarantee regarding the suitability of its products for any particular purpose. "Typical" parameters are the average values expected by Cree in large quantities and are provided for information purposes only. These values can and do vary in different applications and actual performance can vary over time. All operating parameters should be validated by customer's technical experts for each application. Cree products are not designed, intended or authorized for use as components in applications intended for surgical implant into the body or to support or sustain life, in applications in which the failure of the Cree product could result in personal injury or death or in applications for planning, construction, maintenance or direct operation of a nuclear facility.

For more information, please contact:

Cree, Inc.
4600 Silicon Drive
Durham, North Carolina, USA 27703
www.cree.com/RF

Sarah Miller
Marketing
Cree, RF Components
1.919.407.5302

Ryan Baker
Marketing & Sales
Cree, RF Components
1.919.407.7816

Tom Dekker
Sales Director
Cree, RF Components
1.919.407.5639

Copyright © 2006-2015 Cree, Inc. All rights reserved. The information in this document is subject to change without notice. Cree and the Cree logo are registered trademarks of Cree, Inc.

Cree, Inc.
4600 Silicon Drive
Durham, North Carolina, USA 27703
USA Tel: +1.919.313.5300
Fax: +1.919.869.2733
www.cree.com/rf

Bibliography

[1] J. R. G. Nickolas Kingsley, Radar RF Circuit Design, Second Edition, Artech House, 2022.

[2] G. B. Admiralty, Handbook of Wireless Telegraphy, London: His Majesty's Stationary Office, 1938.

[3] W. Everitt, Fundamentals of Radio and Electronics 2nd Edition, London: Constable and Company, Ltd., 1958.

[4] F. G. E. L. Paolo Colantonio, High Efficiency RF and Microwave Solid State Power Amplifiers, Tor Vergata, Italy: John Wiley and Son's, Ltd, 2009.

[5] J. Chitode, Industrial Electronics, Pune: Technical Publications, 2009.

[6] M. H. Rashid, Power Electronics Handbook 4th Edition, Butterworth-Heinemann, 2017.

[7] M. K. Kazimierczuk, RF Power Amplifiers, Dayton, Ohio, USA: John Wiley and Son's, Ltd, 2008.

[8] I. Bahl, Fundamentals of RF and Microwave Transistor Amplifiers, Wiley and Son's, Ltd, 2009.

[9] A. Eroglu, Linear and Switch-Mode RF Power Amplifiers, CRC Press, 2017.

[10] M. J. F. Andrei Grebennikov, Switchmode RF and Microwave Power Amplifiers, Academic Press, 2021.

[11] S. C. Cripps, RF Power Amplifiers for Wireless Communications - 2nd Edition, London: Artech House, 2006.

[12] S. A. Maas, Nonlinear Microwave and RF Circuits, Artech House, 2003.

[13] L. B. Rowan Gilmore, Practical RF Circuit Design for Modern Wireless Systems: Active Circuits and Systems, Volume 2, Artech House, 2003.

[14] M. S. Mugisho, "Design of a High Efficiency S-Band Power Amplifier for a CubeSat," in *IEEE*, Cape Town, 2016.

[15] N. B. C. Jose Carlos Pedro, Intermodulation Distortion in Microwave and Wireless Circuits, Boston: Artech House, 2003.

[16] J. L. Walker, The Handbook of RF and Microwave Power Amplifiers, Cambridge University Press, 2012.

[17] Z. Wang, Envelope Tracking Power Amplifiers for Wireless Communications, Artech House, 2014.

[18] J. Wood, Behavioral Modelling and Linearization of RF Power Amplifiers, Boston: Artech House, 2014.

[19] A. H. v. R. J. H. H. Michiel Steyaert, Analog Circuit Design: RF Circuits: Wide-Band, Front-Ends, DAC's Design Mtehodology and Verification for RF and Mixed-Signal Systems Low Power and Low Voltage, Springer Science and Business Media, 2006.

[20] J. G. Mike Golio, RF and Microwave Applications and Systems, CRC Press, 2018.

[21] S. D. MacPherson, An Introduction to High Frequency Small-Signal Amplifier Design, 2002.

[22] N. O. S. Andrei Grebennikov, Switchmode RF Power Amplifiers, Amsterdam: Newnes, 2007.

[23] N. O. Sokal, "Class-E High Efficiency RF/Microwave Power Amplifiers: Principles of Operation, Design Procedures, and Experimental Verification," in *Analog Circuit Design* , Boston, 2003.

[24] D. G. M. Y. V. R. V. K. A. G. M. T. Moïse Safari Mugisho, "Generalized Class-E power amplifier with shunt capacitance and shunt filter," in *IEEE Transactions on Microwave Theory and Techniques*, 2019.

[25] T. Mader, E. Bryerton, M. Markovic, M. Forman and Z. Popovic, "Switched-Mode High-Efficiency Microwave Power Amplifiers in a Free-Space Power-Combiner Array," in *IEEE*, 1998.

[26] J. E. A.J. Wilkinson, "Transmission-Line Load-Network Topology for Class-E Power Amplifiers," in *IEEE Transactions on Microwave Theory and Techniques*, 2001.

[27] A. D. Balwinder Singh, Analog Electronics, New Delhi: Firewall Media, 2007.

[28] R. Diffenderfer, Electronic Devices: Systems and Applications, Kansas City: Thompson Delmar Learning, 2005.

[29] C. Kachhava, Solid State Physics, Solid State Devices and Electronics, New Delhi: New Age International, 2003.

[30] D. K. S. G. N.N. Bhargava, Basic Electronics and Linear Circuits, New Delhi: Tata McGraw-Hill Publishing Company Limited, 1984.

[31] C. Nguyen, Radio-Frequency Integrated-Circuit Engineering, Wiley and Son's, Inc., 2015.

[32] A. G. U.A. Bakshi, Basic Electronics Engineering, Pune: Technical Publications, 2009.

[33] H. Granberg, Radio Frequency Transistors, Boston: Elsevier, 2013.

[34] A. Grebennikov, RF and Microwave Transmitter Design, Jonh Wiley & Sons, 2011.

[35] M. R. A. H. Roohollah Bameri, "A 2.4 GHz Class-E Power Amplifier with High Power Control Range," in *25th Iranian Conference on Electrical Engineering (lCEE20 17)*, 2017.

[36] M. K. K. Tadashi Suetsugu, "Analysis and Design of Class E Amplifier with Shunt Capacitance Composed of Nonlinear and Linear Capacitances," in *IEEE TRANSACTIONS ON CIRCUITS AND SYSTEMS—I: REGULAR PAPERS, VOL. 51, NO. 7*, 2004.

[37] F. H. Raab, "Class-E, Class-C, and Class-F Power Amplifiers Based Upon a Finite Number of Harmonics," in *IEEE TRANSACTIONS ON MICROWAVE THEORY AND TECHNIQUES, VOL. 49, NO. 8*, 2001.

[38] Y. P. K. Y. Peng Chen, "Concurrent High-Efficiency Tri-band GaN Power Amplifier with Continuous Class-E Mode," in *2017 International Conference on Circuits, Devices and Systems*, 2017.

[39] E. W. B. M. M. M. F. Z. P. Thomas B. Mader, "Switched-Mode High-Efficiency Microwave Power Amplifiers in a Free-Space Power-Combiner Array," in *IEEE TRANSACTIONS ON MICROWAVE THEORY AND TECHNIQUES, VOL. 46, NO. 10*, 1998.

[40] P. A. S. C. P. B. K. Z. B. P. N. P. J. F. S. N. O. S. Frederick H. Raab, "Power Amplifiers and Transmitters for RF and Microwave," in *IEEE TRANSACTIONS ON MICROWAVE THEORY AND TECHNIQUES, VOL. 50, NO. 3*, 2002.

[41] H. H. A. Sheikhi, "Analysis and Design of the Novel Class-F/E Power Amplifier with Series Output Filter," in *IEEE Transactions on Circuits and Systems II, Express Briefs, Vol. 69, No. 3*, 2022.

[42] C. S. D-A. Nguyen, "A high-efficiency design for 5-W 2.4/5.8 GHz concurrent dual-band class-E power amplifier," in *Microwave and optical technology letters, 2021, Vol.63 (4)*, 2021.

[43] I. L.-H. D. F.-R. J. L.-Y. M. M.-C. C. P.-W. E. H.-D. J. R.-H. P. M. D. Ochoa-Armas, "A nonlinear empirical I/V model for GaAs and GaN FETs suitable to design power amplifiers," in *International journal of RF and microwave computer-aided engineering, Vol.31 (3)*, 2021.

[44] X. L. Y. Z. T. Q. X. D. W. C. F. G. C. Liu, "Investigation of High Efficiency Parallel Circuit Class-EF Power Amplifiers with Arbitrary Duty-Cycles," in *IEEE transactions on industrial electronics (1982), 2021, Vol.68 (6)*, 2021.

[45] H. J. F. Moloudi, "Broadband class-E power amplifier design using tunable output matching network," in *International journal of electronics and communications, vol. 118*, 2020.

[46] X. Z. W. C. T. S. D. H. L. Zhou, "Wideband Class-F−1 Power Amplifier With Dual-/Quad-Mode Bandpass Response," in *IEEE transactions on circuits and systems. I, Regular papers, vol. 67 (7)*, 2020.

[47] K. W. J.V. de Almeida, "Theory of continuous inverse class-E power amplifier modes and continuous-mode self-distortion," in *Microwave and optical technology letters, Vol.63 (8)*, 2021.

[48] X. G. I. H. K. W. J.V. de Almeida, "High-Efficiency Moderate-Power Amplifier Using Packaged GaN Transistor With Improved Average PAE and Gain for Batteryless IoT Applications," in *IEEE transactions on microwave theory and techniques, Vol.71 (2)*, 2023.

[49] S. C. Bera, Microwave High Power High Efficiency GaN Amplifiers for Communication, Springer Nature Singapore, 2022.

[50] V. A. B.-H. G. J. S. C. Qianqian Liu, "A Class-E RF Power Amplifier with a Novel Matching Network for High-Efficiency Dynamic Load Modulation," in *IEEE International Symposium on Circuits and Systems (ISCAS)*, 2017.

[51] D. P. Kenle Chen, "Design of Highly Efficient Broadband Class-E Power Amplifier Using Synthesized Low-Pass MatchingNetworks," in *IEEE Transactions on Microwave Theory and Techniques, Vol. 59, No. 12*, 2011.

[52] T. A. Filipek, "Design and Optimization of High Efficiency GaN HEMT Class-E Power Amplifiers," in *TENCON 2015 - 2015 IEEE Region 10 Conference*, 2015.

[53] S. G. S. H. S. I. L. U. K. M. a. R. A. Y. Hongtao Xu, "A High-Efficiency Class-E GaN HEMT Power Amplifier at 1.9 GHz," in *IEEE MICROWAVE AND WIRELESS COMPONENTS LETTERS, VOL. 16, NO. 1, JANUARY 2006*, 2006.

[54] A. B. V. F. Mury Thian, "High-Efficiency Harmonic-Peaking Class-EF Power Amplifiers With Enhanced Maximum Operating Frequency," in *IEEE TRANSACTIONS ON MICROWAVE THEORY AND TECHNIQUES, VOL. 63, NO. 2, FEBRUARY 2015*, 2015.

[55] K. M. Ayman O. Ameen, "A 1.75 GHz CMOS Class E RF Power Amplifier and Oscillator," in *2007 Internatonal Conference on Microelectronics*, 2007.

[56] R. N. a. F. M. G. Pouya Aflaki, “Design and implementation of an inverse class-F power amplifier with 79 % efficiency by using a switch-based active device model,” in *2008 IEEE radio and wireless symposium [front matter]*, 2008.

[57] J. L. K. A. R. W. P. K. S. A. D. L. T. Hwang, “Class-F Power Amplifier with 80.1% Maximum PAE at 2 GHz for Cellular Base-station Applications,” in *IEEE Annual Conference on Wireless and Microwave Technology (WAMICON)*, 2013.

[58] G. C. a. J. C. H. Kim, “A high-efficiency inverse class-F power high-efficiency inverse class-F power,” in *Microw. Opt. Technol. Lett., vol. 50, no.*, 2008.